S-nitrosation of mitochondrial Connexin 43 regulates mitochondrial function: implication for cardioprotection

Inauguraldissertation
zur Erlangung des Grades eines Doktors der Naturwissenschaften
(Dr. rer.nat.)
des Fachbereichs Biologie und Chemie
der Justus-Liebig-Universität Gießen

vorgelegt von
Soetkamp, Daniel
aus Münster

Gießen, September 2014

Die der vorliegenden Arbeit zugrunde liegenden Experimente wurden am Institut für Physiologie der Justus-Liebig Universität oder an anderen gleichwertigen Einrichtung unter der Leitung von Herrn Prof. Dr. Schulz durchgeführt.

1. Gutachter: Herr Prof. Dr. Michael Martin

2. Gutachter: Herr Prof. Dr. Rainer Schulz

Vorsitzender des Prüfungsausschusses: Herr Prof. Dr. Herbert Over

Tag der Disputation: 05.09.2014

If you want to make an apple pie from scratch, you must first create the universe.

Dr. Carl Sagan

Table of Contents

Dedicated to
Nesrin, Gabriel, Theo, and Lisa

1. Introduction

Connexins (Cxs) are a family of integral membrane proteins. They are the basis of channels within membranes allowing the passage of ions and small molecules. These channels are essential in various aspects of vertebrate physiology including the coordination of cellular signaling.

1.1 Connexins

Humans express 21 different connexin (Cx) isoforms, whereas mouse and rat express only 20. Cxs are named according to their molecular weight, which ranges from 23 to 62 kDa. Channels formed by different Cxs vary in solute permeability and their regulation and interaction with other proteins [1, 126, 182, 198]. Cxs are transmembrane (TM) proteins spanning the plasma membrane four times. The TM domain consists of α-helices (TM1-TM4) extending outside the plasma membrane for a significant distance. TM1 and TM2 domains are the pore forming helices with their narrowest region near to the extracellular site of the plasma membrane [174, 198]. The short N-terminal and the longer C-terminal ends face the cytosol. The C-terminal domain displays large variations among connexin isoforms. Two extracellular loops (E1 and E2 between TM1-TM2 and TM3-TM4) and one cytoplasmic loop (CL between TM2-TM3), with a not well conserved sequence, connect the TM domains [1, 126, 198].

In the heart, a variety of Cx isoforms are present. Cx31.9 is located at the atrioventricular nodal region [40]. Cx40 is present in the atrium and Cx45 at the border between myocytes and fibroblasts. Both Cx40 and Cx45 are also found in the conduction system [44]. In endothelial cells Cx43, Cx40, and Cx37 are detectable [34]. However, the predominant isoform in cardiomyocytes is Cx43. The majority of cellular Cx43 forms gap junctions (GJs) at the terminal intercalated disks of cardiomyocytes. However, in low density Cx43 is also located at the lateral sides of the cardiomyocyte sarcolemma where it forms hemichannels (HCs) [78, 185, 223].

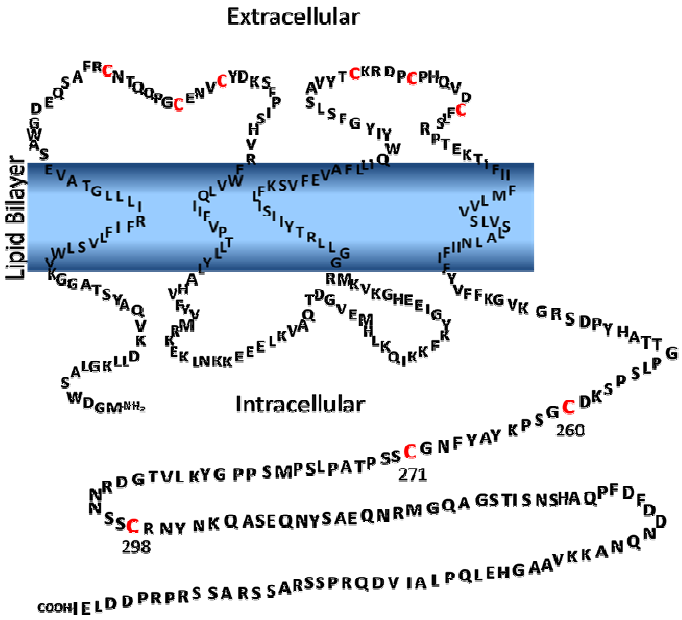

Figure 1.1: Schematic display of rat Cx43. Schematic representation of the primary structure of Cx43 and its orientation in the outer membrane. Cysteine residues of the amino acid sequence are labeled in red [modified from Lampe and Lau, 2000].

The C-terminal tail of Cx43 contains a variety of domains interacting with other proteins such as tubulins, tyrosine kinases, ubiquitin ligases, zonula occludens 1, and sodium (Na^+) channels [3, 4, 117, 256, 291]. Furthermore, phosphorylation mainly takes place at the C-terminal domain. Thus far, three distinct forms of Cx43 (P_0, P_1, P_2) with different molecular weights have been detected in the heart by Western blot analysis. P_0 has been viewed as dephosphorylated Cx43 while P_2 is believed to represent the fully phosphorylated form of Cx43 [278]. Cx43-phosphorylation sites are species-dependent: in mice there are 24 identified sites, in rats 21, and in humans 19 sites [127, 278]. These sites are the target of several kinases, such as protein kinase A (PKA), protein kinase C (PKC), protein kinase G (PKG), protein tyrosine kinases, mitogen-activated protein kinases (MAPK), casein kinases and protein phosphatases [158, 242].

1.2 Gap junctions and hemichannels

Six Cx43 assemble to form HCs, which contribute to cellular volume regulation [218], the release of ATP and NAD^+ from the cytosol [71], and the release of signaling molecules into the extracellular fluid activating survival pathways [55]. The two extracellular loops of Cx43 contain six conserved cysteines that can form

intramolecular disulfide bonds. These disulfide bonds are essential for connecting two opposing HCs of neighboring cells thereby forming a pore. Accumulation of pores form GJs [9, 90, 233], which connect the cytosol of neighboring cells allowing the passage of molecules with a size up to 1 kDa [89, 130]. GJs have been characterized as unspecific aqueous pores with a diameter of 0.8–1.4 nm, which is the only selective parameter [175]. There is certain evidence that casts doubt on the unselectively of Cx-formed channels. First, the permeability to fluorescence dyes decreases with increasing negative charge of the dye molecule, which suggests that the Cx-formed channel pore has a slight, fixed negative charge [32, 89]. Supporting this observation is the relatively low chloride (Cl^-)/ potassium (K^+) permeability compared to Na^+/K^+ for GJs determined by y_j ratios or bi-ionic potentials [33, 196, 281]. Secondly, according to several studies, Cx-formed channels are highly selective for monovalent cations with a higher permeability for K^+ than Na^+ (suggested ranking: K>Na>Lithium (Li)>Trimethylaluminium (TMA)> Triethanolamine (TEA)) [17, 33, 142, 262, 279, 280, 287]. However, the main forces determining fluxes via membranes are chemical and electrical gradients between membranes. Fluxes of molecules through GJs and HCs are regulated by channel assembly and degradation [233], as well as by channel open probability [259]. Cx43 GJs are highly dynamic structures with a high turnover rate of a few hours (half-life of Cx43 ranges from 1–3 hours) and a rapid redistribution [15, 157, 255].

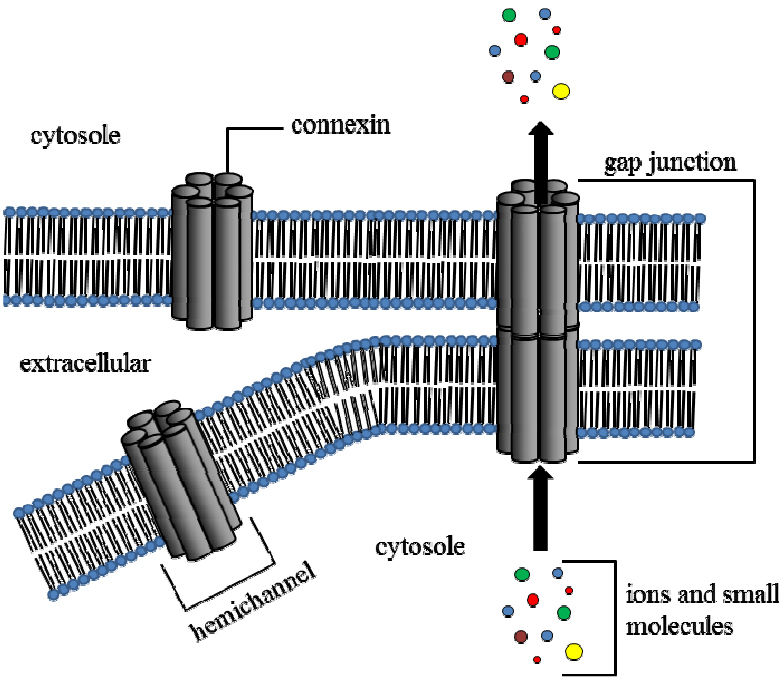

Figure 1.2: Schematic illustration of GJ assembly.

1.3 Regulation of connexin

The regulation of pore diameter and open probability of Cx-formed GJs and HCs is a complex mechanism and is so far not fully understood. Several Cx domains are involved in Cx43-formed channel opening. The N-terminal domain is involved in voltage-dependent gating [11, 98, 154, 215], while the C-terminal domain is involved in regulation of open probability and protein-protein interactions [1, 3, 91, 117, 126]. The CL region interacts with the C-terminal domain regulating channel opening during cellular acidification [73, 121].

GJs are mostly open for mediating continuous electric and chemical signals between cells, whereas HCs at the sarcolemma have a low open probability. Nevertheless the low open probability of HCs is enough to release signaling molecules of a physiological relevant amount into the extracellular space. Thus, HCs are involved in autocrine and paracrine signaling under physiological conditions [39, 52, 260, 298]. The p38 mitogen-activated protein kinase dependent pathway on the one hand reduces communication via GJs while on the other hand increases HCs permeability. The cytokine mediated increase in HCs permeability is blocked by application of a sulfhydryl reducing agent, which, however, does not affect GJs permeability. This finding suggests, that both types of Cx-formed channels are targeted by PKs, but their functional response is different [225].

Ions which can pass through Cx43-formed channels are able to regulate its conductance. Calcium (Ca^{2+}) induced reduction of GJ open probability has been reported for cardiomyocytes [72, 199]. Large changes in Ca^{2+} concentrations reduce gap junction conduction, whereas a low concentration does not affect GJ permeability [180, 232]. The suggested binding site of the positively charged Ca^{2+} and proton (H^{+}) ions is located at the CL [259].

In addition, Cx-formed HC open probability is regulated by Ca^{2+}. HC open probability is enhanced by a positive membrane potential and low extracellular Ca^{2+} levels [59, 86, 98, 163]. Under pathological conditions, sustained HC opening leads to metabolite loss, Ca^{2+} influx, equilibration of ionic gradients, and cellular damage. Blockade of HC opening reduces cardiomyocyte volume overload and irreversible injury following ischemia/reperfusion [289]. Under physiological conditions, the negative voltage of the membrane on the cellular side and millimolar concentrations of extracellular Ca^{2+} keep the HC open probability low [41, 48, 59, 86, 98, 163, 238].

However, HC opening can still be induced at high extracellular Ca^{2+} by several factors, including ischemia, inflammation, extracellular alkalinization, and Cx dephosphorylation [8, 60, 83, 113, 136, 166, 202, 227, 239, 251].

The phosphorylation of Cx43 at serine, threonine, and tyrosine residues mediates GJ remodeling and HC opening at the plasma membrane during ischemic events in the brain, kidney, and heart [59, 78, 113, 165]. Phosphorylation of Cx43 affects GJ communication in a positive and negative manner [21, 35, 64, 139, 157, 193]. The site specific phosphorylation sites of Cx43 targeted by PKC, MAPK, and protein-tyrosine kinase $pp60^{src}$, have been identified (Figure 1.3) [159, 172, 234, 290]. Phosphorylation of Ser368 by PKC decreases the selectivity for large hydrophilic compounds and negatively charged solutes, while increasing the selectivity for positively charged ions, which maintains electrical cell-cell coupling [10, 81, 155, 159]. During ischemia this mechanism minimizes the spread of damage inducing compounds to healthy neighboring cells. Furthermore, Cx43 phosphorylation is involved in its intracellular transportation as well as the assembly of GJs which influence intercellular communication [284].

On the other hand, dephosphorylation of Ser368 increases HC-permeability and thereby increasing the fluxes of metabolites and second messengers, Ca^{2+} induced cellular damage, and subsequently induces apoptosis [60, 113, 136, 161, 165, 283]. Studies using liposomes with nonphosphorylated Cx43-formed HCs have shown low permeability, whereas liposomes with induced HC phosphorylation showed greater permeability, indicating that dephosphorylation can be sufficient for HC opening. Supporting this notion, channels formed by mutated Cx43 - without the Ser368 phosphorylation site - stay preferentially open [10]. However, this effect was exclusively found for Cx43 at the intercalated disks and Ser368 phosphorylation was not found elsewhere [81, 176, 256, 258].

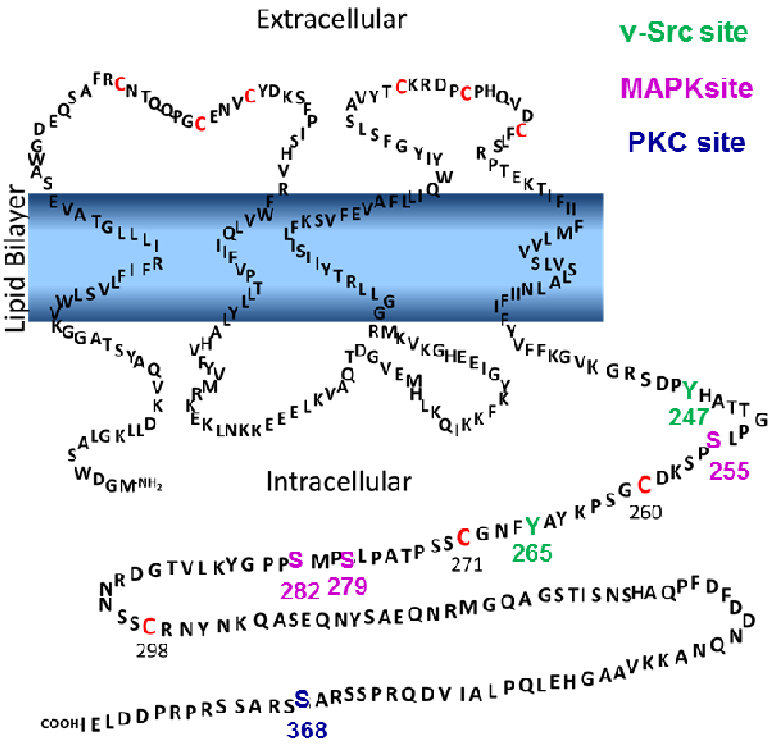

Figure 1.3: Schematic representation of the primary structure of rat Cx43 and its phosphorylation sites targeted by v-Src, MAPK, and PKC [modified from Lampe and Lau, 2000].

Therefore, there are specific ways of increasing HC permeability: dephosphorylation by ATP depletion, activation of Ca^{2+} dependent phosphatases, oxidation by reactive oxygen species (ROS) [61], and a rapid turnover rate of Cx43 by additional insertion of HCs into the membrane [224]. Indeed, HC opening in astrocytes is blocked during metabolic inhibition by scavenging ROS with Trolox. Interestingly, in the metabolically inhibited astrocytes treated with cyclosporine A (CsA), an increase in HC permeability was still possible even though dephosphorylation was inhibited. In fact, this suggests that the redox potential plays a role in HC opening [60, 61, 224]. Supporting this notion, Tumor necrosis factor (TNF-α) and interleukin-1β induced p38 MAPK activation leads to an increase in nitric oxide (NO) synthase (NOS) activity, which induces Cx43 HC opening in astrocytes [51, 216, 224, 226, 294]. Accordingly, application of low concentrations of NO induces increased Cx43 HC permeability. The free radical NO can attach covalently to free thiol groups of cysteine residues, which is a reversible redox-dependent post-translational protein modification called S-nitrosation (SNO) [82]. Studies have shown that NO and metabolic inhibition increases the permeability of Cx-formed channels to hydrophilic fluorescent molecules in astrocytes. Agents like Trolox and melatonin, which scavenge free

radicals like NO, lower dye uptake by reducing SNO without affecting Cx43 phosphorylation, whereas application of NO donors increase dye uptake. This suggests that SNO and not Cx43 dephosphorylation is the critical factor for increased Cx43-formed channel open probability [224]. Furthermore, SNO of the cysteine residue 271 increases and denitrosation decreases permeability of Cx43 myoendothelial GJs in the vessel wall [261]. Apart from its pore-forming capabilities, Cx43 interacts with a great variety of intracellular proteins involved in intracellular signaling and breakdown products of Cx43 (such as its C-terminus) might act as transcription factor [27]. The C-terminal domain of rat Cx43 was detected in the nucleus of cardiomyocytes and HeLa cells, where it inhibits cell proliferation [65].

1.4 Myocardial ischemia/reperfusion injury and its reduction by preconditioning

Myocardial infarction occurs species-dependently during occlusion of a major coronary artery for more than 20 minutes. While reperfusion is mandatory to ultimately reduce infarct size, reperfusion itself might contribute to the development of irreversible myocardial injury (the so called reperfusion injury). Since the extent of myocardial infarction predicts patient's prognosis, the search for strategies to reduce irreversible myocardial injury is still ongoing [109].

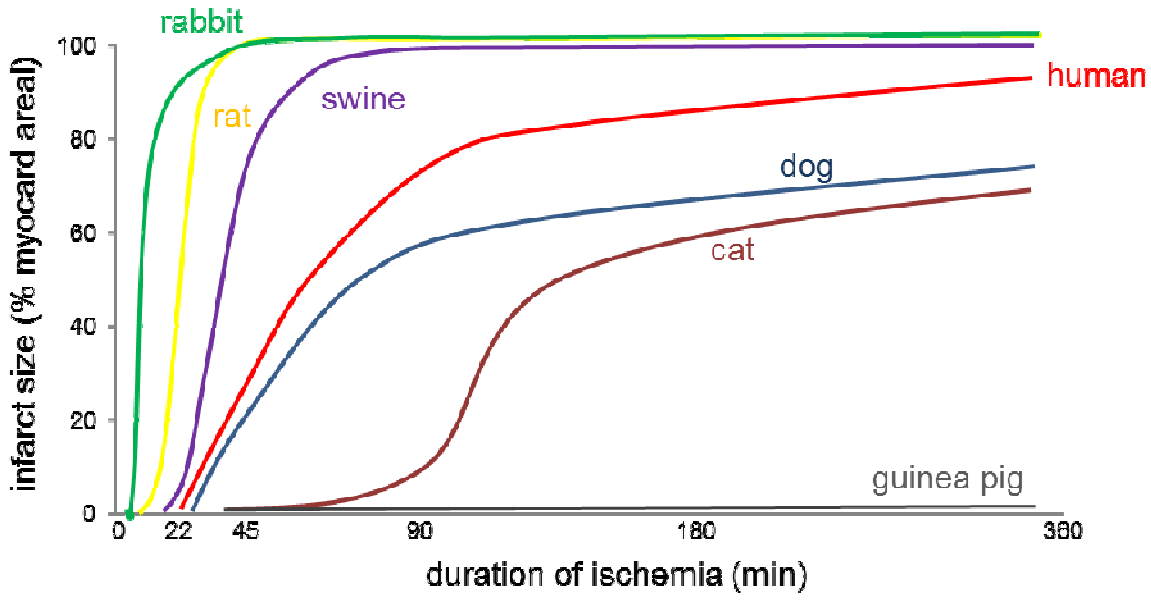

Figure 1.4: Time course of myocardial infarct development following complete coronary occlusion in different species [modified from Schaper et al., 1988].

Interestingly, brief episodes of ischemia and reperfusion protect the heart and delay the irreversible tissue damage caused by a subsequent more prolonged ischemia and reperfusion. This phenomenon has been termed ischemic preconditioning (IPC) and was first described by Murry et al. [56, 192]. IPC reduces the extent of apoptosis [179, 192, 195, 209], reduces the infarct size [299], and protects against arrhythmia in mice [236], rats [104, 249, 285], rabbit [57], and dog [143], but not in pig [102, 203, 228, 248]. The trigger phase of IPC is characterized by release of adenosine, bradykinin, opioids, and other G-protein coupled membrane receptor activating pathways [18, 19, 93, 100, 153, 171, 194, 201, 272] such as reperfusion injury salvage kinases (RISK) and survivor activating factor enhancement (SAFE) pathways. While the kinases of RISK (Akt/ERK1/2/GSK-3β), kinases of SAFE (TNF-α/JAK/STAT-3) [25, 85, 112, 119, 187, 189], and the protein kinase G/PKC pathway [63], contribute to cell survival, the modulation of AMP-activated protein kinase, Pim-1, and proteins of the Bcl-2 family may also play a role [16, 46, 49, 50, 129, 188].

Preconditioning can also be induced by pharmacological agents, for example by potassium channel openers like diazoxide, pinacidil, and nicorandil [115, 204, 237]. Diazoxide is supposed to be a selective mitochondrial ATP-dependent potassium (mitoK_{ATP}) channel opener inducing a low conduction state of the mitochondrial permeability transition pore (MPTP) located in the inner mitochondrial membrane. Prolonged opening of the MPTP destroys the proton gradient and thus the mitochondrial membrane potential, leads to mitochondrial swelling, rupture of the outer and inner mitochondrial membrane and finally loss of cardiomyocyte viability [144].

Short episodes of ischemia and reperfusion applied at a distant tissue or organ, such as extremities, also render the heart resistant to a prolonged period of ischemia, thereby inducing a phenomenon called remote ischemic preconditioning (rIPC) [31, 111, 213, 214, 271]. Recent studies showed that rIPC limited the injury in patients with acute myocardial infarction [69]. The protective signal is supposed to be directed to the heart by the interaction of humoral factors and neuronal transmission [2, 74, 75, 95, 135, 169, 250]. An increasing amount of data suggests that rIPC has protective mechanisms/signaling cascades in common with IPC. Signaling molecules such as adenosine, bradykinin, and opioids also trigger cardioprotection by rIPC. Furthermore, activity of common cardiac prosurvival kinases are also upregulated and increased phosphorylation was detected for ERK1/2-MAPK, JNK1/2-MAPK,

PKCε-isoform, signal transducer and activator of transcription (STAT) 3, STAT-5, and protein kinase B (Akt) [23, 114, 120, 128, 295]. In mice, pigs, and humans it has been shown that episodes of blood pressure cuff inflation and deflation in an extremity increases the circulating NO and nitrite in the blood [148, 220, 221].

1.5 Role of Cx43 in cardioprotection by preconditioning (PC)

Preconditioning (PC) reduces the dephosphorylation of Cx43 caused by ischemia leading to reduction of electric uncoupling and HC opening [134, 186, 241]. The preserved phosphorylation of Cx43 during IPC is likely to be linked to increased activity of PKC and p38 [241], as well as decreased association to protein phosphatases [274]. However, pretreatment with heptanol, a GJ uncoupling agent, blocks IPC suggesting that Cx43 is essential for the signal transduction cascade of IPC's cardioprotection [162]. Supporting evidence of Cx43's role in cardioprotection came from experiments with heterozygous Cx43-deficient mice, in which cardioprotection by IPC was lost [244, 245]. Surprisingly, in isolated cardiomyocytes of Cx43-deficient mice, IPC induced cardioprotection was also abolished, suggesting a role of Cx43 in cardioprotection independent from GJs [167].

While Cx43 is located at the sarcolemma (GJs and HC), it is also present in cardiomyocyte subsarcolemmal mitochondria (SSM), but not in interfibrillar mitochondria (IFM) which are present between myofibrils [24, 28, 231]. These two distinct subpopulation of mitochondria differ, besides their localization, in their morphology and function [229]. Evidence for the presence of Cx43 in mouse, rat, pig, and human left ventricle mitochondria was demonstrated by fluorescence-activated cell sorting, Western blot analysis, as well as confocal and electron microscopy [24]. Cx43 is imported via the regular mitochondrial import machinery, which was demonstrated by co-immunoprecipitation studies showing interactions of Cx43 with the translocase of the outer membrane 20 (TOM20) and heat shock protein 90 [230]. Following IPC, the amount of mitochondrial Cx43 (mtCx43) was rapidly increased and the increased amount was stable for the following 90 minutes. Evidence for the cardioprotective relevance of mtCx43 is attested by inhibition of the import of Cx43 into mitochondria, attenuating diazoxide-induced cardioprotection [230]. *In vitro* cross-linking studies on mitochondria showed complexes of a molecular weight comparable with that of Cx43 hemichannels [184]. Supporting this notion, the two

hemichannel blockers carbenoxolone and heptanol reduced mitochondrial uptake of Lucifer Yellow dye [184]. In addition, mitochondrial ADP stimulated complex 1 respiration was reduced by inhibiting Cx43-formed channels with mimetic peptides, by 18α-glycyrrhetinic acid (18αGA), or genetic modification of Cx43. Furthermore, in Cx43 overexpressing HL-1 cells, mitochondrial oxygen consumption was significantly increased [26].

The main source of ROS production is the flavin mononucleotide site of complex 1 and the Q cycle of complex III [6, 43, 190, 276]. Excessive ROS production leads to cell death, whereas moderate ROS formation contributes to cardioprotection. MitoK_{ATP} channels in the inner mitochondrial membrane have a regulatory effect on ROS production and K^+ influx caused by opening of mitoK_{ATP} channels and subsequent ROS formation are considered to mediate cardioprotection [26, 184, 200]. Mitochondrial ROS formation mediates signal transduction via redox-based post-translational protein modifications.

In permeabilized cardiomyocytes achieved from wild type mice, in astrocytes, and in isolated mitochondria from mouse left ventricles, the application of Cx43 inhibitors 18αGA and carbenoxolone reduced mitochondrial K^+ uptake [29, 152]. Additional studies showed that replacement of Cx43 by Cx32 also led to decreased mitochondrial K^+ influx, confirming a modulatory role of Cx43 in regulating mitochondrial K^+ fluxes [108, 184]. Diazoxide-induced generation of ROS was reduced in Cx43 deficient cardiomyocytes, whereas valinomycin, a potassium ionophore, and menadione produced equal amounts of ROS in wild type and Cx43 deficient cardiomyocytes and afforded subsequent cardioprotection. Thus, mtCx43 appears to be an essential part of the signal transduction cascade of endogenous cardioprotection [20, 103, 115, 205].

1.6 NO in cardioprotection

NO and its metabolites have a cardioprotective impact and reduce ischemia/ reperfusion injury [58, 63, 79, 173, 183, 254]. Following IPC, SNO of sulfhydryl residues for a wide spectrum of proteins was found to be significantly increased [150]. Interestingly, studies identified S-nitrosothiols in mitochondria following IPC, attesting SNO's influence on mitochondrial function and mitochondrial derived cardioprotection. Furthermore, SNO of proteins correlates with prevention of cell

death following prolonged ischemia and reperfusion [53, 191, 212, 263], and the reversible post-translational modification shielding cysteine from potential oxidation by ROS is thought to be the underlying protective mechanism [264, 266, 302]. ROS induced protein modifications are mainly irreversible, altering the function of proteins or even denaturing them. Thus increased ROS production during ischemia/reperfusion injury can lead to sustained myocardial dysfunction [307]. Therefore, the amount of SNO plays a critical role during ischemia/reperfusion injury.

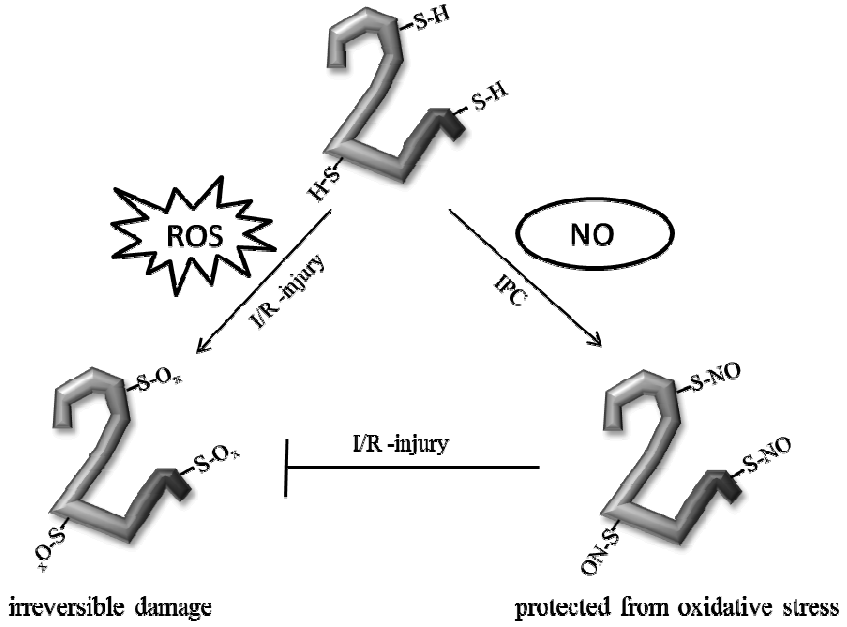

Figure 1.5: Schematic display of protection by NO. Increased ROS formation during ischemia/reperfusion injury causes to irreversible cysteine oxidation (Ox) and myocardial dysfunction (left). Conversely, IPC increases SNO of proteins leading to cardioprotection by shielding cysteine residues from oxidative stress (right) [modified from Kohr et al., 2011].

In the myocardium NO is synthesized by three different isoforms of nitric oxide synthase (NOS) [305], including neuronal NOS (NOS_1), inducible NOS (NOS_2), and endothelial NOS (NOS_3). NOS_1 and NOS_3 are constitutively expressed [12], whereas the inducible isoform NOS_2 is expressed following stress or pathological conditions [7]. In addition, NO can be generated independently from NOS by reduction of nitrite in a non-enzymatic manner [147, 177]. Treatment with NO donors like S-nitrosoglutathione leads to increased SNO of proteins and cardioprotection [263]. NO is also involved in cardioprotective signaling [119, 263] and NO´s role in post-translational modification of proteins has been increasingly recognized in recent years [240, 247, 264], especially during endogenous cardioprotective interventions [150]. Therefore, the balance between ROS and NO is essential for the regulation of

cardioprotection. SNO has been shown to play an important role in the regulation of metabolism, signal transduction, and the regulation of myocardial key proteins. NO has a cyclic guanosine monophosphate (cGMP)-dependent and cGMP-independent effect on final target proteins. The cGMP-dependent pathways are regulated by NO modification of guanylate cyclase, which increases cGMP levels thereby regulating downstream cGMP-dependent kinases like PKG, which transmits cardioprotective signals to the mitochondria [63, 137, 303]. CGMP-independent pathways are directly regulated by SNO of proteins [105, 118, 178]. Among the target proteins which are regulated by SNO is the L-type Ca^{2+} channel [265], the sarcoplasmic reticulum Ca^{2+} -ATPase [263], and the sarcoplasmic Ca^{2+} release channel [99, 286]. SNO also decreases the activity of mitochondrial proteins such as cytochrome c oxidase [301], F_1F_0ATPase [263], cyclophilin D [197], and mitochondrial complex 1 [54]. The NO donor 2,2′-(hydroxynitrosohydrazino)-bis-ethanamine inhibits the respiratory complex IV (cytochrome C oxidase) after long-term exposure in pulmonary artery endothelial cells, which is likely to be responsible for NO toxicity in lung endothelial cells [301]. A study showed that cardioprotection induced by IPC or by application of GSNO decreased F_1-ATPase α1 subunit activity leading to a slower decline of ATP following prolonged ischemia [263]. Cyclophilin D mediates MPTP opening, which is reduced by application of the NO donor GSNO in wild type, but not in Cyclophilin D deficient mouse embryonic fibroblasts [197]. Application of a selective mitochondrial SNO donor inhibits mitochondrial complex 1 activity during the first 5 minutes of reperfusion in ischemic tissue, thereby protecting from oxidative damage by decreasing ROS production [54]. Additional SNO of proteins has been identified, among them are aconitate hydratase, aldehyde dehydrogenase, α-ketogluterate dehydrogenase, creatine kinase, malate dehydrogenase, and thioredoxin [53, 149, 263]. Therefore, application of NO donors provides cardioprotection and reduces infarct size following ischemia/reperfusion injury with SNO of proteins being essential for cardioprotection. However, the full range of SNO targeted proteins, that influence myocardial function or those have a cardioprotective role have not been yet identified.

1.7 Aim of study

The present investigation's goal is to characterize the role of connexin 43 in mitochondrial function. Nitric oxide and mitochondrial connexin 43 play a role in the signal transduction cascade of cardioprotection. Since SNO regulates Cx43 at the sarcolemma, the question arises whether or not S-nitrosation regulates mitochondrial connexin 43 as well. Therefore, it is of interest if S-nitrosation of mitochondrial connexin 43 alters mitochondrial ion fluxes and generation of reactive oxygen species, since mitochondrial potassium fluxes and moderate increased formation reactive oxygen species are important for cardioprotection by preconditioning. The exact mechanism of how mitochondrial connexin 43 mediates ischemic preconditioning is unclear. Activation of the signal transduction cascade of ischemic preconditioning influences the posttranslational modification of several mitochondrial proteins. Thus, it is of interest whether or not S-nitrosation of mitochondrial connexin 43 is increased following ischemic preconditioning, remote ischemic preconditioning, or application of nitric oxide donors. Addressing these questions would elucidate a missing link in the signal transduction cascade of cardioprotection by ischemic preconditioning. Furthermore connecting nitric oxide and mitochondrial connexin 43 to the signal transduction cascade of cardioprotection would identify a potential pharmacological target that could reduce the damage of a myocardial infarct in patients suffering from pre-infarction symptoms.

2. Materials and Methods

2.1 Materials

2.1.1 Chemicals

Acetone	Callbiochem, La Jolla, CA, USA
Acetonitrile (ACN)	Callbiochem, La Jolla, CA, USA
Adenosine-diphosphate	Sigma-Aldrich, Heidenheim
Albumin standard	Thermo Fisher Scientific Inc., Darmstadt
Ammonium carbonate (NH_4CO_3)	Callbiochem, La Jolla, CA, USA
Amplex UltraRed reagent	Thermo Fisher Scientific Inc., Darmstadt
Antimycin A	Sigma-Aldrich, Heidenheim
Ascorbate	Sigma-Aldrich, Heidenheim
N-(biotinyl)-N-(iodoacetyl)ethylenediamine (BIAM)	Sigma-Aldrich, Heidenheim
Blotting grade blocker non-fat dry milk	Bio-Rad, Munich
Bovine serum albumin	Sigma-Aldrich, Heidenheim
Bis(sulfosuccinimidyl)suberate (BS3)	Life Technologies, Darmstadt
Calcium chloride ($CaCl_2$)	Roth, Karlsruhe
Carbenoxolone	Sigma-Aldrich, Heidenheim
Coomassie Brilliant Blue R-250	Sigma-Aldrich, Heidenheim
Complete Protease Inhibitor (EDTA free)	Roche Diagnostics, Grenzach
Cyclosporine A (CsA)	Sigma-Aldrich, Heidenheim
D-glucose	Roth, Karlsruhe
Dimethyl sulfoxide (DMSO)	Sigma-Aldrich, Heidenheim
Disodium phosphate (Na_2HPO_4)	Roth, Karlsruhe
Dithiothreitol (DTT)	Pierce, Rockford , IL, USA
Dynabeads Protein G DynaMag^{TM}	Thermo Fisher Scientific Inc., Darmstadt
DyeLight maleimide sulfhydryl-reactive dyes	Pierce Biotechnology, Rockford, IL, USA

Ethanol	Merck, Darmstadt
Ethylene diamine tetra acetic acid (EDTA)	Roth, Karlsruhe
Ethylene glycol-bis(β-aminoethyl ether)-tetraacetic acid (EGTA)	Sigma-Aldrich, Heidenheim
Formic acid	Merck, Darmstadt
Glibenclamide	Sigma-Aldrich, Heidenheim
L-Glutamatic acid potassium salt	Sigma-Aldrich, Heidenheim
Glycine	AppliChem, Darmstadt
Gramicidin	Invitrogen, Darmstadt
HEPES	Roth, Karlsruhe
Horseradish peroxidase (HRP)	Roche Diagnostics, Grenzach
Hydrogen chloride (HCl)	Merck, Darmstadt
Hydrogen peroxide (H_2O_2)	Roche Diagnostic, Grenzach
Isoflurane	Forane®, Abott GmbH, Wiesbanden
Ketanest S	Pfitzer, Münster
Lucifer Yellow CH dilithium salt	Sigma-Aldrich, Heidenheim
Magnesium chloride ($MgCl_2$)	Roth, Karlsruhe
Magnesium sulfate ($MgSO_4$)	Roth, Karlsruhe
Malate	Sigma-Aldrich, Heidenheim
Methanol	Roth, Karlsruhe
3-(N-morpholino)propanesulfonic acid (MOPS)	Sigma-Aldrich, Heidenheim
Neocuproine	Sigma-Aldrich, Heidenheim
N-ethylmaleimide (NEM)	Sigma-Aldrich, Heidenheim
Sodium nitrite ($NaNO_2$)	Sigma-Aldrich, Heidenheim
NuPAGE transfer buffer (20x)	Life Technologies, Darmstadt
Oligomycine	Sigma-Aldrich, Heidenheim
Percoll	GE Healthcare, Solingen
Phosphatase inhibitor	Roche Diagnostics, Grenzach
Pluronic® F127	Invitrogen, Darmstadt
Ponceau S solution for electrophoresis	Serva, Heidelberg
Potassium-binding benzofuran isophthalate acetoxymethyl ester (PBFI-AM)	Life Technologies, Darmstadt
Potassium chloride (KCl)	Roth, Karlsruhe

Potassium dihydrogen phosphate (KH_2PO_4)	Merck, Darmstadt
Proteinmarker Precision Plus ProteinTM	BioRad, Munich
Rhodamine B-Isothiocyanate-dextrane (RITC-dextrane)	Sigma-Aldrich, Heidenheim
Rompun	Bayer, Leverkusen
Rotenone	Sigma-Aldrich, Heidenheim
Sodium dodecyl sulfate (SDS)	Roth, Karlsruhe
S-nitrosoglutathione (GSNO)	Santa Cruz, Heidelberg
S-nitroso-N-acetyl-DL-penicillamine (SNAP)	Life Technologies, Darmstadt
Sodium-binding benzofuran isophthalate acetoxymethyl ester (SBFI-AM)	Life Technologies, Darmstadt
Sodium bicarbonate ($NaHCO_3$)	Roth, Karlsruhe
Sodium carbonate (Na_2CO_3)	Roth, Karlsruhe
Sodium chloride (NaCl)	Roth, Karlsruhe
Sodium hydroxide (NaOH)	Roth, Karlsruhe
Sodium phosphate (NaH_2PO_4)	Sigma-Aldrich, Heidenheim
Streptavidin-agarose beads	Sigma-Aldrich, Heidenheim
Succinate	Sigma-Aldrich, Heidenheim
Sucrose	MP Biomedicals, Eschwege
Tetraethylammonium chloride (TEA-Cl)	Sigma-Aldrich, Heidenheim
Tetramethylammonium chloride (TMA-Cl)	Sigma-Aldrich, Heidenheim
Tris-Base	Merck, Darmstadt
Tween-20	AppliChem, Darmstadt
Urea	Sigma-Aldrich, Heidenheim
Valinomycin	Sigma-Aldrich, Heidenheim
XT Reducing agent (20x)	Bio-Rad, Munich
XT Sample buffer (4x)	Bio-Rad, Munich

2.1.2 Antibodies and enzymes

Table 2.1: Used primary and secondary antibodies

Antibody	Distributor	Dilution
Rabbit polyclonal anti-rat connexin 43	Sigma-Aldrich (C6219), Heidenheim	1:1000
Mouse monoclonal anti-rat sodium/potassium (Na^+/K^+)-ATPase α-1	Millipore (# 05-369), Temecula, CA, USA	1:500
Mouse monoclonal anti-dog sarcoplasmic calcium 2 (SERCA2)-ATPase	Sigma-Aldrich (S1314), Heidenheim	1:500
Rabbit monoclonal anti-human histone deacetylase 2 (HDAC2), clone Y461	Millipore (# 04-229), Temecula, CA, USA	1:500
Mouse monoclonal anti-rabbit Glycer-aldehyde-3-phosphate dehydrogenase (GAPDH)	Hytest (# 5G4), Turku, Finland	1:5000
Rabbit polyclonal anti-human translocase of the outer membrane 20 (Tom20)	Santa Cruz (sc-11415), Santa Cruz, CA, USA	1:2000
Rabbit polyclonal anti-human voltage-dependent anion channel (VDAC)	Abcam (ab34726), Cambridge, UK	1:1000
Rabbit polyclonal anti-human manganese dismutase (MnSOD)	Millipore (# 06-984), Temecula, CA, USA	1:2000
Rabbit anti-phospho-connexin43 (S368)	Cell Signaling (# 3511), Leiden, Netherlands	1:1000
Rabbit anti-phospho-connexin43 (S365) and rabbit anti-phospho-connexin43 (S373)	prepared by Paul Lampe Lab, Fred Hutchinson Cancer Research Centre, USA [257]	1:500
Goat anti-rabbit IgG, HRP linked	Cell Signaling (# 7074), Leiden, Netherlands	1:5000
Horse anti-mouse IgG, HRP linked	Cell Signaling (# 7076), Leiden, Netherlands	1:5000

Nargase protease	Sigma-Aldrich, Heidenheim
GAP26, Connexin Mimetic peptide *(VCYDQAFPISHIR)*	AnaSpec, Seraing, Belgium

2.1.3 Kits

Lowry assay: BioRad DC Protein Assay	BioRad, Munich
Chemiluminescent substrate Pico	Healthcare Life Sciences, Freiburg
Chemiluminescent substrate Femto	Healthcare Life Sciences, Freiburg

2.1.4 Buffer and solutions

Physiological saline	Braun Melsungen AG, Melsungen
Isolation buffer	250 mM sucrose, 10 mM HEPES, 1 mM EGTA, pH 7.4 adjusted with Tris-base
30% Percoll solution	30% Percoll (sterile filtered) in Isolation buffer
Krebs-Henseleit buffer	120 mM NaCl, 11, mM D-glucose, 25 mM $NaHCO_3$, 1.75 mM $CaCl_2$, 4.7 mM KCl, 1.2 mM $MgSO_4$, and 1.2 mM KH_2PO_4, pH 7.4 adjusted with 95% O_2/CO_2
Phosphate buffered saline (PBS)	pH 7.4, Merck Millipore, Schwalbach

Buffers used for biochemical methods:

Cell lysis buffer	10% cell lysis buffer (10x), 10% ”Complete” protease inhibitor mix (10x)
HEPES buffer	250 mM HEPES-NaOH, 1 mM EDTA, and 0.1 mM neocuproine, pH 7.7
RIPA lysis buffer	Invitrogen, Grand Island, NY, USA

Buffers used for precipitation:

Conjugate buffer	20 mM NaH_2PO_4, 0.15 M NaCl, pH 7-9
Quenching buffer	1 M Tris-HCl
IP buffer	PBS with 0.05% Tween-20

Buffers used for SDS-PAGE and Western blot:

MOPS buffer	20x MOPS buffer
Comaisse blue staining	0.1% Coomassie Brilliant Blue R-250, 50% methanol, and 10% glacial acetic acid
Transfer buffer	20x NuPAGE Tranfer buffer, 10% v/v methanol

Buffers used for antibody detection:

Blocking solution	5% w/v blotting grade blocker non-fat dry milk in TBST
TBS	10 mM Tris, 150 mM NaCl, pH 7.6
TBST	0.1% Tween-20 in TBS

Buffers used for proteomic analyses:

Reduction solution	10 mM DTT, 25 mM NH_4CO_3
Alkylation solution	25 mM NEM in 25 mM NH_4CO_3, 1 mM EDTA
Washing buffer	25 mM NH_4CO_3 in 50% v/v ACN
Trypsin solution	12.5 ng/µl in 25 mM NH_4CO_3, 1 mM EDTA

Buffers used for analysis of mitochondrial function :

Incubation buffer	125 mM KCl, 10 mM MOPS, 1.2 mM KH_2PO_4, 1.2 mM $MgCl_2$, 20 µM EGTA, pH 7.4
Isosmotic potassium buffer	150 mM KCl, 7 mM NaCl, 2 mM KH_2PO_4, 1 mM $MgCl_2$, 6 mM MOPS, 6

	mM succinate, 0.25 mM ADP, 0.5 µM rotenone, pH 7.2
Glutamate/Malate buffer	5 mM glutamate, 2.5 mM malate in incubation buffer
Succinate buffer	5 mM succinate, 2 µM rotenone in incubation buffer
TEA buffer	120 mM TEA-Cl, 10 mM HEPES, 10 mM succinate, 5 mM KH_2PO_4, 0.1 mM EGTA, 0.5 mM $MgCl_2$, 5 µM rotenone, 0.67 µM oligomycin, pH 7.2
TMA buffer	120 mM TMA-Cl, 10 mM HEPES, 10 mM succinate, 5 mM KH_2PO_4, 0.1 mM EGTA, 0.5 mM $MgCl_2$, 5 µM rotenone, 0.67 µM oligomycin, pH 7.2

2.1.5 Consumables

10% Bis-Tris SDS-Gels	Life Technologies, Darmstadt
C_{18} column ZipTip	Millipore, Billerica, MA, USA
PicoFrit analytical column	New Objective, Woburn, MA, USA
Protran® nitrocellulose transfer membrane (0.2 µm)	Whatman, GE Healthcare, Solingen
Zorbax 300SB-trap column	Agilent Technologies, Santa Clara, CA, USA

2.1.6 Equipment

Allegra™ 64R Centrifuge	Beckman Coulter, Krefeld
Centrifugal evaporator	Heraeus, Hanau
Clary Eclipse spectrophometer	Varian, Mulgrave, Australia
Digital sonifier 450 D Branson	Emerson Technologies,

	Dietzenbach
Dry Block DB-2D	Techne, Burlington Township, NJ, USA
Electrophoresis power supply – EPS 601	GE Healthcare, Solingen
ELISA microplate reader model 680	Bio-Rad, Munich
Laser Doppler Perfusion Imaging (LDPI)	Perimed, Stockholm, Schweden
LTQ Orbitrap Velos mass spectrometer with Eksigent nanoLC-Ultra 1D plus system	Thermo Fisher Scientific, San Jose, CA, USA
Oxygen meter 782	Strahtkelvin, Glasgow, UK
pH 211R Microprosser pH meter	Hanna Instruments, Kehl
Proteome Discover 1.1	Thermo Fisher Scientific, San Jose, CA, USA
Typhoon 9400 variable mode imager	GE Healthcare Lifesciences, Piscataway, NJ, USA
Vascular occluder (6 mm)	Kent Scientific, Torrington, USA
Ventilator side port Inspira	Harvard Apparatus, Hugo-Sachs, March-Hugstetten
X Cell SureLock Novex mini	Invitrogen, Darmstadt
X Cell Blot Module	Invitrogen, Darmstadt

2.2 Methods

2.2.1 Animals

All rodents were treated according to the Guide for the Care and Use of Laboratory Animals published by the US National Institutes of Health (NIH publication no. 85-23, revised 1996) and approved by the Institutional Laboratory Animal Care and Use Committee of the NIH, Bethesda, MD, USA or according to the European Convention for Protection of Vertebrate Animals Used for Experimental and Other Scientific Purposes (Council of Europe Treaty Series No. 123). For Langendorff heart perfusion experiments male Sprague-Dawley rats (190–210 gram and 7-8 weeks old) were anesthetized with pentobarbital and anti-coagulated with heparin. Male Wistar-Janvier rats (190-210 gram and 8–10 weeks old) were used for mitochondrial

permeability experiments and were anesthetized with 2.5% v/v isoflurane. Male C57BL/6J mice used for rIPC studies were 11–14 weeks of age with a body weight ranging from 25–35 gram. They were anesthetized by intra peritoneal (i.p.) injection of ketamine (45 mg/kg) and xylazine (Rompun, 10 mg/kg) according to their body weight. The performed animal experiments were authorized (TVA Nummer: G347/12).

2.2.2 Isolation of mitochondria

All procedures were performed at 4°C to maintain mitochondrial integrity. To prevent light-induced SNO breakdown, samples were kept in the dark during the isolation process. SSM were isolated from left ventricles of male rats or mice as described previously [24]. For functional analysis, the left ventricles of rat hearts were minced in isolation buffer, homogenized with an Ultra Turrax and centrifuged at 800 g for 10 minutes. The resulting supernatant was centrifuged for 10 minutes at 12,200 g and the pellet was resuspended in BSA-free isolation buffer and centrifuged twice at 10,300 g for 5 minutes.

IFM, which lack Cx43, were used as negative controls and isolated as previously described [28]. The hearts were weight; left ventricles were minced, homogenized and centrifuged at 800 g for 10 minutes. The resulting pellet was resuspended) and incubated on ice for 1 minute in 5 ml isolation buffer additional containing 0.5% BSA and nargase (8 U/g. The tissue was homogenized and centrifuged at 800 g for 10 minutes and the supernatant was centrifuged for 10 minutes at 12,200 g. The resulting pellet was resuspended in BSA free isolation buffer and centrifuged twice at 10,300 g for 5 minutes.

For quantitative SNO analysis, a BSA-free isolation buffer supplemented with 0.1 mM neocuproine, EDTA free complete protease inhibitor, and phosphatase inhibitor was used. The mitochondria were isolated as described above from rodent left ventricles. The right ventricles were frozen at -80°C and were used as control. The isolated mitochondria from left ventricles were layered on a 30% Percoll gradient and centrifuged for 30 minutes at 35,000 g. This resulted in a lower fraction containing pure SSM and an upper fraction containing cell debris. The lower fraction was collected and washed three times with isolation buffer by centrifuged at 10,200 g for 5 minutes.

Protein concentrations were determined by the Lowry assay using BSA as a standard. For quantitative analysis the purity of isolated mitochondria was validated by Western blot analysis confirming the absence of non-mitochondrial cellular proteins (Na^+/K^+-ATPase, SERCA2a, HDAC2, and GAPDH) and the enrichment of mitochondrial proteins (VADC, MnSOD, and TOM20). Mitochondria were stored at -80°C.

2.2.3 Analyses of mitochondrial membrane potential

A toxic effect of carbenoxolone on mitochondria was analyzed by measuring the membrane potential. A loss of membrane potential indicated MPTP opening or membrane rupture. Mitochondria (0.5 mg/ml) were added to isolation buffer supplemented with 5 mM NaCl and 100 nM rhodamine 123 dye. The rhodamine 123 dye accumulates in membranes in a membrane potential dependent manner. After measuring the fluorescence (λ_{ex} 503 nm; λ_{em} 535 nm) for 3 minutes with a stable mitochondrial membrane potential DMSO, 1 µM, 25 µM, or 35 µM Carbenoxolone were added. A toxic effect is characterized by an increase of fluorescence intensity indicated by a release of membrane accumulated dye caused by a loss of membrane potential.

2.2.4 Measurements of mitochondrial autofluorescence

Mitochondrial autofluorescence was measured by using NADPH (λ_{ex} 340 nm; λ_{em} 460 nm) as a fluorescence indicator for mitochondrial integrity. For testing carbenoxolone toxicity, 1 mg SSM was applied after 30 seconds measuring the level of baseline fluorescence in 2 ml isolation buffer. Then, after measuring mitochondrial autofluorescence for 3 minutes DMSO, 1 µM, 25 µM, or 25 µM carbenoxolone was applied. A decline of mitochondrial autofluorescence indicates a mitochondrial loss of NADPH due to MPTP opening or membrane rupture.

2.2.5 Dye permeation experiments

Dye permeation experiments were performed according to Miro-Casas et al. [184]. Freshly isolated mitochondria were pelleted by centrifugation at 10,200 g for 3 minutes at 4°C and resuspended at a concentration of 400 µg/ml in isosmotic succinate buffer. Mitochondria were assigned to groups either supplemented with 1 µM, 10 µM, or 25 µM of the hemichannel blocker carbenoxolone, 0.5 mM NO donor S-nitroso-N-acetyl-DL-penicillamine (SNAP), 1 mM of NO donor S-nitrosoglutathione (GSNO), a combination of NO donor and carbenoxolone, or 5 µl DMSO. Additional mitochondria from Langendorff perfused hearts receiving IPC or that were control perfused were assigned to dye permeation experiments. As a control, IPC receiving or control mitochondria were exposed to UV light for 5 minutes to remove light sensitive SNO modifications. After a 5 minute incubation period at 25°C and 650 rpm, 50 µM of the Cx43 hemichannel-permeable dye Lucifer Yellow CH dilithium salt (LY) and 25 µg/ml of the hemichannel-impermeable dye rhodamine B isothiocyanate-dextran 10S (RITC-dextran) were added and samples were incubated for 25 minutes at 25°C and 650 rpm. Subsequently, mitochondria were washed and resuspended in 200 µl succinate buffer. Fluorescence of LY (λ_{ex} 430 nm; λ_{em} 535 nm) and RITC-dextran (λ_{ex} 545 nm; λ_{em} 600 nm) was measured by a 96-microplate fluorometer at high sensitivity. As a negative control, experiments were performed with ultrasound treated (20 seconds, amplitude 50%) mitochondria to exclude interference of dye and membrane fragments, as well as with IFM to confirm Cx43 hemichannel-specific effects.

2.2.6 Mitochondrial potassium uptake

Experiments for measuring velocity of mitochondrial K^+ influx were modified from Miro-Casas et al. [184]. Freshly isolated mitochondria were resuspended at a concentration of 400 µg/ml in isolation buffer. Either 1 µM, 10 µM, or 25 µM carbenoxolone, 0.5 mM SNAP, the combination of both, or 5 µl DMSO was added to mitochondria and incubated for 20 minutes at 25°C and mixed at 650 rpm. The experiments were repeated with the use of 1 mM physiologically relevant NO donor GSNO instead of SNAP. Subsequently, mitochondria were loaded with 10 µM acetoxymethyl of potassium-binding benzofuran isophthalate (PBFI) for 10 minutes at

25°C and 650 rpm. The benzofuran isophthalate derivatives with their cell-permeant acetoxy methyl (AM) are able to permeate mitochondria. Once inside the mitochondria the lipophilic AM group is cleaved by unspecific esterases, resulting in a charged form of the potassium indicator, which is not able to pass mitochondrial membranes. K^+ depletion from the mitochondrial matrix was achieved by adding 3 volumes of tetraethylammonium (TEA) buffer, which replaces K^+ in the mitochondrial matrix. Subsequently, mitochondria were washed, sedimented at 10,200 g and 4°C for 3 minutes, and resuspended in 30 µl isolation buffer. The kinetics of mitochondrial K^+ uptake were measured after a KCl pulse of 140 mM at alternated excitations at 340/380 nm and emission at 500 nm by a fluorometer in 2 ml isolation buffer at medium sensitivity. In order to measure the K^+ permeability for the Cx43 hemichannel only, during measurements, MPTP opening was blocked by adding 1 µM CsA [110], the proton channel of the ATP-synthase was blocked with 1µg/ml oligomycin, and opening of ATP-dependent potassium channels was blocked by 5 µM glibenclamide [246, 267]. The experiments were repeated without these inhibitors to investigate the influence of NO donors on the K^+ influx under physiological conditions. The K^+ influx during the first 2 seconds after the KCl-pulse, was determined by the increase of the PBFI fluorescence ratio of 340/380 nm per second in different treatment groups. As a positive control, K^+ influx was determined after addition of 5 nM valinomycin, which is highly sensitive to sodium and potassium and functions as a sodium and potassium specific transporter across membranes. In order to confirm a Cx43 specific effect, experiments were also performed with IFM instead of SSM.

2.2.7 Mitochondrial sodium uptake

Experiments for measuring the velocity of mitochondrial Na^+ influx were performed similarly as measuring potassium influx. Mitochondria were treated either with 25 µM carbenoxolone, 0.5 mM SNAP, 1 mM GSNO, the combination of NO donor and carbenoxolone, or 5 µl DMSO and then loaded with 10 µM acetoxymethyl of sodium-binding benzofur (SBFI) instead of using PBFI. Sodium depletion was then performed with tetramethylammonium (TMA) buffer. After subsequent washing, the kinetics of mitochondrial Na^+ uptake were measured after a NaCl pulse of 10 and 140 mM at alternated excitations at 340/380 nm and emission at 500 nm by a fluorometer. This was performed in 2 ml isolation buffer as well as in 2 ml succinate buffer

supplemented with inhibitors for MPTP, ATP-synthase, and ATP-dependent potassium channels as described above at high sensitivity. Na^+ influx of the first 2 seconds after the NaCl-pulses was determined by the increase of the SBFI fluorescence ratio of 340/380 nm per second of the six different treated groups. As a positive control, Na^+ influx was determined after addition of 5 nM gramicidin, which has a similar function as valinomycin and forms a channel for potassium and sodium, but does not interfere with SBFI dye as does valinomycin.

2.2.8 ROS production

One mg of freshly isolated SSM or IFM were added to 2 ml incubation buffer containing 5 mM glutamate and 2.5 mM malate as a substrate, 10 U/ml horseradish peroxidase (HRP), and 50 µM Amplex UltraRed reagent. Amplex UltraRed is a fluorogenic substrate for HRP that reacts with hydrogen peroxide (H_2O_2). For estimating the NO-mediated influence of mtCx43 on ROS production either 25 µM carbenoxolone, 0.5 mM SNAP, 1mM GSNO, a combination of a NO donor and carbenoxolone, or 20 µl dH_2O was added 30 seconds before the measurement was started. Additional experiments were completed inhibiting Cx43 by using the Cx43 mimetic peptide Gap26. Analysis of ROS formation was performed by a fluorometer at an extinction and emission wavelength of 568/581 nm. Mitochondrial H_2O_2 production was measured for 4 minutes and the increase of H_2O_2 was expressed in nmol/min/mg protein by comparing the data to a standard curve estimated with H_2O_2. After 4 minutes of measurement, 2 µg/ml of mitochondrial complex III inhibitor antimycin A was added for inducing mitochondrial ROS overproduction, which served as a positive control. Furthermore experiments were repeated in presence of 30 nM FCCP or 2 µM of complx 1 inhibitor rotenone.

2.2.9 Rat heart perfusion protocols

Excised rat hearts were placed in ice-cold Krebs-Henseleit buffer and the hearts were Langendorff perfused in retrograde fashion with oxygenated Krebs-Henseleit buffer (95% O_2/5% CO_2, pH 7.4) at a constant pressure of 100 cm water at 37°C. Hearts were randomly assigned to either a control group perfused for 40 minutes under normoxic conditions or an ischemic preconditioned (IPC) group in which the hearts

were perfused for 20 minutes under normoxic conditions followed by four cycles of 5 minutes ischemia and 5 minutes reperfusion [170, 263]. Perfusion was performed in the dark to prevent breakdown of SNO modifications. Control experiments were also performed by daylight confirming light sensitivity of SNO modifications.

2.2.10 In vivo remote ischemic preconditioning

The following method of the induction of cardioprotection by remote ischemic preconditioning or application of nitrite was performed by Dominik Semmler from the Cardiovascular Research Laboratories of the Heinrich Heine University Düsseldorf. C57BL/6J mice were anesthetized by i.p. injection of ketamine (45 mg/kg) and xylazin (Rompun 10 mg/kg) and a tracheal tube was inserted for mechanical ventilation, which was performed according to the individual body weight at a tidal volume of 2.1 - 2.5 ml and a respiratory rate of 140 breaths per minute. The mice were supplemented with 100% oxygen via a rodent ventilator (Minivent) side port. Around the right upper hindlimb a small vascular occluder with internal inflation pressure of 200 mmHg (6 mm), measured digitally, was used to arrest the hindlimb perfusion. The rIPC mouse model achieved 4 cycles of 5 minutes hindlimb ischemia followed by 5 minutes of reperfusion. The control group was perfused for 40 minutes. rIPC was stimulated by pharmacological preconditioning induced by injection of 48 nM nitrite into the cavity of the left ventricle, whereas the control group received an equal volume of 50 µl physiological saline. The chest was opened through a midline sternotomy. Mouse hearts were excised and mitochondria were isolated as described above.

2.2.11 Labeling and precipitation of SNO modified proteins

A modified biotin switch method was used for labeling and quantification of SNO protein modifications as previously described [133]. SSM protein samples (250 µg) and controls (250 µg IFM, and 250 µg right ventricle of hearts) diluted in HEPES buffer supplemented with EDTA free complete protease inhibitor, phosphatase inhibitor, 0.1 mM neocuproine, and 2.5% SDS (wt/vol), were pressed 5 times through a 27 gauge needle. To block free thiols, 50 mM N-ethylmaleimide (NEM) was used. After incubation for 20 minutes at 50°C with gentle mixing every 5 minutes, free thiols were labeled with NEM and could not be modified. This procedure was stopped by

removing NEM via cold acetone precipitation (-20°C). The samples were then resuspended in HEPES buffer with 1% SDS (wt/vol) containing 1 mM ascorbate for reduction of SNO modified cysteine residues. Reduced SNO groups were labeled with N-(biotinoyl)-N-(iodoacetyl)ethylenediamine (BIAM). Prior to incubating samples with streptavidin-agarose beads for precipitation of SNO modified proteins, 2 µl of loading control was taken. Precipitation was performed overnight with rotation at 4°C in the dark. Samples were washed three times with HEPES buffer, eluted in 30 µl sample buffer with 10 M urea and heated at 95°C for 5 minutes. Specificity of the biotin switch method was proven by adding 10 mM or 100 mM DTT before eluting the sample, which breaks the disulfide bound between the thiol group and biotin. Western blot analysis was subsequently performed.

2.2.12 Analysis of NO donor impact on mtCx43 phosphorylation

The influence of NO donors on mtCx43 phosphorylation was analyzed. Mitochondria were incubated either with 1 µM carbenoxolone, 0.5 mM SNAP, 1 mM GSNO, the combination of a NO donor and carbenoxolone, or 5 µl DMSO in incubation buffer. Subsequent mitochondrial purity was achieved by Percoll gradient centrifugation as described above. Phosphorylation of Cx43 was then investigated by Western Blot analysis was performed with Phospho-connexin 43 antibodies directed against serine residues Ser365, Ser368, and Ser373.

2.2.13 Western blot analysis

Right ventricles (RV) of hearts were minced and used as positive controls. All controls were diluted with RIPA lysis buffer or cell lysis buffer and centrifuged at 13,000 g for 10 minutes at 4°C. Protein concentration of supernatants was estimated using the Lowry assay using BSA as a standard. Both mitochondrial samples and controls were separated by electrophoresis on 10% Bis-Tris SDS-Gels and transferred to nitrocellulose membranes. Protein transfer was controlled by membrane staining with Ponceau S. After blocking with 5% (w/v) nonfat dry milk, membranes were incubated with primary antibodies diluted according to product instructions in 5% (w/v) nonfat dry milk (see table 2.1). The corresponding IgG HRP-conjugate combined with chemiluminescent substrate or corresponding DyLight

maleimide sulfhydryl-reactive dyes combined with fluorescence emission at 700 nm were used as secondary antibodies and scanned on a Typhoon 9400 variable mode imager.

2.2.14 Precipitation of mtCx43 and SNO labeling for proteomic analysis

Immunoprecipitation (IP) was performed for enriching proteins of interest for proteomic analysis. Five hundred µg SSM, from either IPC or control perfused rat hearts in HEPES buffer were supplemented with EDTA free complete protease inhibitor, phosphatase inhibitor, 0.1 mM neocuproine, and pressed 5 times through a 27 gauge needle. Then samples were lysed by adding 2.5% SDS. Free thiols were labeled with NEM for 20 minutes at 50°C. After acetone precipitation, SNO modifications were reduced with ascorbate and labeled with 55 mM iodoacetamide. Polyclonal rabbit anti-Cx43 antibody was used for IP assays. Dynabeads Protein G DynaMag^{TM}-2 was cross-linked to 5 µg antibody with bis(sulfosuccinimidyl)suberate (BS3) to reduce the antibody presence according to product instructions. Dynabeads (1.5 mg) were washed with conjugate buffer and incubated with 5 mM BS3 in conjugate solution with rotation for 30 minutes. Crosslinking reactions were quenched by adding 1 M Tris-HCl with rotation for 15 minutes. Dynabeads were washed three times with IP buffer supplemented with EDTA-free complete protease inhibitor, phosphatase inhibitor, and 0.1 mM neocuproine. Five µg of rabbit anti-Cx43 or negative control rabbit IgG1 were added and incubated for 30 minutes with rotation forming antibody-Dynabead complexes. After washing, 500 µg of SSM and IFM fraction samples or total homogenate was added and the mixture was incubated with rotation overnight at 4°C. Samples were then washed 3 times with 200 µl PBS, eluted in 100 µl PBS, and added to new tubes. After discarding the supernatant, beads were resuspended in 30 µl XT Sample buffer with XT Reducing agent and proteins were eluted from beads by heating for 5 minutes at 95°C. Samples were then separated by SDS-gel electrophoresis. For visualizing protein bands SDS gels were Coomassie stained. After washing the gel with dH_2O, the gel was stained by incubation for 20 minutes with Coomassie solution. Then the gel was washed 5 times with dH_2O and destained with dH_2O at 4°C overnight.

2.2.15 Identification of SNO cysteine residues by LC-MS/MS analysis

The pretreatment of samples analyzed by mass spectrometrically analyses was performed by the author or by the research group of Prof. Dr. Lochnit from the biochemical institute of the Justus-Liebig University Giessen. Coomassie stained SDS gel bands of 43 kDa were cut out into small pieces to facilitate enzyme access. To remove the Coomassie dye and SDS traces, gel pieces were washed three times and incubated for 15 minutes with 25 mM NH_4CO_3 in 50% acetonitrile (ACN). Traces of ACN were removed using a centrifugal evaporator for complete dryness. Gel pieces were rehydrated for one hour at 56°C in reduction solution. Resulting free thiols of peptides were blocked with an alkylating solution followed by incubation for 45 minutes at room temperature in the dark. Gel pieces were then washed with 25 mM NH_4CO_3 in 50% ACN and samples were dried via centrifugation by using a centrifugal evaporator. The gel pieces were then trypsinized and digestion was performed overnight at 37°C. The supernatants were transferred to new tubes and gel pieces were incubated twice for 15 minutes on ice with 0.1% formic acid in 50% ACN to extract the remaining protein. All supernatants were combined and concentrated via centrifugal evaporation to a volume of 10 µl. After adding 15 µl of 0.1% formic acid, samples were cleaned with a C_{18} column. Liquid chromatography tandem MS (LC-MS/MS) was performed by Prof Dr. Günther Lochnit from the Biochemical Institute of the Justus-Liebig University or by Dr. Marian Gucek from the NIH in Bethesda, MD, USA using a LTQ Orbitrap Velos mass spectrometer coupled to an Eksigent nanoLC-Ultra 1D plus system that uses collision-induced dissociation (CID) fragmentation. Samples were loaded with a flow rate of 6 µl/minutes on to a Zorbax 300SB-trap column. Separation was performed using a reversed-phase PicoFrit analytical column with a 40 minutes linear gradient of 5–40% acetonitrile in 0.1% formic acid at a flow rate of 250 nl/minutes. LTQ Orbitrap Velos settings were chosen as follows: spray voltage 1.5 kV, and full MS mass ranger of *m/z* 230-2,000. Analysis was implemented in a data-dependent mode with one MS1 high-resolution (60,000) scans for precursor ions, and six data-dependent MS/MS scan for precursor ions above the threshold ion count of 2,000 with collision energy of 35%.

2.2.16 MASCOT database analysis

The LTQ Orbitrap Velos raw data output was analyzed with Proteome Discover 1.1 (Thermo Fisher Scientific) with the NIH six-processor MASCOT cluster search engine (http://biospec.nih.gov, version 2.3) using the following criteria: database. Swiss-Prot (Swiss Institute of Bioinformatics); taxonomy, *Rattus norvegicus* (rat); enzyme, trypsin; miscleavages 3; variable modifications, NEM and iodoacetamide (carbamidomethyl); MS peptide tolerance 25 ppm, and MS/MS tolerance 0.8 Da. An ion score that measured if the MS/MS spectra matched the stated peptide was allocated. Ion scores were measured in 10 x $\log_{10}$ (P), representing the probability of a random match (expectation value). Therefore, a high score represents a confident match as described by Perkins et al. (1999).

2.2.17 Statistics

Data are presented as mean ± SEM. Normal distribution of data was analyzed using a non-parametric Kolmogorov–Smirnov test. Unpaired Student´s *t* test was used between the two groups of IPC and control mitochondria of Western blot data and dye permeation data to determine the difference in the mean values. Unpaired Student´s *t* tests were used between the two groups of IPC and control rat left ventricular mitochondria, as well as between rIPC and control mouse left ventricular mitochondria of Western blot data and dye permeation experiments. This was used to determine the difference in the mean values of SNO modifications of mtCx43 data between two groups. Data of LY, K^+ uptake, Na^+ uptake and ROS formation were compared by two-way repeated measures ANOVA and Fisher`s LSD. Statistical significance was determined at $p<0.05$.

3. Results

NO plays a role in cardioprotection by preconditioning and is known to alter the function of several proteins involved in cardioprotective signaling. MtCx43 is part of the signal transduction cascade of preconditioning and regulates mitochondrial function.

3.1 SNO of mtCx43 influences mitochondrial function

It is of interest if SNO of mtCx43 plays a role in altering mitochondrial function. Mitochondrial function was analyzed by measuring mitochondrial permeability for dyes and specific ions, as well as mitochondrial ROS generation with exposure to either NO donors and/or Cx43-formed channel inhibitors.

3.1.1 Estimation of carbenoxolone toxicity

Carbenoxolone was used to reduce the open probability of Cx43-formed channels. To define the adequate concentration of carbenoxolone, its mitochondrial toxicity was analyzed. Loss of mitochondrial membrane potential or loss of mitochondrial auto-fluorescence was used to indicate mitochondrial damage. Thus, the release of membrane potential dependent accumulated rhodamine 123 dye and the subsequent increase in fluorescence intensity was analyzed under exposure to concentrations of 1 µM, 25 µM, 35 µM carbenoxolone, and DMSO used as a vehicle. The mitochondrial membrane potential was only lost in the presence of 35 µM carbenoxolone indicating a toxic effect of carbenoxolone solely at high concentrations (Figure 3.1).

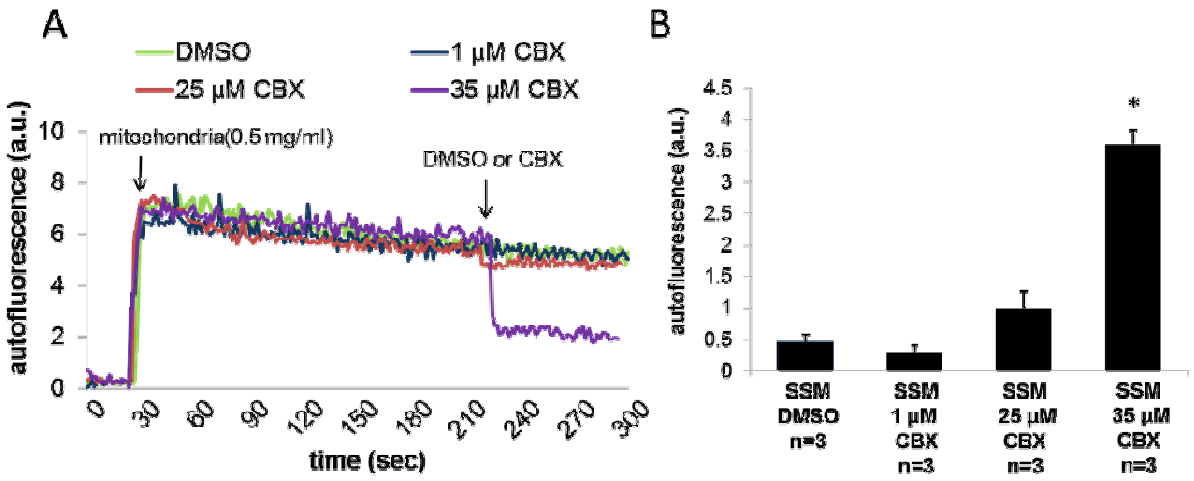

Figure 3.1: Analyses of carbenoxolone toxicity measuring mitochondrial membrane potential. Subsarcolemmal mitochondria (SSM) were loaded with rhodamine 123 dye, which accumulates in membranes in a membrane potential dependent manner. Mitochondria were applied to the rhodamine 123 containing solution after 90 seconds leading to decline of fluorescence intensity indicating mitochondrial dye uptake. Subsequently, after 210 seconds 1 µM, 25 µM, 35 µM carbenoxolone (CBX), or DMSO were administered. An increase of fluorescence intensity indicated loss of membrane potential (A). The difference of arbitrary units (a.u.) of fluorescence intensity before and after application of carbenoxolone are shown as means ± SEM of 3 replicates per group. * ($p<0.05$) indicates significant differences between groups (B).

Additional mitochondrial autofluorescence measurements were performed to analyze the toxic effect of carbenoxolone. Measurements were performed by using NADPH (λ_{ex} 340 nm; λ_{em} 460 nm) as a fluorescence indicator for mitochondrial integrity. Application of 35 µM carbenoxolone rapidly decreased mitochondrial autofluorescence (Figure 3.2). Carbenoxolone concentrations of up to 25 µM, which were used in this study, had no effect on mitochondrial membrane potential and autofluorescence indicating the nontoxic effects of carbenoxolone used in this study.

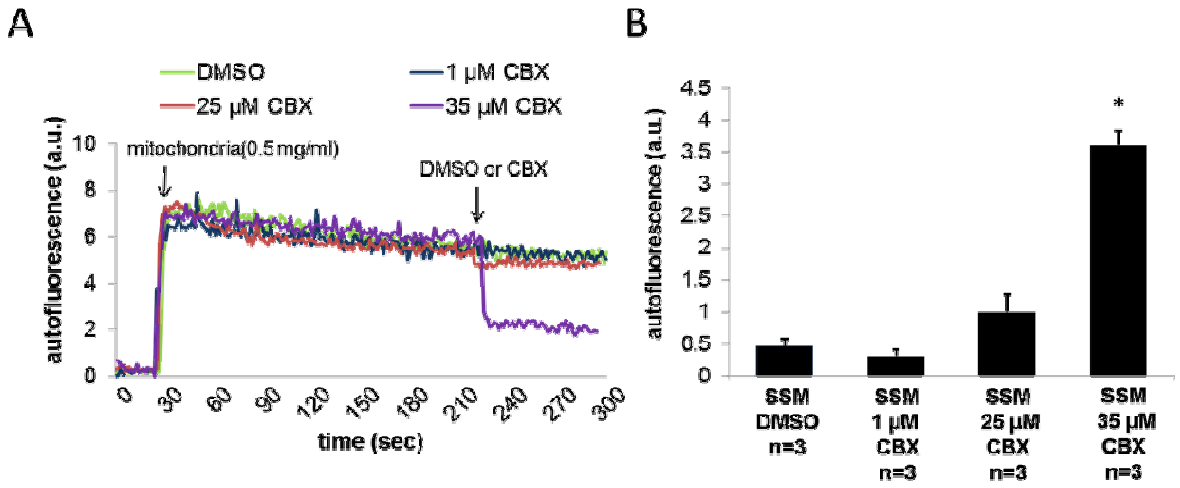

Figure 3.2: Analyses of carbenoxolone toxicity measuring mitochondrial autofluorescence. Subsarcolemmal mitochondria (SSM) were applied to cuvettes and fluorescence of NADPH (λ_{ex} 340 nm; λ_{em} 460 nm) was measured after 30 seconds. After 210 seconds, 1 µM, 25 µM, 35 µM carbenoxolone (CBX), or DMSO was applied. The decrease of fluorescence intensity indicated loss of mitochondrial membrane integrity (A). The difference of arbitrary units (a.u.) of fluorescence intensity before and after application of carbenoxolone are shown as means ± SEM of 3 replicates per group. * ($p<0.05$) indicates significant differences between groups (B).

3.1.2 Analysis of NO's impact on mitochondrial permeability

Analyses of mitochondrial permeability were performed to investigate the influence of NO donors on mitochondrial function with and without inhibition of Cx43-formed channels. Rat mitochondria were treated either with 5 µl DMSO, 1 µM or 25 µM carbenoxolone, 0.5 mM SNAP, 1 mM GSNO, or a combination of a NO donor and carbenoxolone. Fluorescence analyses were performed after exposure to 50 µM LY and 25 µg/ml RITC-dextran (Figure 3.3).

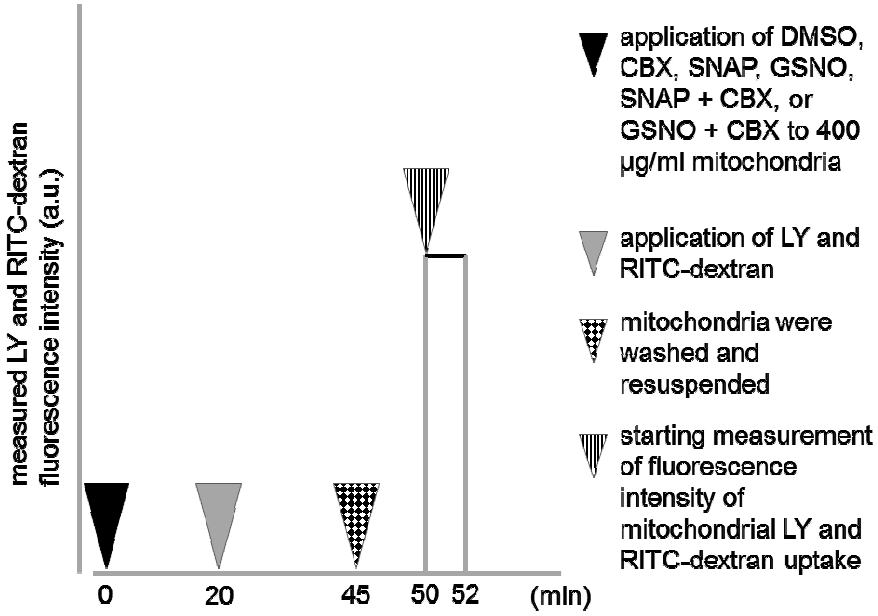

Figure 3.3: Schematic display of experimental setup for measuring mitochondrial LY dye uptake.

Mitochondrial LY fluorescence intensity was significantly increased after application of the NO donor SNAP compared to DMSO as control by 38.4 ± 9.3% (n=12, $p<0.05$). The increase in LY uptake was slightly lower in mitochondria treated with the NO donor GSNO, but still GSNO increased LY uptake by 28.1 ± 7.4% (n=12, $p<0.05$) compared to control. The NO-mediated increase in mitochondrial LY uptake was abolished in the presence of carbenoxolone, which at a concentration of 1 µM decreased LY uptake by 17.7 ± 2.9% compared to DMSO control (n=12, $p<0.05$), by 36.7 ± 2.7% (SNAP + carbenoxolone versus SNAP; n=12, $p<0.05$) compared to SNAP, and by 33.4 ± 1.8% (GSNO + carbenoxolone versus GSNO; n=12, $p<0.05$) compared to GSNO treated SSM (Figure 3.4A). The fluorescence intensity of the HC impermeant dye RITC-dextran showed no difference throughout the different treatments (n=12, p=ns) (Figure 3.4B). A concentration of 25 µM carbenoxolone caused a similar decrease of LY uptake. The LY fluorescence intensity was reduced by 17.4 ± 5.9% (n=6, $p<0.05$) in mitochondria treated with 25 µM carbenoxolone compared to DMSO control (Figure 3.4C). Mitochondrial treatment with carbenoxolone at a concentration of 25 µM did not influence the measured fluorescence intensity of RITC-dextran (Figure 3.4D).

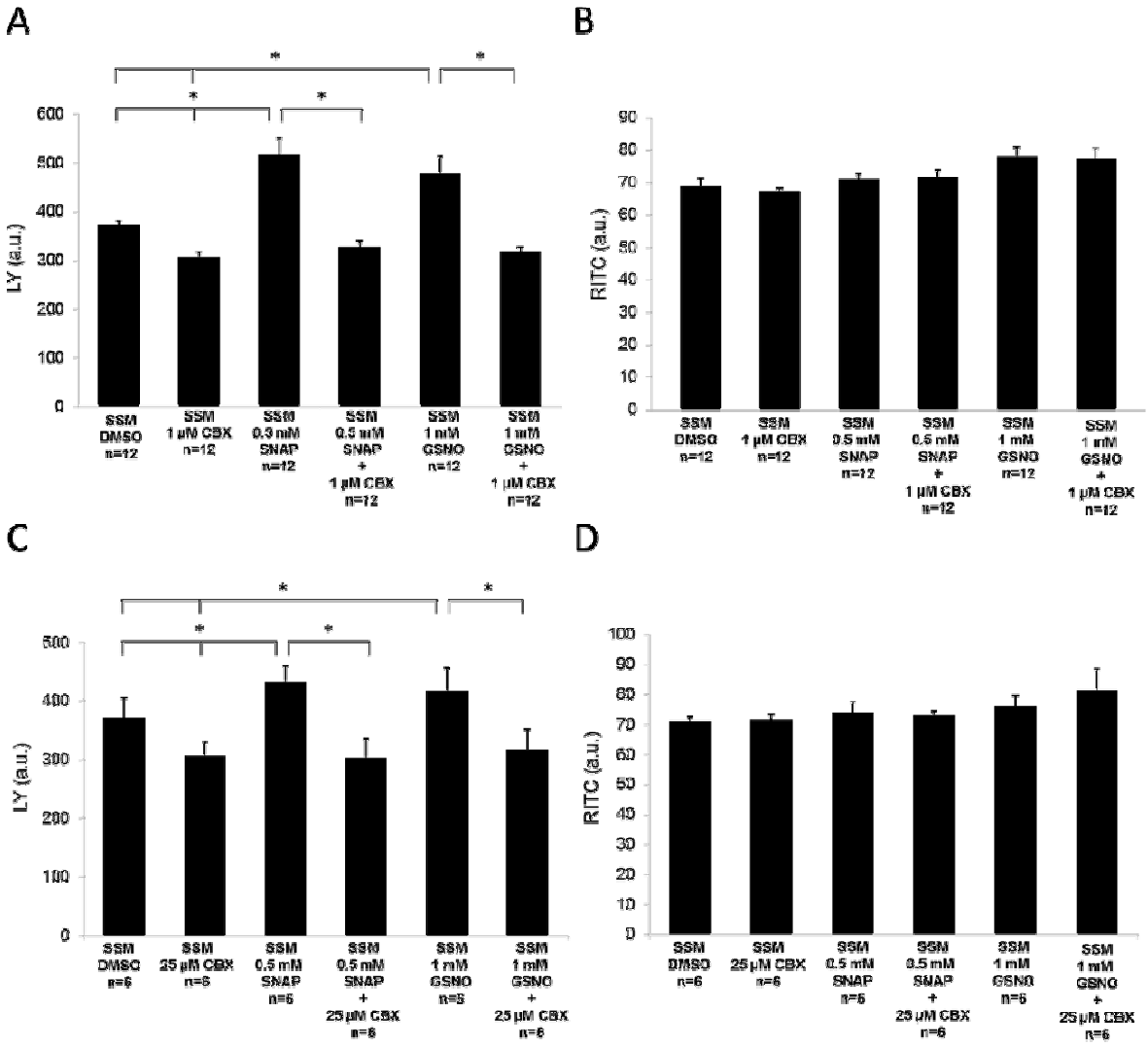

Figure 3.4: LY dye uptake of SSM. SSM were treated either with 1 µM (A+B) or 25 µM (C+D) carbenoxolone (CBX), S-nitroso-N-acetyl-DL-penicillamine (SNAP), S-nitrosoglutathione (GSNO), a combination of NO donor and hemichannel blocker (SNAP + carbenoxolone; GSNO + carbenoxolone), and dimethyl sulfoxide (DMSO; used as solvent). Dye uptake of the hemichannel permeable dye LY (A+C) and the hemichannel impermeable dye RITC-dextran (B+D) was measured and expressed as arbitrary units of fluorescence. Data are shown as mean ± SEM of 6–12 replicates per group from intact SSM. * ($p<0.05$) indicates significant differences versus marked groups.

The experiments were also performed with IFM instead of SSM. Experiments with IFM did not show an altered dye uptake between different treatment groups (n=7, p=ns) (Figure 3.5). Since IFM do not contain Cx43, these experiments support a Cx43 specific effect of increased permeability caused by SNO.

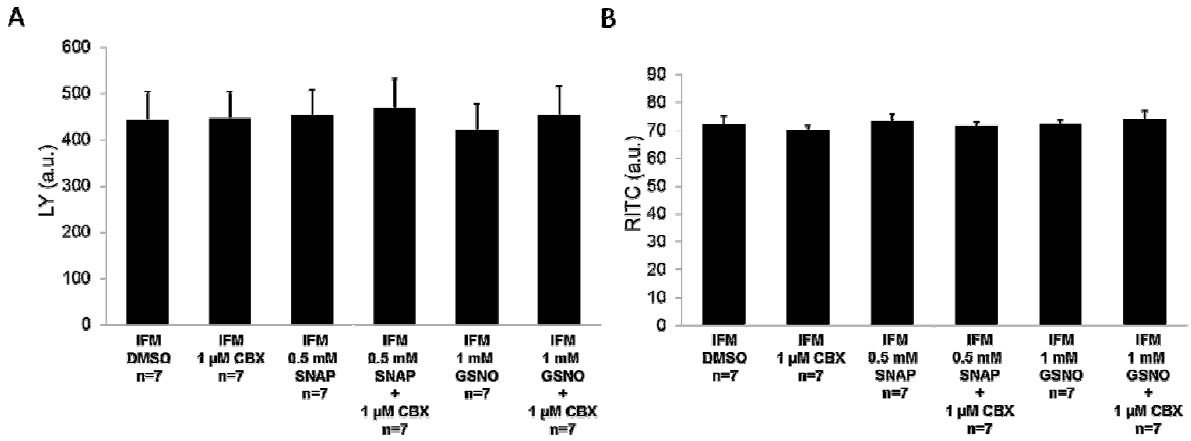

Figure 3.5: LY dye uptake of IFM. IFM were used as a negative control lacking Cx43. After treatment either with 1 µM carbenoxolone (CBX), S-nitroso-N-acetyl-DL-penicillamine (SNAP), S-nitrosoglutathione (GSNO), a combination of NO donor and hemichannel blocker (SNAP + carbenoxolone; GSNO + carbenoxolone), or dimethyl sulfoxide (DMSO; used as solvent), dye uptake of the hemichannel permeable dye LY (A) and the hemichannel impermeable dye RITC-dextran (B) was measured and expressed as arbitrary units of fluorescence. Data are shown as mean ± SEM of 7 replicates per group of IFM from rat left ventricles (LVs).

Additionally, to exclude any false positive or false negative results by agent induced accumulation of LY in membrane fragments, the experiments were also performed with ruptured SSM. SSM received an ultrasound treatment, which ruptures the mitochondrial membranes. These studies with ultrasound treated mitochondria displayed no difference in LY uptake among different treated groups (n=7, p=ns). Also in this case fluorescence intensity of RITC-dextran did not differ between the different protocols (n=7, p=ns) (Figure 3.6).

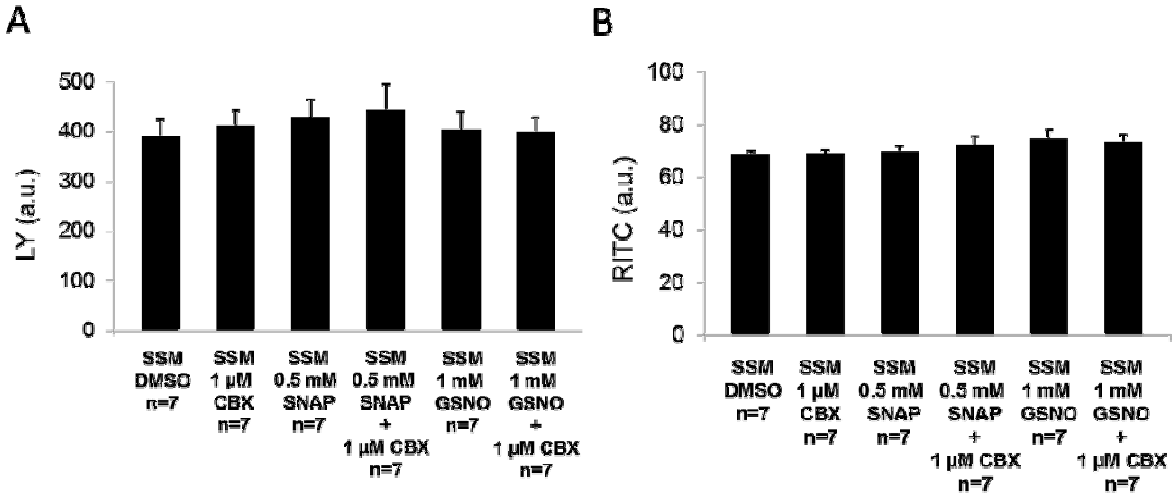

Figure 3.6: LY dye uptake of ultrasound treated SSM. SSM were either incubated with carbenoxolone (CBX), S-nitroso-N-acetyl-DL-penicillamine (SNAP), S-nitrosoglutathione (GSNO), a combination of a NO donor and hemichannel blocker (SNAP + carbenoxolone; GSNO + carbenoxolone), or dimethyl sulfoxide (DMSO; used as solvent). After incubation with LY and RITC-dextran mitochondria were ruptured by ultrasound. Possible dye interaction with membrane fragments were analyzed by measuring LY dye (A) and RITC-dextran dye (B), which were expressed as arbitrary units of fluorescence. Data are shown as mean ± SEM of 7 replicates per group of ultrasound treated mitochondria from rat LVs.

3.1.3 Mitochondrial potassium uptake

Mitochondria were incubated separately either with 1 µM, 10 µM, or 25 µM carbenoxolone, 0.5 mM SNAP, 1 mM GSNO, a combination of NO donor and carbenoxolone, or 5 µl DMSO used as a vehicle. The velocity of potassium (K^+) influx into the matrix of mitochondria from rat left ventricles was estimated by measuring the increase of the 340/380 nm fluorescence intensity ratio for 2 seconds after addition of a 140 mM KCl pulse. The potassium indicator PBFI consists of fluorophores linked to nitrogen of crown ether which confers selectivity to K^+. Upon ion binding the excitation maxima of PBFI shifts to a shorter wavelength causing a change in ratio of energy absorbed at 340/380 nm. In order to measure the K^+ permeability through Cx43 hemichannels, other mitochondrial channels including ATP-dependent potassium channels, ATP-synthase, and MPTP were blocked with glibenclamide, oligomycin, and cyclosporine A. Mitochondria treated with NO donors showed a significantly higher refilling rate of K^+. The velocity of K^+ uptake was 227.9 ± 30.1% higher in SNAP treated mitochondria compared to DMSO control (n=10, $p<0.05$).

Application of the NO donor GSNO increased the velocity of K^+ influx by 122.6 ± 28.1% (n=7, p<0.05) compared to control. The NO mediated increases of mitochondrial K^+ influx by SNAP and GSNO were significantly blocked by carbenoxolone at a concentration of 1 µM. With carbenoxolone application, velocity of K^+ influx decreased by 153.2 ± 24.4% (n=17, p<0.05) compared to DMSO control, decreased by 112.1 ± 4.5% in SNAP (SNAP + carbenoxolone versus SNAP; n=7, p<0.05), and decreased by 170 ± 4.3% (GSNO + carbenoxolone versus GSNO; n=7, p<0.05) compared to GSNO treated mitochondria (Figure 3.7). In contrast, IFM did not show alterations of K^+ influx in response to NO donors or carbenoxolone (n=7; p=ns) (Figure 3.8).

The experimental set up was proven by applying valinomycin, a K^+-specific ionophore, which transports K^+ ions through membranes following their electrochemical gradient. Among different treatment groups of mitochondria no difference in velocity of mitochondrial K^+-influx was detected for the first two seconds after application of 5 nm valinomycin conforming equal loading of PBFI dye. The measured increase of fluorescence intensity subsequent to valinomycin application confirmed integrity of mitochondrial membranes during experimental measurements (Figure 3.7C, 3.8C and 3.9C).

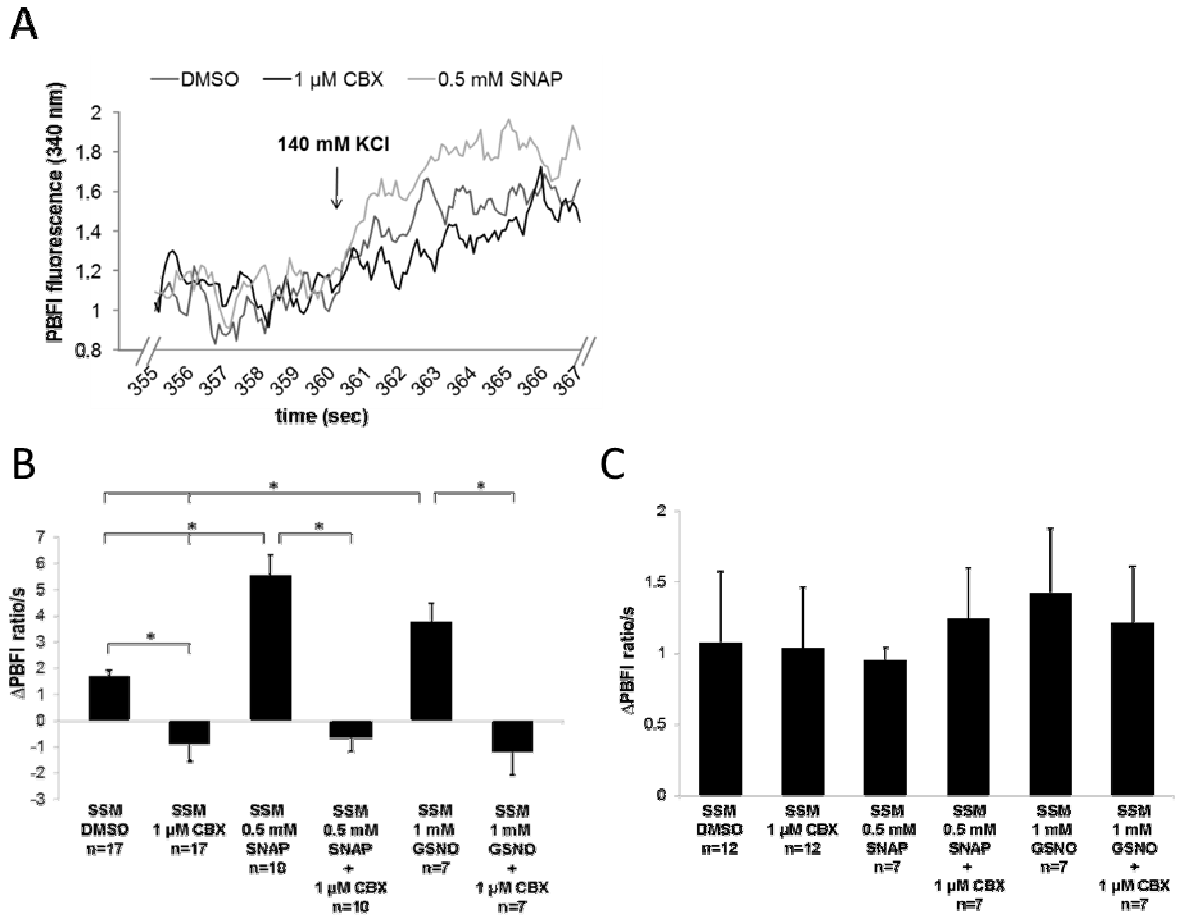

Figure 3.7: K^+ permeability of SSM. Analysis of K^+ influx was measured in SSM from the LVs of rat hearts treated either with 1 µM carbenoxolone (CBX), S-nitroso-N-acetyl-DL-penicillamine (SNAP), S-nitrosoglutathione (GSNO) a combination of NO donor and hemichannelblocker (SNAP + carbenoxolone; GSNO + carbenoxolone), or dimethyl sulfoxide (DMSO; used as solvent). The increase in the PBFI fluorescence ratio (arbitrary units) was measured after an initial KCl pulse of 140 mmol. Oligomycin, glibenclamide, and cyclosporine were present during the entire experiment to measure K^+ influx exclusively via Cx43 hemichannels (A). The rate of PBFI fluorescence ratio (340/380 nm) change from mitochondria in different treatments was estimated for the initial 2 seconds after the addition of a KCl pulse (B). Valinomycin, a K^+ transporter, was added for validation of equal PBFI loading of intact mitochondria (C). Data correspond to mean ± SEM of 6–17 replicates per group. * ($p<0.05$) indicates significant differences between marked groups.

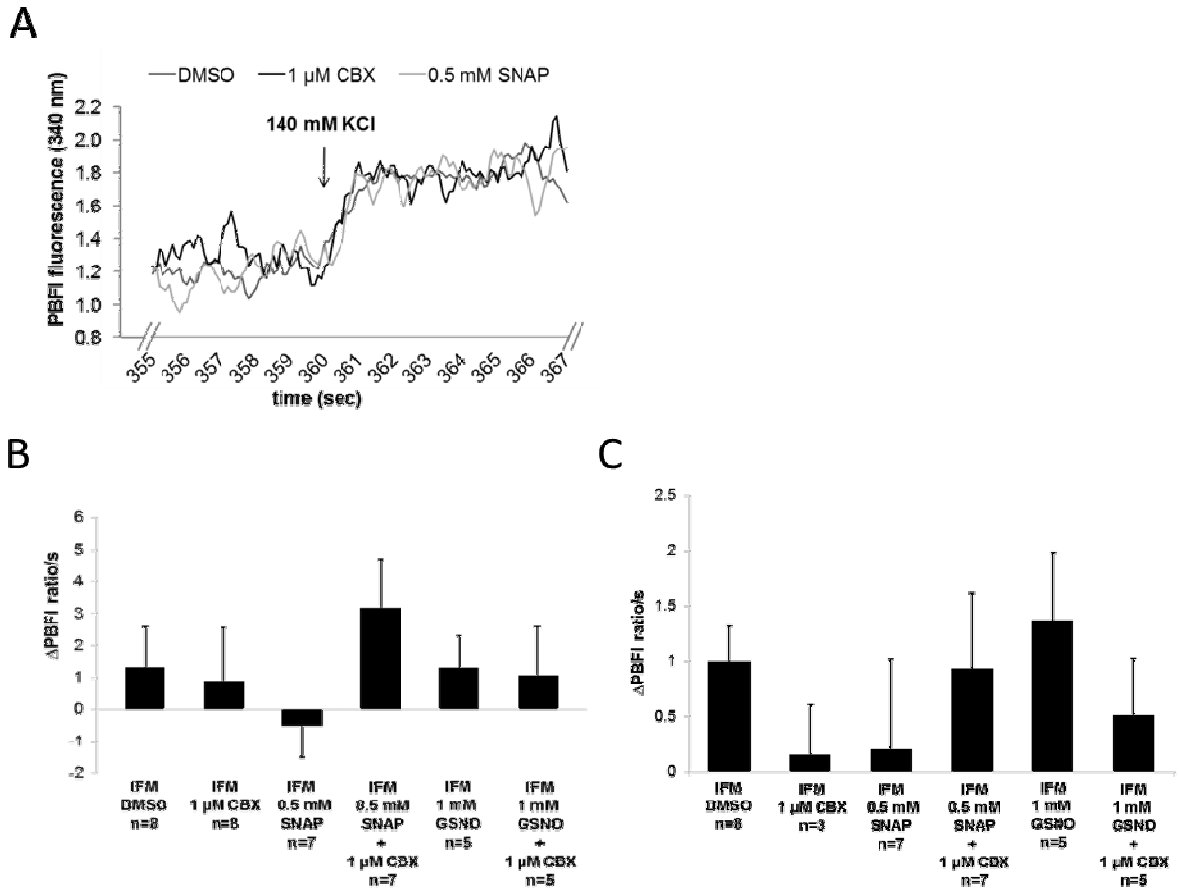

Figure 3.8: K^+ permeability of IFM. Analyses were performed with IFM to address the NO mediated increase in K^+ influx in the absence of Cx43. The increase in the PBFI fluorescence ratio (arbitrary units) was measured after an initial KCl pulse of 140 mM. Oligomycin, glibenclamide, and cyclosporine were present during the entire experiment to measure K^+ influx exclusively via Cx43 hemichannels (A). The rate of change of the PBFI fluorescence ratio (340/380 nm) from mitochondria in different treatments was estimated for the initial 2 seconds after the addition of a KCl pulse (B). Valinomycin, a K^+ transporter, was added for validation of equal PBFI loading of intact mitochondria (C). Data correspond to mean ± SEM of 5–8 replicates per group. * ($p<0.05$) indicates significant differences between marked groups.

In addition, K^+ influx was inhibited in concentrations of 10 µM carbenoxolone by 140.5 ± 34.2% compared to DMSO control (n=8, $p<0.05$) and decreased by 332.1 ± 21.6% compared to SNAP treated mitochondria (SNAP + carbenoxolone versus SNAP; n=8, $p<0.05$). With 25 µM of carbenoxolone, K^+ influx was decreased by 990.0 ± 151.2% compared to DMSO control (n=7, $p<0.05$), decreased compared to SNAP treated mitochondria by 172.5 ± 36.5% (SNAP + carbenoxolone versus SNAP; n=7, $p<0.05$) and decreased by 167.2 ± 25.5% compared to GSNO treated samples (GSNO + carbenoxolone versus GSNO; n=7, $p<0.05$) (Figure 3.9). Confirming, that carbenoxolone had a similar inhibitory effect in a concentration range from 1–25 µM.

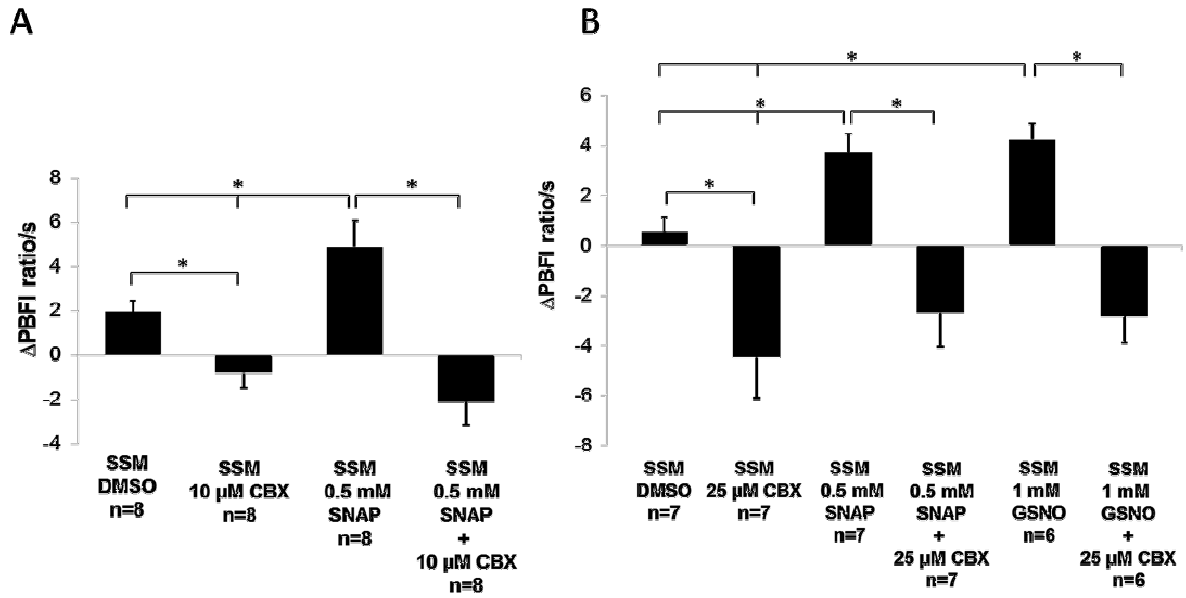

Figure 3.9: Mitochondrial K^+ permeability with 10 µM CBX. Analysis of K^+ influx was measured in SSM treated either with 10 µM carbenoxolone (CBX) (A), or 25 µM carbenoxolone (B), S-nitroso-N-acetyl-DL-penicillamine (SNAP), S-nitrosoglutathione (GSNO), a combination of NO donor and hemichannelblocker (SNAP + carbenoxolone; GSNO + carbenoxolone), or dimethyl sulfoxide (DMSO; used as solvent). The increase in the PBFI fluorescence ratio (arbitrary units) was measured after an initial KCl pulse of 140 mmol. Oligomycin, glibenclamide, and cyclosporine were present during the entire experiment. The rate of PBFI fluorescence ratio (340/380 nm) change from mitochondria was estimated for the initial 2 seconds. Data correspond to mean ± SEM of 6–8 replicates per group. * ($p<0.05$) indicates significant differences between marked groups.

SNO mediated K^+ influx through Cx43 hemichannels was also measured without additional mitochondrial channel blockers. The data showed a NO mediated increase of K^+ influx, which was weaker with SNAP versus DMSO (138.9 ± 30.7%, n=7, $p<0.05$) compared with SNAP versus DMSO with additional mitochondrial channel blockers. GSNO also increased K^+ permeability compared to control (119.7 ± 16.0%, n=7, $p<0.05$) as was the case in experiments where the K^+ permeability for Cx43 HCs was measured in the presence of inhibitors. The NO mediated increase of K^+ influx was blocked by carbenoxolone (154.6 ± 10.1% for 0.5 mM SNAP with 1 µM carbenoxolone and 103.8 ± 25.2% for 1 mM GSNO with 1 µM carbenoxolone; n=7, $p<0.05$) (Figure 3.10).

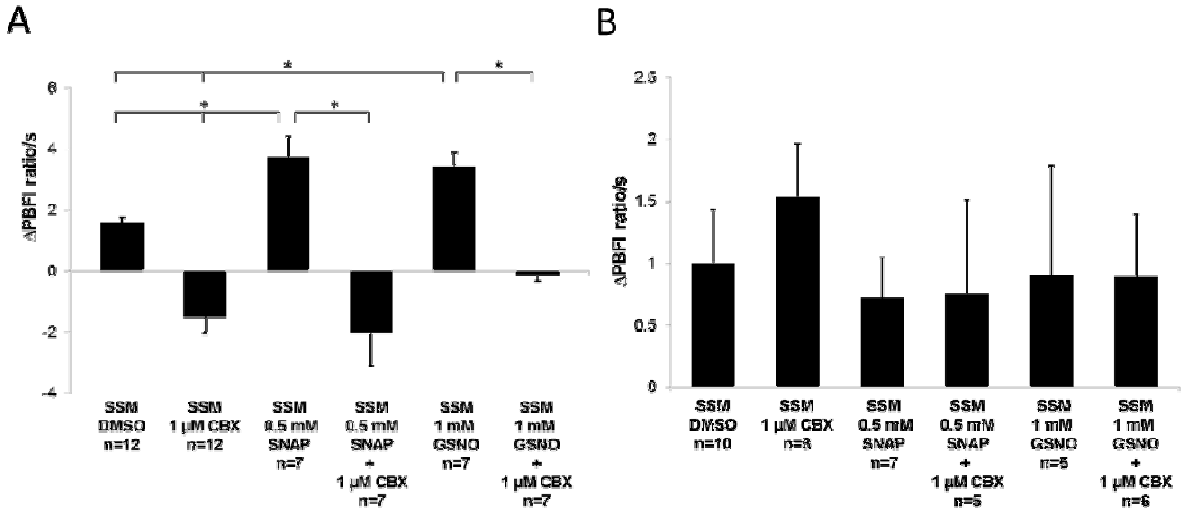

Figure 3.10: Mitochondrial K^+ permeability with 25 µM CBX. Analysis of K^+ influx under physiological conditions was measured without adding additional mitochondrial channel blockers to SSM from LVs of rat hearts (A). Mitochondria were either treated with carbenoxolone (CBX), S-nitroso-N-acetyl-DL-penicillamine (SNAP), S-nitrosoglutathione (GSNO), a combination of NO donor and hemichannel blocker (SNAP + carbenoxolone; GSNO + carbenoxolone), or dimethyl sulfoxide (DMSO; used as solvent). The increase in the PBFI fluorescence ratio of 340/380 nm (arbitrary units) was measured for 2 seconds after an initial KCl pulse of 140 mM. The K^+ transporter valinomycin was added for validation of equal PBFI loading and confirming integrity of mitochondrial membranes (B). Data correspond to mean ± SEM of 6–12 replicates per group. * ($p<0.05$) indicates significant differences between marked groups.

3.1.4 Mitochondrial sodium uptake

Permeability for Na^+ was measured using sodium binding benzoflur (SBFI). The sodium sensitive indicator functions similarly to PBFI. Mitochondrial sodium influx was calculated based on an extinction shift and estimated by calculation of a 340 nm/380 nm ratio. Mitochondrial Na^+ was depleted and then measurements were performed at 340 nm and 380 nm in a fluorometer with high sensitivity. Velocity of mitochondrial Na^+ influx was estimated after a sodium chloride pulse of a physiological concentration of 10 mM and after an application of 140 mM sodium chloride. Additional inhibitors for MPTP, ATP-synthase, and ATP-dependent potassium channels were supplemented to strengthen a Cx43 hemichannel dependent effect. Measurements performed in isolation buffer under steady state IV conditions at 340 nm (Figure 3.11A) and 380 nm (Figure 3.11B) showed no relevant mitochondrial sodium influx after treatment either with 1 µM carbenoxolone, 0.5 mM SNAP, 1 mM GSNO, a combination of NO donor and carbenoxolone, or 5 µl DMSO.

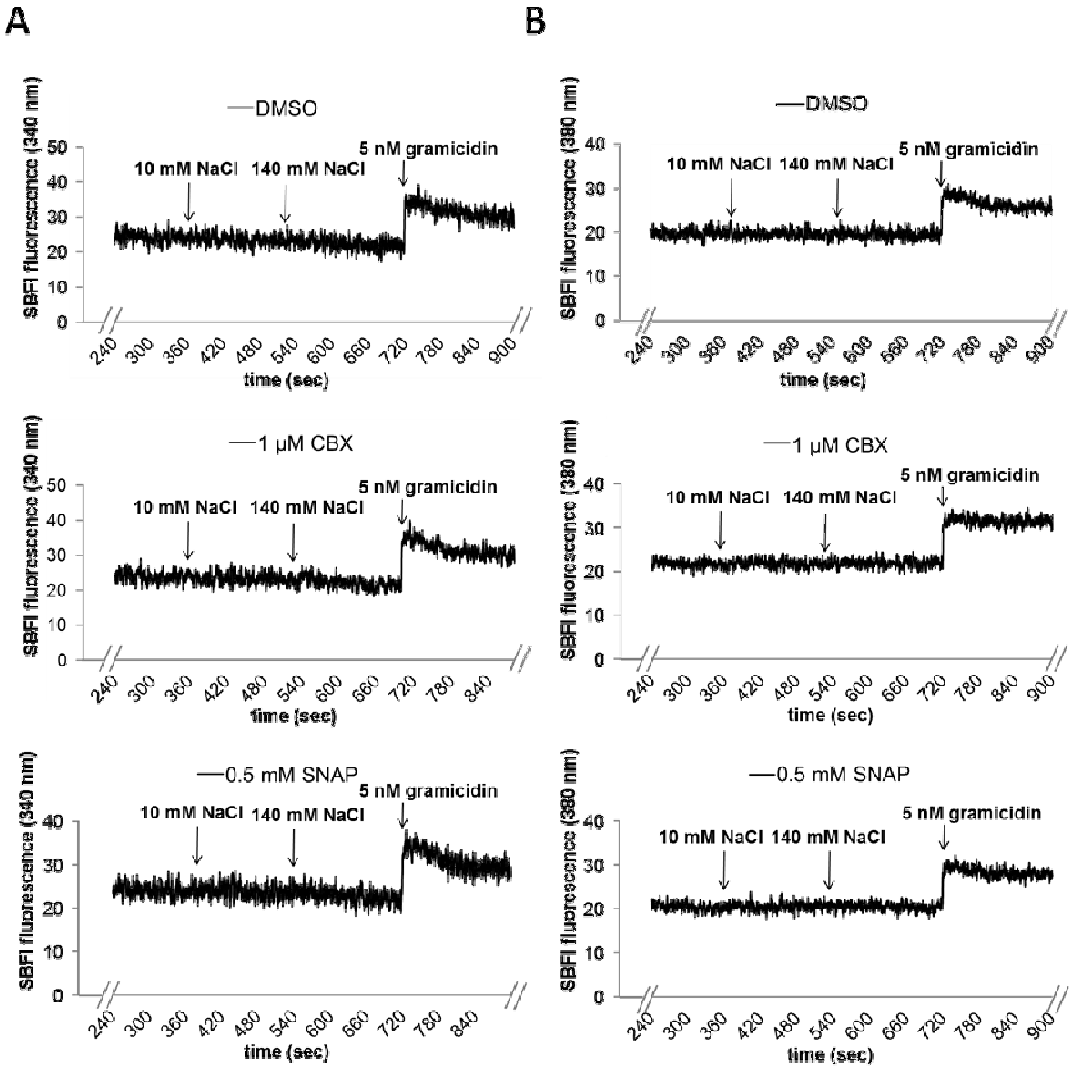

Figure 3.11: Mitochondrial sodium (Na^+) permeability. Na^+ influx was measured in isolated subsarcolemmal mitochondria (SSM) from the left ventricles of rat hearts. Mitochondria were treated either with carbenoxolone (CBX), S-nitroso-N-acetyl-DL-penicillamine (SNAP), S-nitrosoglutathione (GSNO) a combination of a NO donor and hemichannel blocker (SNAP + carbenoxolone; GSNO + carbenoxolone), or dimethyl sulfoxide (DMSO; used as solvent). Measurements were performed in isolation buffer supplemented with oligomycin, glibenclamide, and cyclosporine A inhibiting the mitochondrial channels, MPTP, ATP-synthase, and ATP-dependent potassium channels to increase the effect of Cx43 hemichannel permeability. The intensity of SBFI fluorescence was measured from mitochondria in different treatments (here representative shown for DMSO, carbenoxolone, and SNAP) at excitations of 340 nm (A) and 380 nm (B) during the addition of 10 mM and 140 mM sodium chloride (NaCl) pulses, as well as application 5 nM gramicidin used as control. Data for mitochondrial Na^+ permeability was not analyzed for the 5 replicates per group, because of the lack of Na^+ influx.

Application of 5 nM gramicidin led to a Na^+ influx with a non-differing velocity among treatment groups which confirmed sufficient and equal mitochondrial SBFI loading (Figure 3.17).

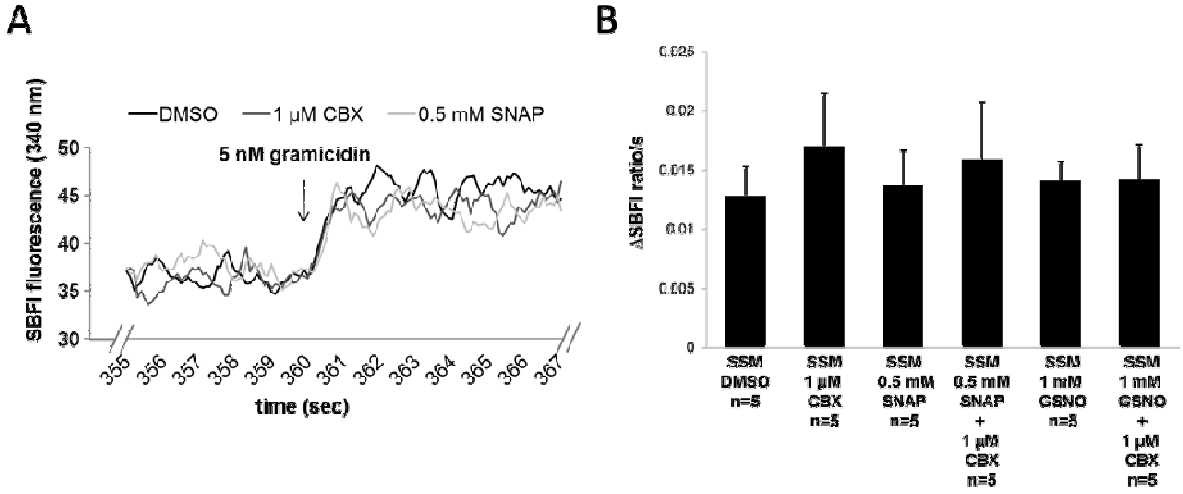

Figure 3.12: Mitochondrial sodium (Na^+) influx using a Na^+ transporter. The experimental set up of Na^+ influx measurements was controlled by application of 5nM Na^+ transporter gramicidin after application of Na^+ pulses (A). The rate of SBFI fluorescence ratio (340/380 nm) change from mitochondria in different treatments was estimated for the initial 2 seconds after the addition of gramicidin (B). Data correspond to mean ± SEM of 5 replicates per group.

The experiments were also performed in succinate buffer under energized conditions with rotenone inhibiting complex I favoring complex II respiration. The Na^+ influx was analyzed for 2 seconds after a 10 mM and a 140 mM sodium chloride pulse (Figure 3.13). With the 140 mM pulse, mitochondrial Na^+ influx was highly increased in succinate buffer compared to the experiments performed under steady state IV conditions. Between groups only non-significant changes in Na^+ fluxes were measured (n=6, p=ns). Overall, only low Na^+ fluxes were measured compared to the measurements of K^+ fluxes suggesting that mitochondrial Cx43 HCs have certain ion selectivity.

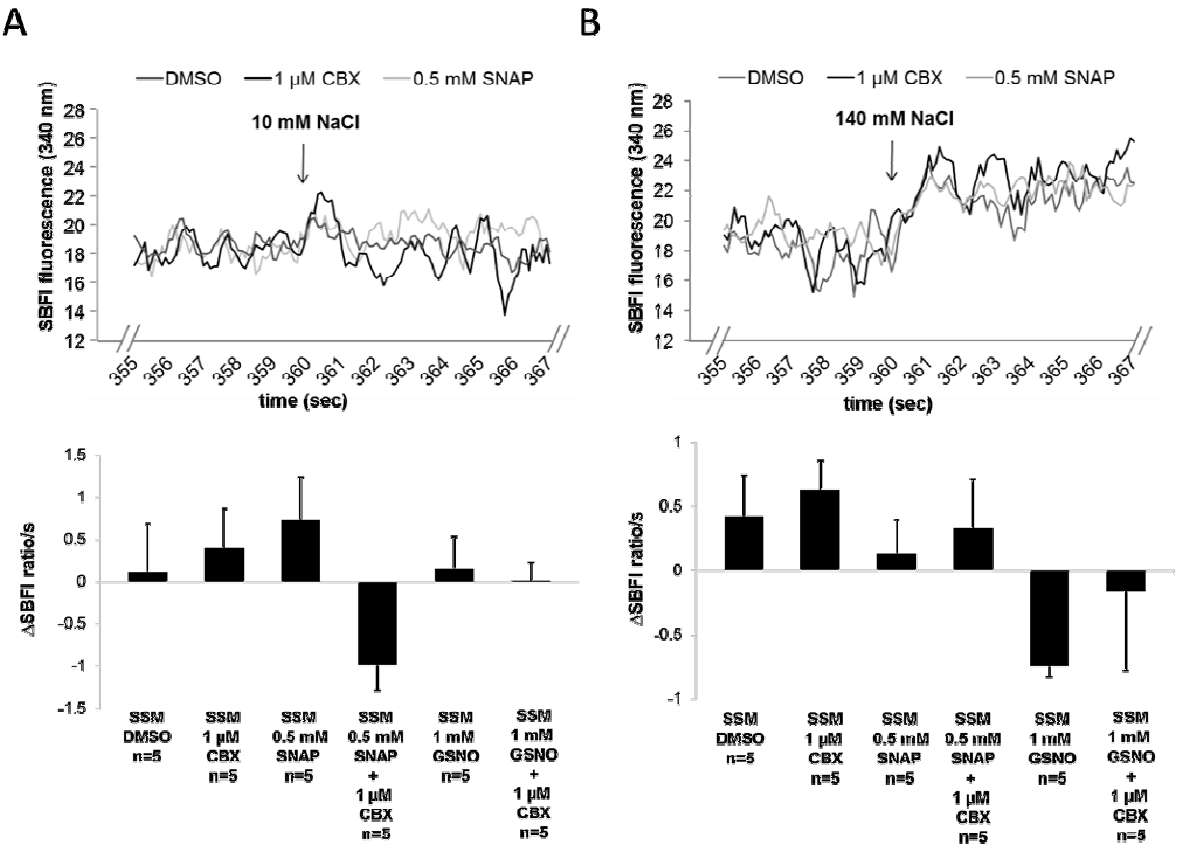

Figure 3.13: Mitochondrial sodium (Na^+) permeability during complex II respiration. Subsarcolemmal mitochondria (SSM) were isolated from the left ventricles of rat hearts and either treated with carbenoxolone (CBX), S-nitroso-N-acetyl-DL-penicillamine (SNAP), S-nitrosoglutathione (GSNO), a combination of a NO donor and hemichannel blocker (SNAP + carbenoxolone; GSNO + carbenoxolone), or dimethyl sulfoxide (DMSO; used as solvent). Measurements were performed in succinate buffer. Specificity of Cx43 hemichannel permeability was increased in the measurements by supplementing oligomycin, glibenclamide, and cyclosporine A through inhibiting of mitochondrial channels, MPTP, ATP-synthase, and ATP-dependent potassium channels. The rate of SBFI fluorescence ratio (340/380 nm) change from mitochondria in different treatments was measured during the addition of 10 mM (A) and 140 mM (B) sodium chloride (NaCl) pulses. The fluorescence increase was analyzed for the first two seconds following to the pulse. Data correspond to mean ± SEM of 5 replicates per group.

The gramicidin induced Na^+ influx did not differ between treatment groups of mitochondria also in case of experiments performed in succinate buffer favoring mitochondrial complex II respiration (Figure 3.14).

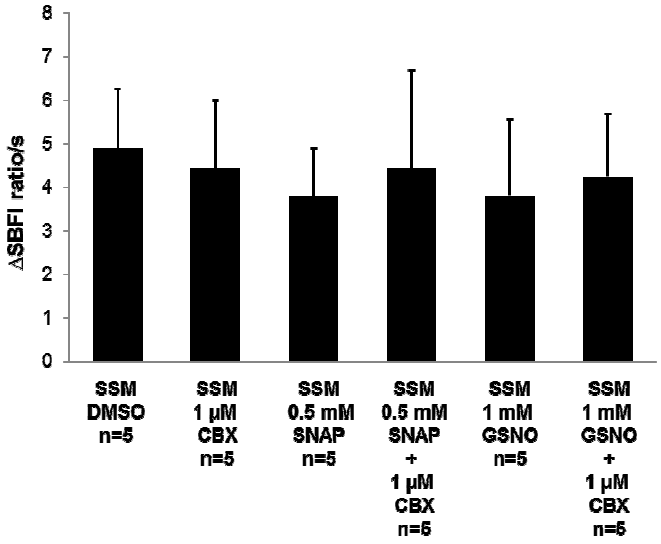

Figure 3.14: Control of mitochondrial SBFI loading. Equal SBFI loading of different subsarcolemmal mitochondrial (SSM) treatment groups (details, see text) was controlled by measuring sodium influx after application of 5 nM sodium transporter gramicidin. The rate of SBFI fluorescence ratio (340/380 nm) change from mitochondria in different treatments was estimated for the initial 2 seconds after the addition of gramicidin. Data correspond to mean ± SEM of 5 replicates per group.

3.1.5 ROS production

Endothelial NOS docks to the mitochondrial outer membrane producing local NO [94], therefore, whether or not NO can regulate ROS via SNO of mitochondrial Cx43 is of interest. Mitochondrial ROS production was measured with 25 µM carbenoxolone, 0.5 mM SNAP, 1 mM GSNO, a combination of NO donor and carbenoxolone, or 20 µl dH_20. ROS production was measured with glutamate/malate as a substrate for complex 1 respiration with ADP stimulation. The application of NO donor SNAP enhanced ROS formation by 22.9 ± 1.8% (n=9, $p<0.05$) compared to control. Application of NO donor GNSO led to an increase of ROS production by 40.6 ± 7.1% (n=9, $p<0.05$) compared to control. The NO mediated increases were abolished by application of 25 µM carbenoxolone (Figure 3.15A). Antimycin A blockades the electron transfer form coenzyme Q to cytochrome C at respiration chain complex III, thus leading to circulation of electrons between complex I and complex III causing maximal ROS formation. Therefore antimycin A was used as a

control and was applied at the end of baseline ROS formation measurements. After antimycin A application ROS formation was increased approximately by 6–12 times compared to baseline ROS generation. After antimycin A application, in samples receiving GSNO, ROS formation was significantly reduced by 44.2 ± 7.7% (n=9, p<0.05) compared to other treatment groups (Figure 3.15B).

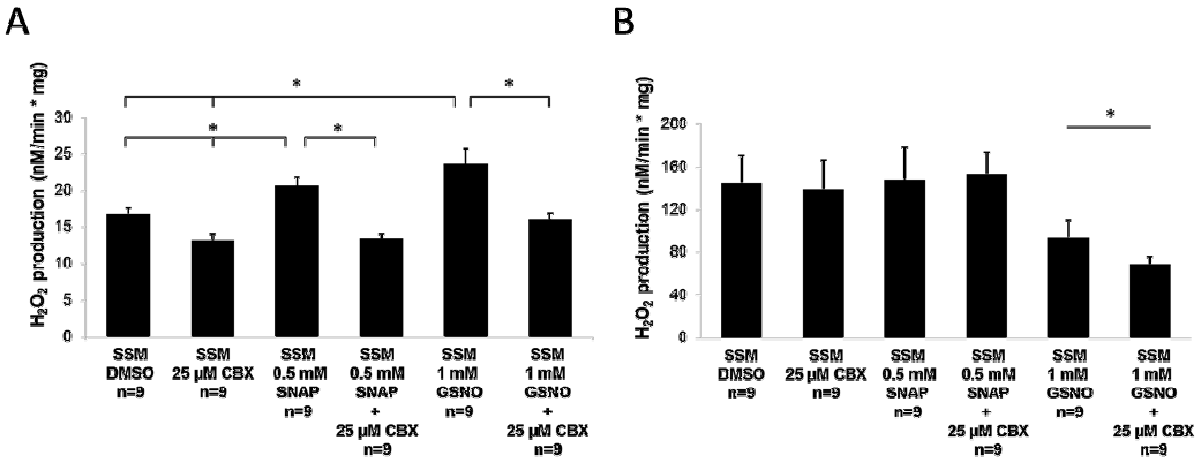

Figure 3.15: Nitric oxide influence on ROS formation (H_2O_2 production) of subsarcolemmal mitochondria (SSM). Measurements of ROS generation (H_2O_2 production) were performed on freshly isolated SSM treated with carbenoxolone (CBX), S-nitroso-N-acetyl-DL-penicillamine (SNAP), S-nitrosoglutathione (GSNO), a combination of a NO donor and hemichannel blocker (SNAP + carbenoxolone; GSNO + carbenoxolone), or dH_2O. Mitochondrial H_2O_2 production was measured during ADP stimulated complex 1 respiration for 4 minutes and the increase of H_2O_2 was expressed in nM/min/mg protein by comparing the data to a standard curve (A). Subsequently, antimycin A was added for measuring maximal mitochondrial ROS production serving as a positive control (B). Data correspond to mean ± SEM of 9 replicates per group. * (p<0.05) indicates significant differences between marked groups or significant difference between marked and non-marked groups.

IFM were used to validate Cx43-dependent increases of ROS formation due to NO. Application of NO donors in IFM decreased ROS production. SNAP decreased ROS formation by 14.4 ± 4% (n=9, p<0.05) compared to control and GSNO by 13.8 ± 4%, n=9, p<0.05) compared to control. Carbenoxolone had no significant inhibitory effect on ROS production with ADP stimulated complex 1 respiration (n=9, p=ns) (Figure 3.16).

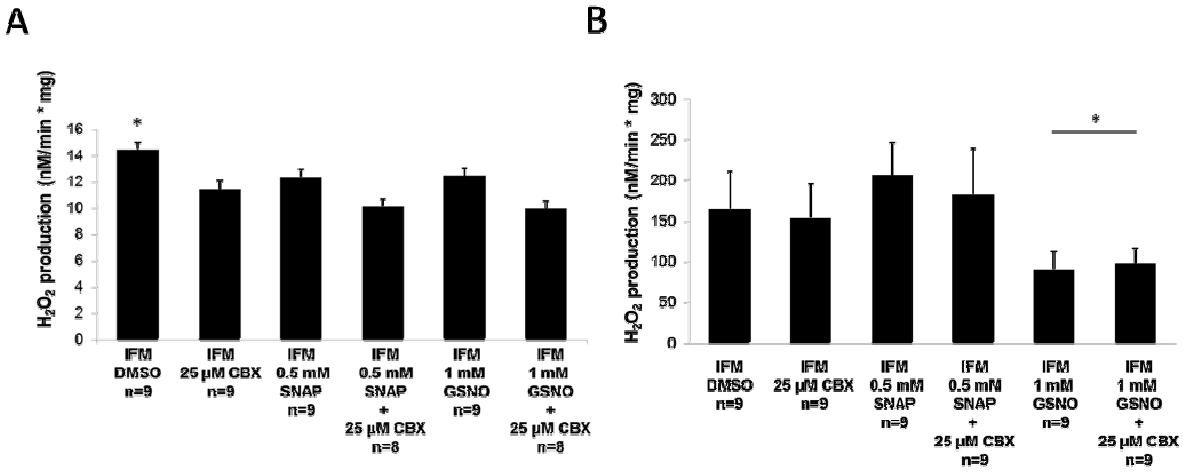

Figure 3.16: Nitric oxide influence on ROS formation (H_2O_2 production) of interfibrillar mitochondria (IFM). Measurements of ROS generation was performed on freshly isolated IFM treated with carbenoxolone (CBX), S-nitroso-N-acetyl-DL-penicillamine (SNAP), S-nitrosoglutathione (GSNO), a combination of a NO donor and hemichannel blocker (SNAP + carbenoxolone; GSNO + carbenoxolone), or dH_2O. Mitochondrial H_2O_2 production was measured during ADP stimulated complex 1 respiration for 4 minutes and the increase of H_2O_2 was expressed in nM/min/mg protein by comparing the data to a standard curve (A). Subsequent antimycin A was added for measuring maximal mitochondrial ROS production serving as a positive control (B). Data correspond to mean ± SEM of 9 replicates per group. * ($p<0.05$) indicates significant differences between marked and unmarked groups.

The impact on mitochondrial ROS generation of 1 µM GSNO or 48 nM GSNO was investigated. Again, mitochondrial ROS production was increased by 20 ± 3.7% (n=16, $p<0.05$) in samples treated with 1 µM GSNO compared to control and 50 nM GSNO increased mitochondrial ROS formation by 14.3 ± 2.8 (n= 13, $p<0.05$) compared to control.

The Cx43 mimetic peptide Gap26 binds to the first extracellular loop of Cx43, thereby inhibiting Cx43 HC opening [288], whereas carbenoxolone inhibits formation of Cx43-formed channels [70]. Mitochondria treated with Gap26 showed no alterations in baseline ROS formation, but Gap26 abolished the NO induced increase in ROS formation. In Gap26 treated SSM the ROS formation was decreased about 14.3 ± 2.8 (n= 13, $p<0.05$) compared to GSNO treated mitochondria (Figure 3.17).

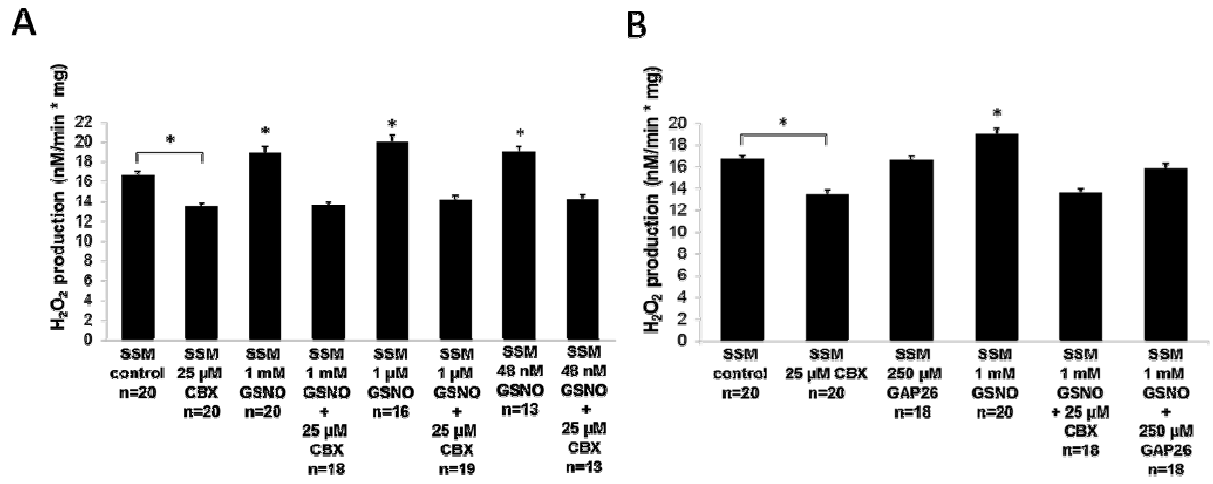

Figure 3.17: Low concentration nitric oxide influence on ROS formation (H_2O_2 production) of subsarcolemmal mitochondria (SSM). Measurements of ROS generation were also performed on freshly isolated SSM with low concentrations (1 µM and 48 nM) of S-nitrosoglutathione (GSNO) (A), and additional experiments were performed with Cx43 mimetic peptide GAP26, an inhibitor of Cx43 hemichannels or carbenoxolone (CBX). Mitochondrial H_2O_2 production was measured during ADP stimulated complex 1 respiration and was expressed in nM/min/mg protein. Data correspond to mean ± SEM of 13–20 replicates per group. * ($p<0.05$) indicates significant differences between marked groups or significant difference between marked and unmarked groups.

Additionally ROS measurements were performed with the respiratory complex I inhibitor rotenone. Inhibition of complex I lead to increased formation of the primary electron donor ubisemiquinone. The present data show increased mitochondrial ROS formation after rotenone application. However, mitochondrial ROS formation did not differ in the presence of rotenone in different mitochondrial treatment groups (n=6, p=ns) and the NO mediated increase of ROS formation was abolished (Figure 3.18).

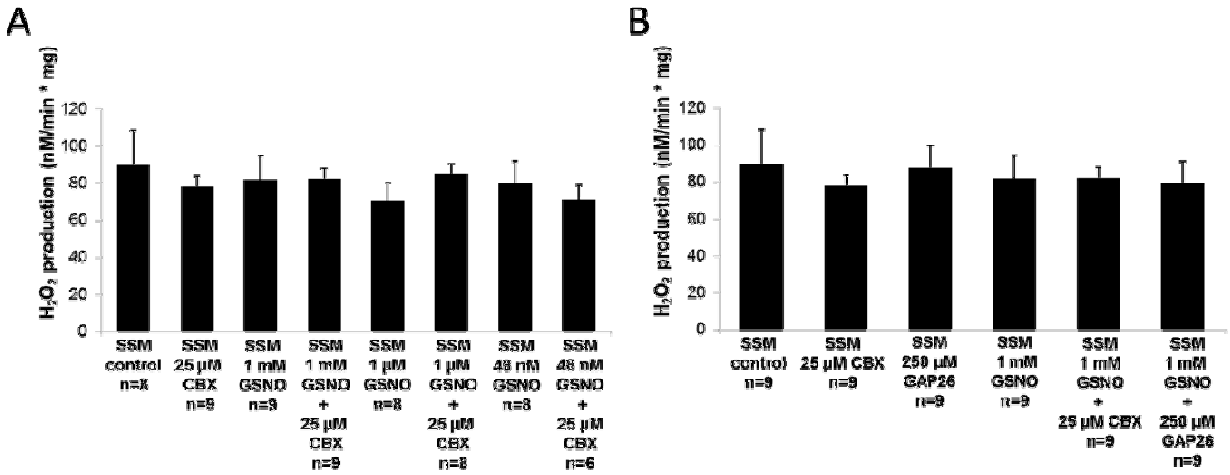

Figure 3.18: Nitric oxide influence on ROS formation (H_2O_2 production) of subsarcolemmal mitochondria (SSM) with inhibition of respiration chain complex I. Measurements of ROS generation were performed on SSM in the presence of respiration chain complex I inhibitor rotenone (A and B). Mitochondrial H_2O_2 production was measured during ADP stimulated complex 1 respiration and was expressed in nM/min/mg protein. Data correspond to mean ± SEM of 6–9 replicates per group.

The respiratory chain uncoupling agent FCCP, which inhibits mitochondrial membrane potential, was used as a negative control. Application of FCCP significantly decreased ROS formation, and ROS generation did not differ between different treatment groups (Figure 3.19).

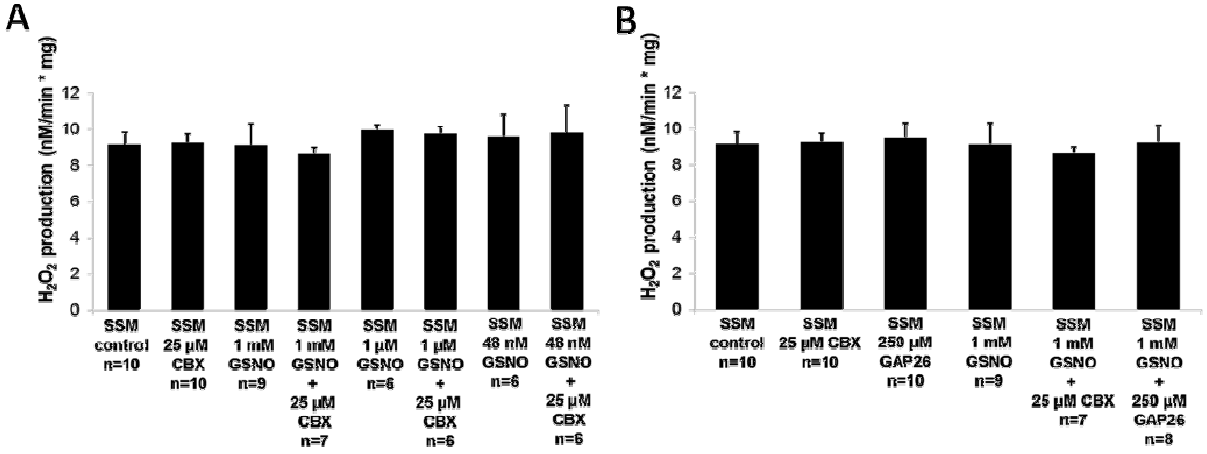

Figure 3.19: Nitric oxide influence on ROS formation (H_2O_2 generation) of subsarcolemmal mitochondria (SSM) with respiration chain uncoupling. Measurements of ROS generation were also performed on SSM in the presence of respiration chain uncoupler FCCP (A and B). Mitochondrial H_2O_2 production was measured during ADP stimulated complex 1 respiration and was expressed in nM/min/mg protein. Data correspond to mean ± SEM of 6–10 replicates per group.

3.1.6 Quantification of SNO modified mtCx43 after NO donor application

SNO quantification analyses were performed on mitochondria isolated by density gradient ultracentrifugation. Purity of mitochondrial preparation was determined by the absence of immunoreactivity for antibodies directed against markers of the plasma membrane (Na^+/K^+-ATPase), sarcoplasmic reticulum (SERCA2 ATPase), nucleus (HDAC), cytosol (GAPDH) and enrichment of mitochondrial proteins (TOM20 and MnSOD) (Figure 3.20A). A modified biotin switch method was utilized for labeling SNO modified proteins with biotin (BIAM) (Figure 3.20B). Following precipitation and Western blot analysis, intensity of the 43 kDa bands representing SNO-modified mtCx43 was significantly increased in mitochondria incubated with NO donors. Samples treated with GSNO, SNAP, or a combination of a NO donor and Cx43 HC blocker carbenoxolone showed an increase in SNO modifications of mtCx43 in average by 109.2 ± 21.5% ($n=7$, $p<0.05$) compared to mitochondria not treated with a NO donor (Figure 3.20C,D and E). The reason for applying the HC blocker carbenoxolone was to exclude it's NO interfering properties. Additionally as a control, DTT was applied to NO donor treated and biotin labeled samples to break disulfide bounds confirming specificity of the biotin switch method. In samples treated with 100 mM DTT the Cx43 band was not present or was highly reduced (Figure 3.20D). In mitochondria treated with 10 mM DTT and the NO donor SNAP the amount of SNO modified mtCx43 was significantly reduced by 59.7 ± 7.6% compared to NO treated samples and reduced by 15.8 ± 7.8% ($n=7$, $p<0.05$) compared to untreated samples (Figures 3.20C and 3.20E).

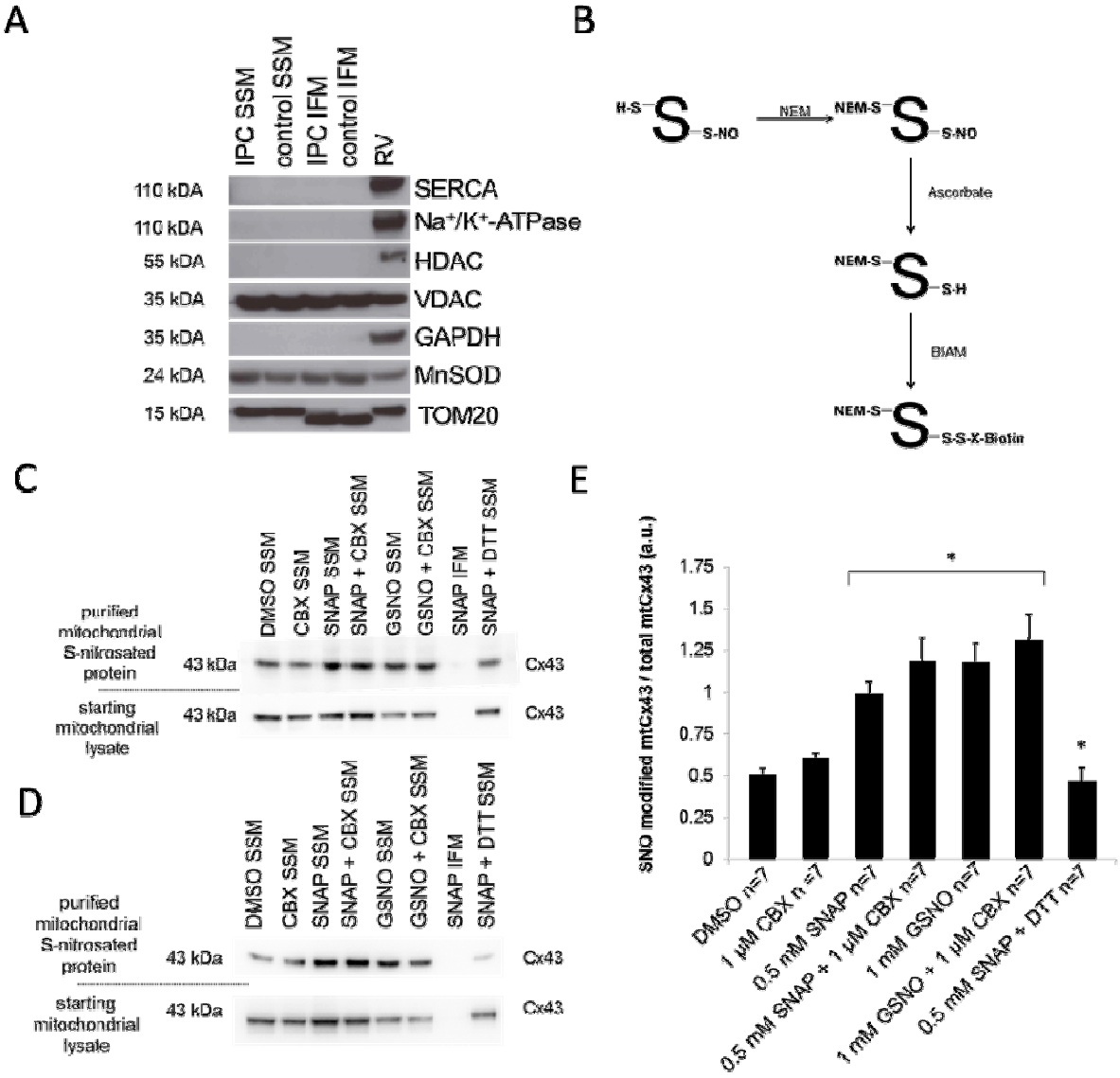

Figure 3.20: Quantification of SNO modified mtCx43 for nitric oxide treated mitochondria. SNO quantification was performed on mitochondria treated either with carbenoxolone (CBX), S-nitroso-N-acetyl-DL-penicillamine (SNAP), S-nitrosoglutathione (GSNO), a combination of NO donor and hemichannel blocker (SNAP + carbenoxolone; GSNO + carbenoxolone), or dimethyl sulfoxide (DMSO; used as solvent). Purity of subsarcolemmal mitochondria (SSM) and interfibrillar mitochondria (IFM) preparations was determined by the absence of immunoreactivity for antibodies directed against cellular markers and enrichment of mitochondrial proteins (A). Using a modified biotin switch method, SNO modified cysteine residues of mitochondrial proteins were labeled with biotin (B). Subsequent to precipitation of biotin labeled SNO modified proteins, Western blot analyses were performed for mtCx43 (C+D). Biotin labeled mitochondria were treated with 10 mM DTT (C) or 100 mM DTT (D) for validation of the specificity of the biotin switch method. Band signal intensity of purified SNO modified mtCx43 was normalized to a loading control taken from the starting mitochondrial lysate, representing the total amount of loaded mtCx43. * ($p<0.05$) indicates significant difference to unmarked groups. Results are expressed as mean ± SEM of 7 replicates per group (E).

3.1.7 Identification of mtCx43 phosphorylation induced by NO

Changes in mtCx43 phosphorylation status, which can also affect HC open probability, were analyzed subsequent to NO donor exposure and addition of HC blocker carbenoxolone. SSM were incubated either with 1 µM carbenoxolone, 0.5 mM of NO donor SNAP, 1 mM of NO donor GSNO, a combination of a NO donor and carbenoxolone, or 5 µl DMSO used as a vehicle. The Western blot analysis showed only changes in mtCx43 phosphorylation for serine residue 365 (pS365) in response to administration of NO donor SNAP. MtCx43's pS365 was tendentially increased by 71.4 ± 33.4% (n=4, p=ns) in SNAP treated samples compared to the control group (Figure 3.21B). Phosporylation of the Cx43 epitopes S368 and S373 were not altered among different treatment groups (n=4, p=ns) (Figure 3.21B and 3.21C).

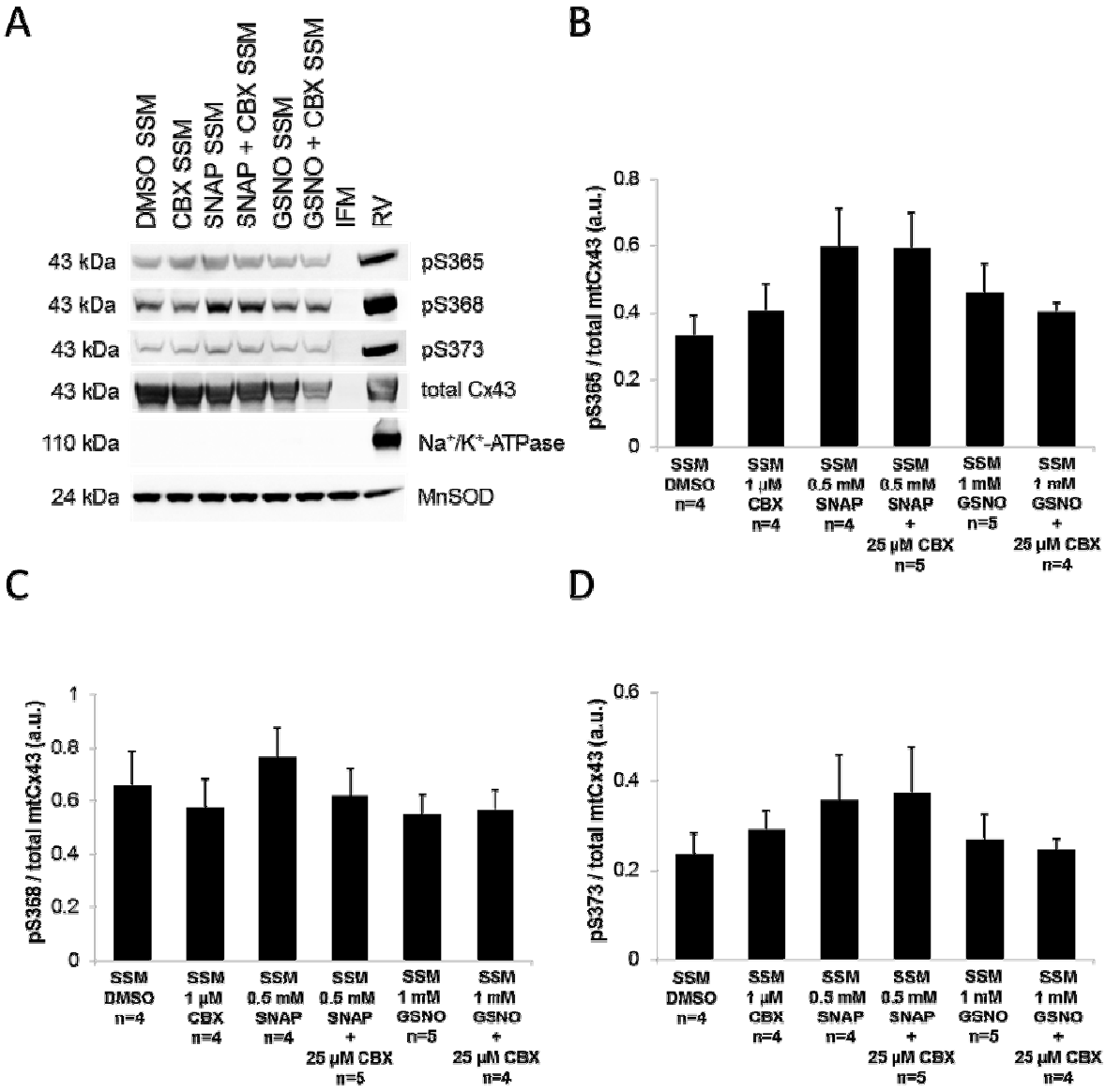

Figure 3.21: Western blot analyses of Cx43 serine phosphorylation. Subsarcolemmal mitochondria (SSM) treated either with carbenoxolone (CBX), S-nitroso-N-acetyl-DL-penicillamine (SNAP), S-nitrosoglutathione (GSNO), a combination of a NO donor and the hemichannel blocker (SNAP + carbenoxolone; GSNO + carbenoxolone), or dimethyl sulfoxide (DMSO; used as solvent) were isolated by Percoll gradient ultracentrifugation. Purity of preparations was determined by the absence of immunoreactivity for antibodies directed against markers of the plasma membrane (Na^+/K^+-ATPase) and increase of mitochondrial protein (MnSOD). Band intensity of Cx43 phosphorylated serine residues S365 (pS365), S368 (pS368), and S373 (pS373) were normalized to total mtCx43 (A). Relative amount of serine phosphorylation was quantified and expressed as a ratio normalized to total mtCx43 ratio (B-D). * ($p<0.05$) indicates a significant difference in comparison with unmarked groups. Results are expressed as mean ± SEM of 4–5 replicates per group.

3.2 The link between SNO of mtCx43 and the signal transduction cascade of preconditioning

In order to identify a link between SNO of mtCx43 and the signal transduction cascade of cardioprotection, preconditioned mitochondria were analyzed for the rate of dye permeability and the amount of posttranslational SNO modification of mtCx43. Additionally, proteomic approaches were used to identify SNO modified cysteine residues.

3.2.1 Analysis of mitochondrial dye permeability after IPC

The dye permeability of mitochondria receiving IPC was analyzed to support a possible link between SNO of mtCx43 and the signal transduction cascade of cardioprotection. Therefore, SSM were isolated from the LV of rat hearts, which received IPC or were control perfused in Langendorff experiments. Following incubation with 50 µM of the HC permeable dye LY or 25 µg/ml of the HC impermeable dye RITC-dextran, mitochondria receiving IPC showed a 13 ± 4.6% higher LY fluorescence intensity (n=4, $p<0.05$) compared to control mitochondria. Additional experiments were performed with IPC and control mitochondria which were exposed for 10 minutes to daylight. These experiments were done to confirm a SNO dependent effect of increased mitochondrial dye permeability due to IPC, since SNO protein modifications are light sensitive. After exposure to daylight, preconditioned and control mitochondria did not show a difference in LY uptake (n=4, p=ns). Fluorescence intensity of RITC-dextran did not differ among treatment groups (n=4, p=ns) (Figure 3.22).

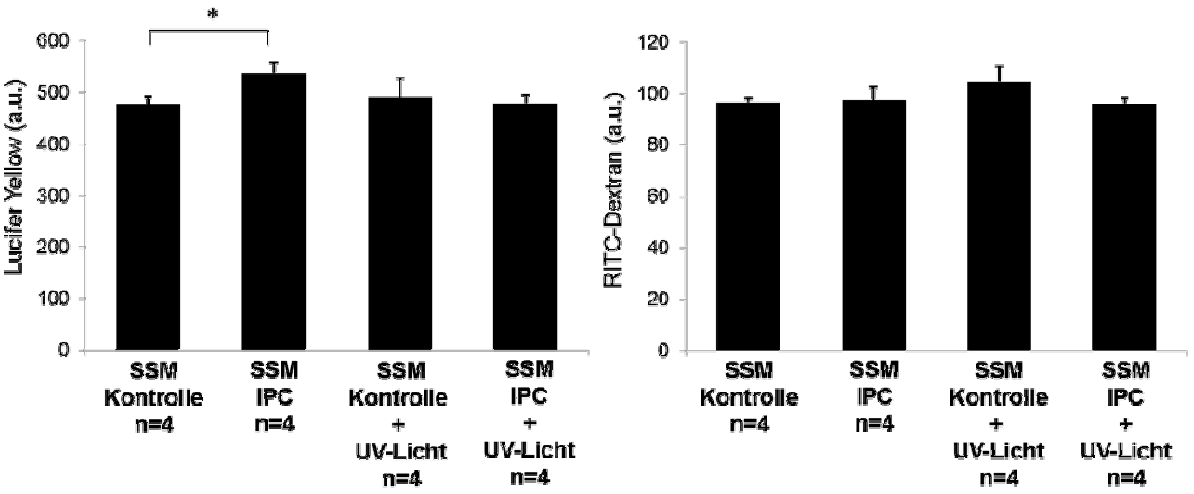

Figure 3.22: Mitochondrial Lucifer yellow (LY) dye uptake of mitochondria isolated from preconditioned hearts. Rat hearts were Langendorff perfused, one group received IPC and the other group was control perfused. Subsequent dye uptake of the hemichannel permeable dye LY (left panel) and the hemichannel impermeable dye RITC-dextran (right panel) of isolated mitochondria was measured. Dye uptake was quantified by measuring fluorescence intensity expressed as arbitrary units. As a control, mitochondria were exposed to daylight, which breaks down light sensitive SNO modifications before incubation with dyes. Data are shown as mean ± SEM of 4 replicates per group. * ($p<0.05$) indicates significant differences between groups.

3.2.2 Quantification of SNO modified mtCx43 after IPC

In order to investigate if SNO of mtCx43 is increased with IPC, rat hearts were once again assigned to a Langendorff perfusion protocol. One group of hearts was preconditioned, while the other group was constantly normo-perfused (control). Subsequent to isolation of mitochondria by ultra-gradient centrifugation, the purity of the mitochondrial preparation was analyzed by Western blot analysis for the absence of immunoreactivity of antibodies for cellular marker proteins and enrichment of mitochondrial proteins (Figure 3.23A). Western blot analysis was also performed to quantify the amount of Cx43 per mitochondrion and showed an increase of 64.8% ± 17% (n=8, $p<0.05$) (Figures 3.23B and C). This confirms previously published data that demonstrate that the mitochondrial amount of Cx43 is increased after IPC.

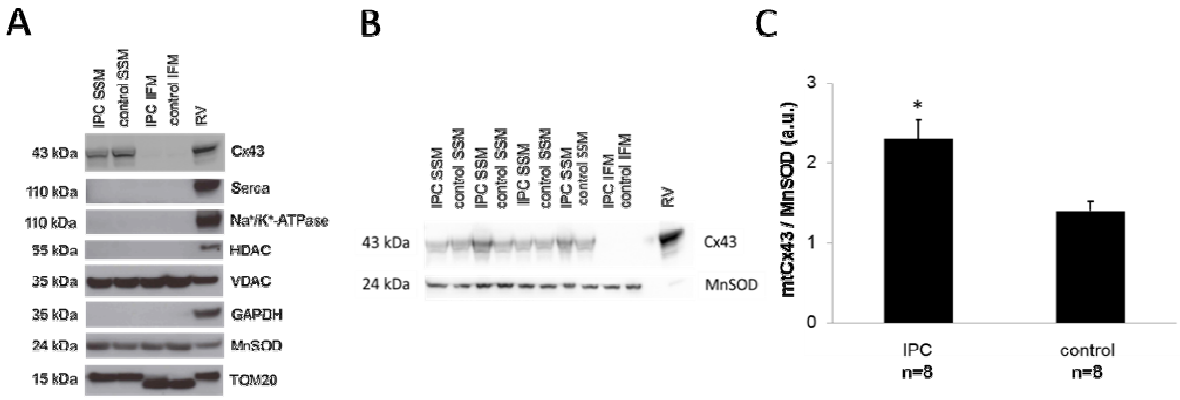

Figure 3.23: Quantification of mtCx43 after ischemic preconditioning (IPC). Rat hearts were assigned to a Langendorff perfusion model. One group was preconditioned while the other was constantly normo-perfused (control). SNO quantification of mtCx43 was performed on mitochondria isolated by Percoll gradient ultracentrifugation. Western blot analysis showed that mtCx43 is increased following IPC when normalized to mitochondrial protein MnSOD (B and C). Results are expressed as mean ± SEM of 8 replicates of IPC and control perfused hearts. * ($p<0.05$) indicates significant difference between groups.

A modified biotin switch method for labeling SNO modified cysteine residues was used and the amount of SNO modified mtCx43 was quantified for each group. The quantification of SNO modified mtCx43 showed that the relative amount of SNO modified mtCx43 was significantly increased by 41.6 ± 1.7% (n=17, $p<0.05$) in preconditioned rat hearts compared to control perfused hearts (Figures 3.24A and B). Additionally, perfusion of rat hearts was performed in daylight and here the increase in light sensitive SNO modification was lost (n=6, p=ns). Furthermore, adding DTT, which breaks down disulfide bounds, after SNO labeling led to a decrease of precipitated protein and the significant difference between the groups was abolished (n=5, p=ns) (Figures 3.24C, D, and E).

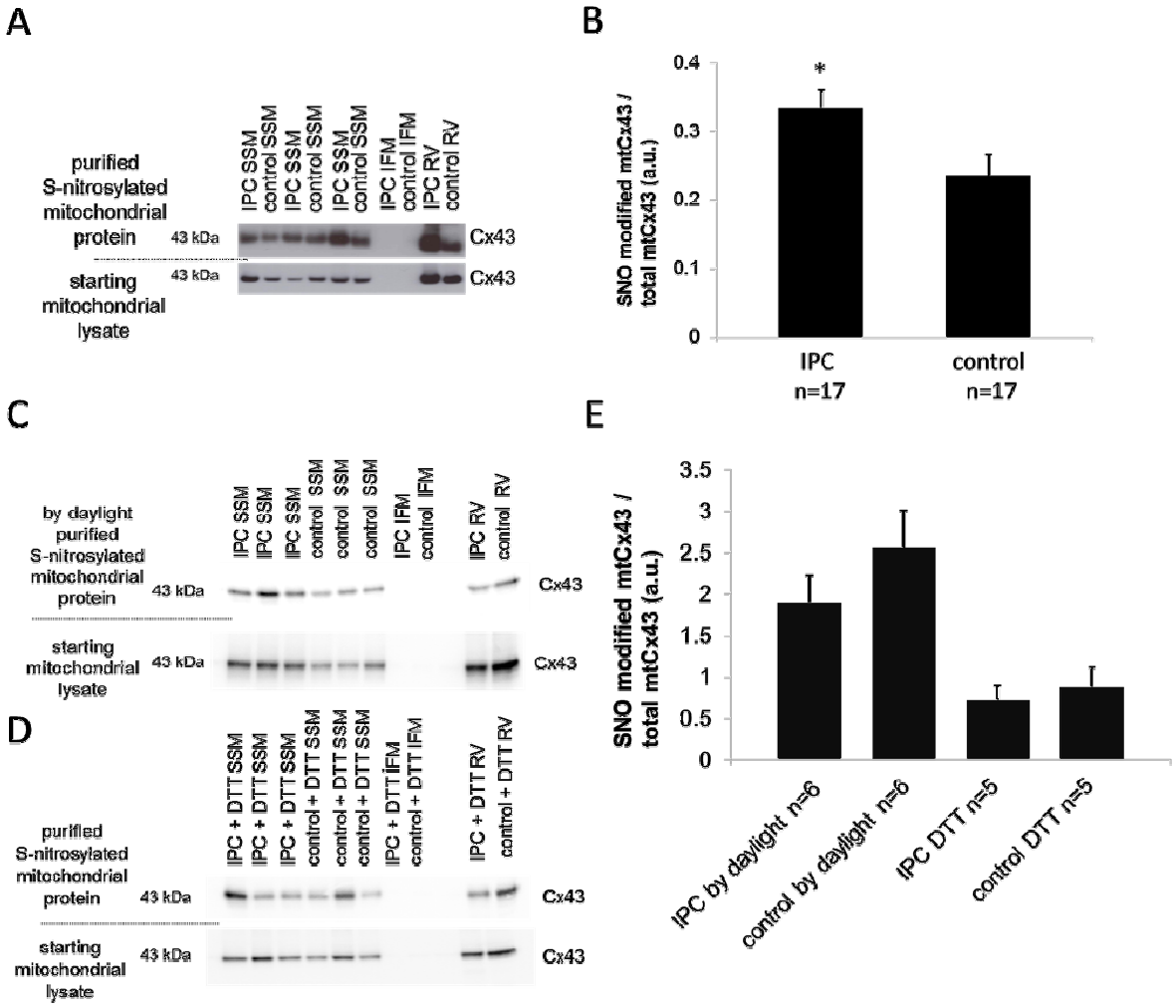

Figure 3.24: SNO quantification of mtCx43 after ischemic preconditioning (IPC). Rat hearts were assigned to a Langendorff perfusion model, either receiving IPC or constantly normoperfusion (control). Using a modified biotin switch method, biotin labeled SNO modified proteins were precipitated; Western blot analyses were performed for mtCx43 (A, C, and D). Interfibrillar mitochondria (IFM) were used as a negative control. The right ventricle of rat hearts was used as a positive control. Band signal intensity of purified SNO modified mtCx43 was normalized to a loading control taken from the starting mitochondrial lysate representing the total amount of loaded mtCx43 (B). In addition, as negative controls, Langendorff experiments were repeated by daylight to remove light sensitive SNO modification (C). Isolated mitochondria were treated with DTT to remove the SNO/biotin label showing specificity of the biotin switch method (D). * ($p<0.05$) indicates significant differences between groups. Results are expressed as mean ± SEM of 14 replicates of IPC and control perfused hearts (B). Five to six replicates per group of negative controls were performed (E).

3.2.3 Quantification of SNO modified mtCx43 after rIPC

SNO of mtCx43 was quantified subsequent to rIPC of mouse hearts. One group of mice received rIPC by hindlimb ischemia and reperfusion, whereas the control group received the same treatments except the peripheral ischemia/reperfusion episodes. SNO of mtCx43 was increased by 65.7 ± 16.9% (n=5, $p<0.05$) in mice receiving rIPC compared to control treated mice. Additionally, mice were pharmacological preconditioned by injection of 48 nM sodium nitrite into the cavity of left ventricle, which increased SNO modified mtCx43 by 59.3 ± 18.2% (n=6, $p<0.05$) compared to control mice receiving sodium chloride injections (Figure 3.25).

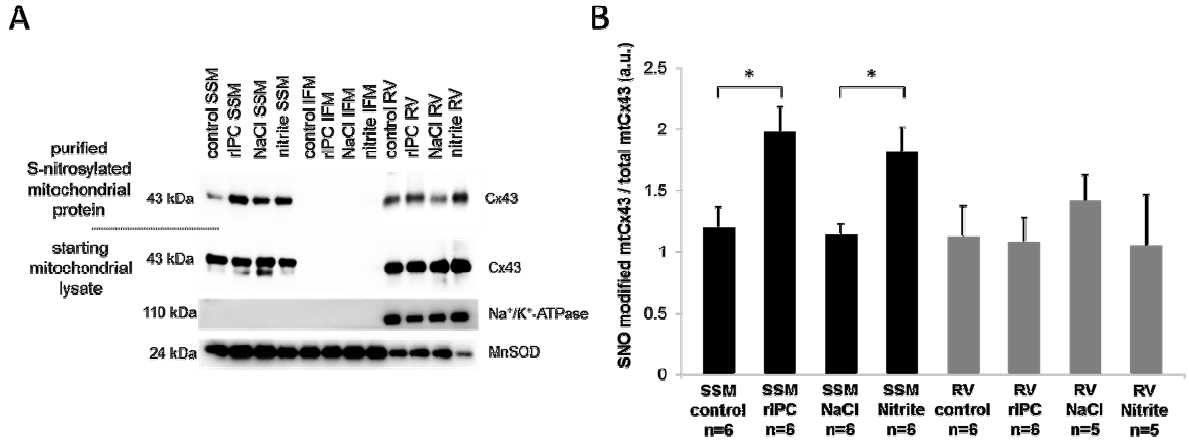

Figure 3.25: SNO quantification of mtCx43 after remote ischemic preconditioning (rIPC). Mice received rIPC by hindlimb ischemia and reperfusion or were pharmacological preconditioned by injection of 48 nM sodium nitrite into the left ventricle. Subsequently subsarcolemmal mitochondria (SSM) were isolated from the left ventricle of these treated mice hearts. Purity of the mitochondrial preparation was confirmed by the absence of immunoreactivity for sarcolemma marker Na^+/K^+-ATPase and enrichment of mitochondrial protein MnSOD. Biotin labeled SNO modified proteins were precipitated and Western blot analyses were performed for mtCx43 (A). Interfibrillar mitochondria (IFM) were used as a negative control. The right ventricle were used as positive a control. Band signal intensity of purified SNO modified mtCx43 was normalized to a loading control taken from the starting mitochondrial lysate representing the total amount of loaded mtCx43 (B). * ($p<0.05$) indicates significant difference between marked groups. Results are expressed as mean ± SEM of 5–6 replicates per group.

In addition, the relative amount of precipitated SNO modified mtCx43 was quantified by normalizing SNO of mtCx43 to total mtCx43 on a Western blot. The results showed that only approximately 0.46 ± 0.01% of the total mtCx43 was SNO modified

in control treated left ventricle of mice hearts (Figure 3.26). The content of SNO of mtCx43 was increased by 60% by rIPC.

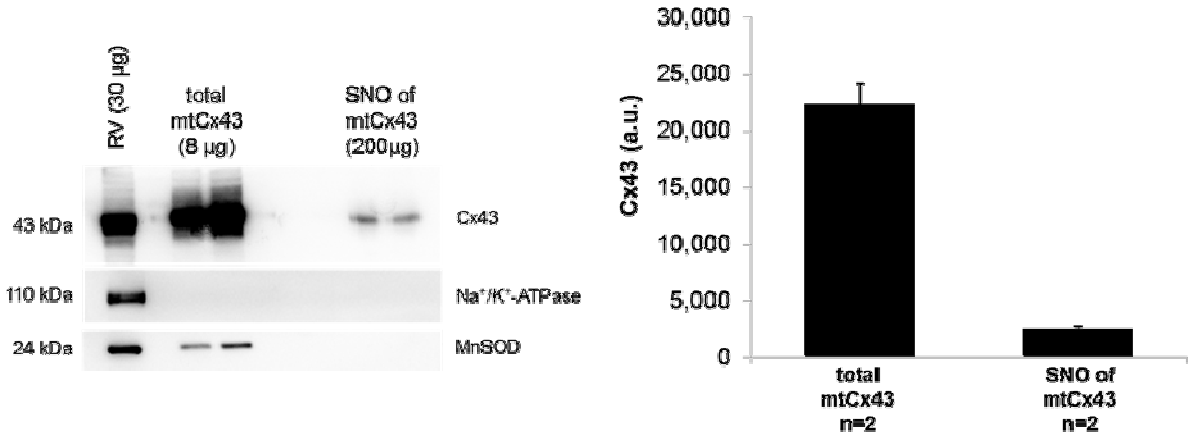

Figure 3.26: Quantification of the relative amount of SNO modified mtCx43. Purity of isolated mitochondria from the left ventricle of mice hearts was confirmed by the absence of immunoreactivity for sarcolemma marker Na^+/K^+-ATPase and enrichment of mitochondrial protein MnSOD. Biotin labeled SNO modified proteins were precipitated and Western blot analyses were performed for mtCx43. The right ventricle of mice hearts were used as positive a control. Results are expressed as mean ± SEM of 2 replicates per group.

3.2.4 Identification of SNO modified cysteine residues of mtCx43

Using liquid chromatography tandem mass spectrometry, SNO modified cysteine residues of mtCx43 were identified following IPC and constantly normo-perfused (control) rat hearts. In IPC treated rat hearts 7 distinct peptides were identified covering 33.5% of Cx43's amino acid (aa) sequence. Analysis of mtCx43 from control perfused rat hearts identified 9 distinct peptides covering 35.3% of the aa sequence (Table 3.1).

Table 3.1: Peptides identified by liquid chromatography tandem mass spectrometry. SNO modified cysteine residues of mtCx43 were labeled with a carbamidomethyl and unmodified cysteine with NEM. Also displayed is the number of peptides identified in 4 trials.

Treatment	Peptide sequence	Range	SNO Cys	Unmodified Cys	No.
IPC	CNTQQPGCENV CYDKSFPISHVR	54 - 76	1: Carbamidomethyl (Cys54)	8: NEM (Cys61)	1
	VAQTDGVNVEM HLK	115 - 128			1
	FKYGIEEHGKVK	135 - 146			2
	SVFEVAFLLIQWY IYGFSLSAVYTCK	163 - 188		25: NEM (Cys187)	1
	RDPCPHQVDCFL SRPTEK	189 - 206		4: NEM (Cys192), 10: NEM (Cys198)	2
	YAYFNGCSSPTA PLSPMSPPGYK	265 - 289	7: (Carbamidomethyl) (Cys271)		1
	LVTGDRNNSSCR	290 - 301		11: NEM (Cys298)	1
Control	CNTQQPGCENV CYDKSFPISHVR	54 - 76	1: Carbamidomethyl (Cys54)	12: NEM (Cys65)	2
	VAQTDGVNVEM HLK	115 - 128			1
	FKYGIEEHGKVK	135 - 146			1
	VKMRGGLLR	145 - 153			1
	RDPCPHQVDCFL SRPTEK	189 - 206	4: Carbamidomethyl (Cys192), 10:Carbamidomethyl (Cys198)	4: NEM (Cy192), 10: NEM (Cys198)	2
	SDPYHATTGPLS PSK	244 - 258			1
	YAYFNGCSSPTA PLSPMSPPGYK	265 - 289	7: (Carbamidomethyl) (Cys271)		1
	LVTGDRNNSSCR	290 - 301		11: NEM (Cys298)	1
	ASSRASSRPR	367 - 376			2

In IPC samples two SNO modified cysteine residues (Cys54 and Cys271) labeled with a carbamidomethyl and five unmodified cysteine (Cys61, Cys187, Cys192, Cys198, and Cys298) with NEM labels were identified. In constantly (control) normoperfused rat hearts four SNO modified cysteine residues of mtCx43 and two unmodified cysteine thiols were detected (Figure 3.27). Cx43 peptides and SNO of mtCx43 were only detectable in low abundance, therefore quantification of SNO modified cysteines by analyzing the ratio of peptide containing carbamidomethyl

labeled cysteines to total detected cysteine residues was not possible with proteomic approaches.

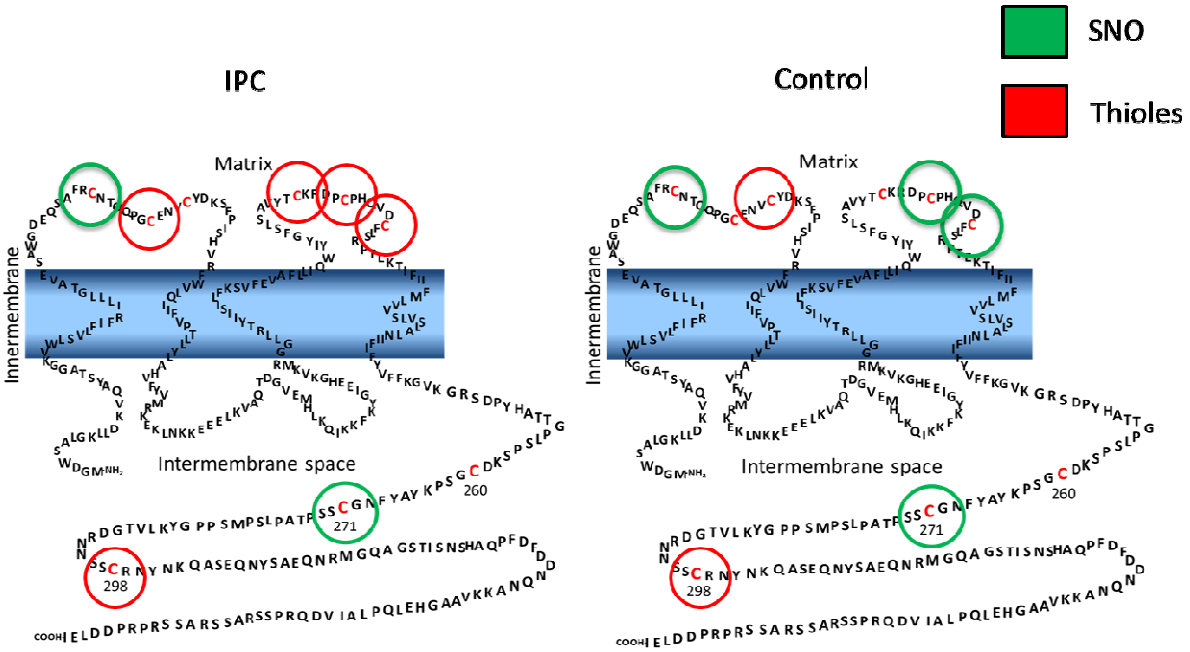

Figure 3.27: Schematic display of mtCx43 showing cysteine modifications identified by proteomic approaches. Mitochondria from ischemic preconditioned (IPC) and constantly (control) normo-perfused rat hearts were analyzed by proteomic approaches for identifying SNO modified cysteine residues of mtCx43. The cysteine residues (C) of mtCx43 are marked in red. Identified cysteine residues by liquid chromatography tandem mass spectrometry are circled in red showing detected unmodified cysteine thiols. Circled in green are SNO modified cysteine residues.

4. Discussion

4.1 S-nitrosation of mtCx43 influences mitochondrial function

Mitochondrial permeability for the LY dye and K^+ are increased following to the application of the NO donors SNAP and GSNO in SSM, but not in IFM. Interestingly, the change in mitochondrial permeability for Na^+ was minor and not influenced by the NO donors. The NO mediated increases in mitochondrial permeability were abolished by the Cx43 hemichannel blocker, carbenoxolone. ROS formation of SSM was also increased in the presence of NO donors. However, the ROS increasing effect of the NO donors was abolished by carbenoxolone or the Cx43 mimetic peptide Gap26, which blocks of HC opening. In contrast to SSM, in IFM ROS formation was decreased in response to NO donors. Furthermore, SNO of mtCx43 was increased in response to the application of NO. These new findings indicate that SNO of mtCx43 contributes to the regulation of mitochondrial permeability, especially for K^+ fluxes and ROS formation, which might be linked to the modified mitochondrial K^+ influx [205].

4.1.1 Reduction of mitochondrial permeability by carbenoxolone confirms the existence of mtCx43 hemichannels

Carbenoxolone, a glycyrrhetinic acid derivative, is a compound known to block gap junctions function by disruption of connexons [96, 293]. Glycyrrhetinic acid derivative intercalate in membranes inducing a conformational change and disrupts connexin hemichannels by direct interaction [67]. Cross-linking studies on mtCx43 confirm the presence of hexamer-like structures in the inner mitochondrial membrane. The existence of mtCx43 HCs is further supported by reduced mitochondrial LY uptake in response to HC blockers carbenoxolone and heptanol. The present results indicate that 1 µM carbenoxolone is sufficient to significantly reduce mitochondrial LY uptake confirming successful disruption and thereby inhibition of mtCx43-formed HCs [167]. In experiments with human fibroblasts 3 µM carbenoxolone reduced inter junctional

communication by 80% and 6 µM completely blocked intercellular transfer of phenylalanine [306].

Carbenoxolone at a concentration of 100 µM led to a rapid decrease of phenylalanine incorporation representing overall protein synthesis, suggesting increased cellular toxicity of the drug at high concentrations [68]. Exposure of 50 µM carbenoxolone led to loss of mitochondrial membrane potential in astrocytes and neurons [283]. Studies on rat liver mitochondria showed that carbenoxolone induced mitochondrial swelling and the collapse of mitochondrial membrane potential via ROS formation and MPTP opening. In the present study, investigating the impact of carbenoxolone on SSM isolated from rat left ventricles showed a loss of mitochondrial membrane potential and mitochondrial integrity in response to 35 µM carbenoxolone. The reason for the greater sensitivity of mitochondria to carbenoxolone in the present study could be due to differences in tissue type or the mitochondrial subpopulation analyzed. However, carbenoxolone concentrations up to 25 µM had no impact on mitochondrial vitality, but significantly reduced LY uptake and velocity of K^+ influx in SSM, but not in IFM lacking Cx43. Therefore, previous findings of reduced mitochondrial permeability caused by connexin HC blockers were confirmed in the present study. Importantly, the Western blot analysis of the present study showed no decrease of SNO of mtCx43 by HC blocker carbenoxolone. Accordingly, carbenoxolone blocks the ion fluxes and their downstream effects mediated by mtCx43 HCs, but not SNO of mtCx43 per se [66, 68].

4.1.2 NO increases mitochondrial permeability

Endogenously, NO can be produced in specific cellular regions via local NOS activation [132, 217]. In cardiomyocytes, specific NOS isoforms located in distinct cellular compartments produce NO in a coordinated manner, thereby allowing the interaction only with co-localized effectors [107, 304]. NOS isoforms have different expression patterns among species. The existence of mitochondrial NOS isoforms was proven by immunohistochemistry in rat liver, brain, kidney, skeletal muscle, and heart [13, 14] and by biochemical analysis in the myocardium [88, 125, 300]. In porcine and rat heart mitochondria the inducible NOS isoform was detected [88, 92], whereas in mice heart mitochondria neuronal NOS is expressed [140]. Furthermore a study showed that caveolae endothelial NOS localizes with mitochondria and docks

to the mitochondrial outer membrane in the human umbilical vein, human endothelial cells, and embryonic kidney cells [94]. However, there are conflicting results regarding the existence of specific mitochondrial NOS isoforms [37, 92, 156, 282]. There is also evidence of NO generation by non-enzymatic release from nitrite independent of NOS isoforms [62], which is suggested to be associated with cardioprotection [252, 253].

In the present study, the NO mediated increase in mitochondrial permeability was measured in SSM, but not in IFM which lack Cx43. The NO mediated increase in mitochondrial permeability was abolished by the connexin HC blocker carbenoxolone. Changes in the phosphorylation status or in the redox state of connexin regulate the open probability of GJs or HCs at the cellular sarcolemma [226, 235]. Studies investigating cellular communication within the vessel wall of the mouse artery showed an increased open probability of Cx43-formed GJs through SNO of cysteine 271, whereas denitrosation by compartmentalized S-nitrosoglutathione reductase decreased GJ permeability [261]. Investigations on astrocytes by Retamal et al. proposed increased GJ permeability with a NO donor application, whereas reducing agents inhibited GJ permeability [224]. In this study, the existence of a similar mechanism for mitochondrial connexin HCs is proposed.

Cx43 HCs located at the sarcolemma are predominantly closed during resting conditions [216]. The results of the present study showed that SSM and IFM had a similar level of LY dye uptake at baseline. This finding indicates that baseline mitochondrial permeability for LY is provided also through other mitochondrial channels and indicates a low open probability mtCx43 HC. A predominant closed confirmation of mtCx43 HC is supported by the fact that, only less than 1% of mtCx43 is SNO modified under baseline conditions. Nevertheless, HC blocker carbenoxolone as well as genetic replacement of Cx43 with Cx32 in mitochondria reduced mitochondrial LY dye permeability. This suggests that at least some mtCx43 HCs are open in SSM under baseline conditions.

In addition to the NO-induced increase in Cx43 HC open probability dephosphorylation of Ser368 is also able to induce HC opening at the plasma membrane. This leads to release of metabolites, second messengers, and Ca^{2+} which causes cellular damage and induces apoptosis of neighboring cells [60, 113, 136, 161, 165, 283].

Several protein kinases located in the mitochondria including PKC [160, 164, 208], protein kinase A [87, 151, 168], and the serine/threonine kinase Akt [22] can phosphorylate mtCx43 HC thereby influencing HC stability and open probability. Thus it could be possible that mtCx43 HC open probability is altered by SNO mediated modification of mitochondrial protein kinase activities. The performed Western blot analysis quantifying serine phosphorylation of mtCx43 showed a tendencially increase in phosphorylation of serine residue 365 in response to the NO donor SNAP. Other tested serine residues or samples treated with the NO donor GSNO displayed no alterations in Cx43 phosphorylation. The serine residue 365 of Cx43 has been viewed as gate keeper in that the epitope must be dephosphorylated in order to allow phosphorylation of the serine residue 368 of Cx43, which in turn is important for the buildup of HC in the sarcolemma [258].

4.1.3 Ion specificity of NO mediated increased mitochondrial permeability

Previous studies have shown that the HC blocker 18α-glycyrrhetic acid reduced mitochondrial K^+ influx. In experiments using Cx43KI32 mice, in which Cx43 is absent and replaced by Cx32, a reduction in mitochondrial K^+ and LY permeability was demonstrated [184]. Cx32 has a highly reduced conductivity for K^+ [108] and is permeable to soluble in a charge dependent manner [97].

The velocity of mitochondrial K^+ influx was increased by NO donors and reduced by carbenoxolone. Thus the NO mediated increase in mitochondrial dye permeability was confirmed by measurements of K^+ influx. The concentration of the K^+ pulses (140 mM) corresponds to the intracellular K^+ concentration. The electrochemical gradient drives K^+ ions into the mitochondrial matrix. Additional mitochondrial potassium channels were inhibited during these measurements: MPTP opening was blocked by cyclosporine A [110], the proton channel of the ATP-synthase was inhibited by oligomycin, and glibenclamide was used to block the opening of ATP-dependent potassium (mitoK_{ATP}) channels [246, 267], the latter being important for cardioprotection by IPC [115, 200]. In the presence of these inhibitors with the addition of carbenoxolone a mitochondrial K^+ influx was still detectable. It is possible, that channels other than mitoK_{ATP} channels could contribute to mitochondrial K^+

fluxes, among them calcium-dependent potassium channels, mitochondrial Kv1.3 potassium channels, and the two-pore potassium channels TASK-3 [268]. The fact that carbenoxolone significantly reduced mitochondrial K^+ influx in the presence of many K^+ channel inhibitors supports the existence of a mtCx43 HC. Blockade of any of the relevant K^+ channels might significantly reduce total mitochondrial matric K^+ levels and thereby inter with ROS formation and the induction of cardioprotection (threshold phenomenon). Relevance of the NO mediated increase of mitochondrial K^+ influx in a physiological context was supported by repeating the experiments without additional K^+ channel inhibitors, which showed slightly reduced but still significant Cx43-dependent increases in the mitochondrial K^+ influx.

It is of interest to note, that mtCx43 HC provide certain ion selectivity. The measured Na^+ influx was minor and neither the NO donors nor carbenoxolone did alter Na^+ fluxes significantly. It is proposed that GJs are rather non-ion specific channels and Cx43 HCs are characterized as size selective pores with negligible charge-dependent selectivity [141]. A number of studies have proposed that Cx43 GJ have certain ion selectivity with a preference for K^+ over Na^+ [287]. This fact could explain the weak Na^+ fluxes which were measured in the present study. In cardiac mitochondria, the Na^+ import is mainly achieved by the Na^+/Ca^{2+} exchanger mediating Na^+ influx in exchange for Ca^{2+} efflux [146] and Na^+ is exported via a mitochondrial Na^+/H^+ exchange system [138]. Metabolic inhibition increases the concentration of Na^+ in the mitochondrial matrix, whereas in energized mitochondria the concentration of Na^+ is lower in the matrix compared to the cytosol [76, 138]. Therefore in the present study, mitochondria performing on state 4 respiration showed a lack of Na^+ influx, whereas a weak Na^+ flux was detectable in mitochondria during complex II respiration. It has to be mentioned further, that a detectable Na^+ influx was only measured in response to a 140 mM sodium chloride pulse. The physiological concentration of intracellular Na^+ in cardiomyocyte ranges approximately 5–10 mM [131]. In response to 10 mM sodium chloride pulses no significant Na^+ influx was detectable even in respiring mitochondria. If a mitochondrial Na^+ influx was measured it was decreased rather than increased in the presence of a NO donor. Since NO inhibits highly selective sodium channels in H144 cells at the cellular surface [5] one alternative explanation for the observed lack of mitochondrial Na^+ influx following NO donors could be a NO induced decrease of mitochondrial Na^+ permeability via inactivation of mitochondrial

sodium channels compensating for a possible increase in Na^+ influx through increased mtCx43 HC open probability.
Taken together, it can be assumed that NO induced mtCx43 HC opening mainly induces mitochondrial K^+ influx.

4.1.4 NO mediated increase in ROS formation in SSM via Cx43

Low amounts of ROS species function as signaling molecules in endogenous cardioprotection [205]. Indeed, cardioprotection induced by diazoxide leads to ROS formation which is dependent on mtCx43 [115]. Furthermore there is evidence that NO triggers preconditioning [30, 269], and that the cardioprotection achieved by the exogenous NO donor SNAP could be abolished by ROS scavengers as well as potassium channel blockers [297]. In the present study mitochondrial ROS formation was increased in response to NO donors in SSM. The NO triggered increase in mitochondrial ROS formation was abolished by uncoupling of Cx43 HCs with carbenoxolone indicating that mtCx43 is essential for NO triggered ROS formation. Furthermore NO induced ROS formation was blocked by the Cx43 mimetic peptide Gap26. Cx43 mimetic peptides have identical sequences to domains of the Cx43 protein. Gap26 binds the first extracellular loop of Cx43 which inhibits GJ formation [84, 292]. More recently studies showed that Gap26 inhibits voltage induced Ca^{2+} currents in ventricular cardiomyocyte indicating an inhibition of Cx43 HC opening [288]. Thus the current data indicates that Cx43 HC opening is a necessary mechanism for NO triggered mitochondrial ROS formation. ROS triggering cardioprotection must be viewed separately from ROS contributing to irreversible injury following sustained episodes of ischemia/reperfusion. Indeed, Chouchani et al. proposed that NO donor induced SNO of mitochondrial complex 1 provided cardioprotection via reduced ROS formation following sustained ischemia and reperfusion [54]. The present study adds one more facet in that, the modification of ROS formation by NO depends on the subpopulation of mitochondria analyzed. Energized IFM in contrary to SSM showed a reduction of ROS formation. The two distinct mitochondrial subpopulations differ in their protein and lipid composition, protein synthesis, respiration capacity, their sensitivity in response to metabolic stress, and Ca^{2+} retention capacity [77, 124, 181, 206, 210, 229]. SSM appear to be the pharmacological target of drugs like diazoxide to induce endogenous

cardioprotection [122] and the present data supports the notion in that NO increases ROS formation only in SSM.

The Complex I and III of the respiratory chain are suggested to be the main sources of mitochondrial ROS formation [275-277]. Several studies provide strong evidence, that mtCx43 regulates ADP stimulated complex 1 respiration via direct interaction. Mitochondrial ROS formation was increased following administration of the respiratory chain complex 1 inhibitor rotenone in the present study confirming previous reports [106, 277]. Interestingly, the NO mediated increase in mitochondrial ROS formation in SSM was no longer seen following inhibition of respiratory chain complex 1 with rotenone suggesting that S-nitrosated mtCx43 interacts with complex 1 to increase ROS formation.

4.1.5 Potential side effects of applied NO donors

The NO donors SNAP and GSNO were used as NO sources in the present study. SNAP is one of the most frequently used exogenous S-nitrosothiol (RSNO) while GSNO (NO glutathione (GSH) as RSNO) is a endogenous key regulator of the cellular redox state and among others modulates metabolic events [45, 222, 243]. The regulatory impact of GSNO is biphasic. Besides the modulation via NO, also GSH can be covalently attached to cysteine thiols, a process which is called S-glutathionylation. Therefore GSNO has the potential to cause both S-nitrosation as well as S-glutathionylation of proteins and it is postulated that following GSNO application a fast transnitrosation reaction is followed by glutathionylation which replaces modifications induced by S-nitrosation as well as oxidation [101, 207]. Glutathionylation of proteins of the respiratory chain complexes I to III or proteins regulating these complexes could be responsible for the lower ROS formation in response to antimycin A in GSNO treated samples. Anitmycin A maximizes ROS formation by inducing circulation of electrons between respiratory chain complex I and III. Since the NO donor SNAP does not influence ROS production during inhibition of complex IV it is likely that a glutathionylation reaction induced by GSNO inhibits ROS formation in the presence of antimycin A, which might however be time-dependent. Since the nitrosation reaction precedes the glutathionylation reaction following GSNO administration, GSNO might increase ROS formation in the short run while ROS formation is decreased at later time points. In theory GSNO might be the

optimal cardioprotectant since the short initial increase in ROS formation could trigger cardioprotection, while the later on suppression of the production of large amounts of ROS preserves from cell death. Further studies need to be performed for clarifying the role of GSNO's glutathionylation reaction in altering mitochondrial function and its relevance for cardioprotection.

4.1.6 Increase in SNO of mtCx43 by application of NO donors

The effects of NO are dose-dependent. Low concentrations of NO nitrosates increase mitochondrial respiration, whereas high concentration of S-nitrosate results in a reversible inhibition of mitochondrial respiration [36, 38, 42, 47, 270]. Sun et al. showed a dose-dependent effect of GSNO in concentrations between 0.1-1 mM increasing SERCA2a and α-KGDH activity, whereas F1-ATPase activity was inhibited. In the present study ROS formation was estimated with concentrations of 0.5 mM SNAP, 1 mM, 1 µM, and 48 nM GSNO. The NO donors SNAP and GSNO, which were used in the present study, are very poor NO donors delivering NO concentrations of about 0.6% and 0.12% of the administered dose [80]. Furthermore it is worth mentioning that S-nitrosothiols are very sensitive to daylight [296]. Thus, the overall applied NO concentrations should be in the nM range and close to physiological concentrations. Indeed, a concentration of 0.1 mM GSNO applied to Langendorff perfused hearts induced SNO of mitochondrial proteins to a similar extent than an endogenous intervention (IPC) did [263].

4.2 IPC induction of SNO of mtCx43 may mediate cardioprotection

The data of the present study shows that SNO of mtCx43 increases mitochondrial dye permeability, K^+ fluxes, and ROS formation. Potassium influx through the opening of mitoK_{ATP} channels and increase in moderate ROS formation are key elements for the subsequent inhibition of MPTP opening following ischemia/reperfusion and they are two factors necessary for mediating IPC and pharmacological preconditioning [29, 115, 167, 245]. Previous studies suggested that NO-induced mtCx43 HC opening may be one key mechanism mediating cardioprotection. The following

investigations were performed on mitochondria from rat hearts receiving IPC to show that SNO of mtCx43 is part of the signal transduction cascade of cardioprotection.

The open probability of Cx43-formed GJs of myoendothelial cells is increased by SNO of cysteine 271 and denitrosation by compartmentalized S-nitrosoglutathione reductase decreased GJ permeability [261]. SNO of cysteine 271 of mtCx43 was identified by proteomic analysis in rat hearts receiving IPC or control perfusion. Unfortunately, the cysteine residue was detected only in low abundance making quantification impossible considering that only 5% of the total cellular Cx43 is located in mitochondria [230]. Furthermore, only a subpopulation of less than 1% of total mtCx43 was found to be SNO modified in resting mitochondria.

In IPC and control perfused rat hearts cysteine 271 of mtCx43 was found to be SNO modified. The cysteine 271 is responsible for increased open probability of GJ channels at the plasma membrane [261]. Accordingly, SNO of cysteine 271 is a promising candidate for mediating Cx43 HC opening in the inner mitochondrial membrane. Proteomic approaches would most likely indicate that a small portion of mitochondrial HCs are also opened under resting conditions likely due to SNO protein modification.

Furthermore, SNO of mtCx43 was increased in the LV of mice receiving rIPC. The rIPC in a remote organ provides protection from potentially lethal myocardial ischemia/reperfusion injury which is proven by several clinical studies [31, 111, 123, 145]. RIPC also led to increased SNO of mtCx43 in mouse hearts supporting the previous observation that IPC induces SNO of mtCx43. Recently, Rassaf et al. demonstrated that NO contributes to cardioprotection by rIPC [221]. Accordingly, application of nitrite reduced infarct size following ischemia/reperfusion *in vivo* [116]. Nitrite is one of the proposed candidates for transporting the protective signal from the remote organ to the myocardium [221]. The underlying mechanism transmitting the protective signal is not fully understood. However, experiments with eNOS deficient mice provide evidence that NO generation by eNOS is essential for the nitrite mediated cardioprotective effect of rIPC, whereas a cardiac specific role of eNOS was excluded [233]. Nitrite is the stable form of NO. The dose dependent cytoprotective effect of nitrite functions via its reduction to NO which is dependent on myoglobin [79, 116, 273]. Nitrite concentrations of 300–500 nM were detected in the circulating blood of mice, which are much higher concentrations compared to nitroso species [116, 219]. In the present study, application of 48 nM sodium nitrite induced

increased SNO of mtCx43 to an equal extent as rIPC does. This shows that concentrations in the nanomolar range are sufficient to induce a similar amount of mtCx43 SNO as rIPC did. Therefore, nitrite is a potential pharmacological agent which was determined by investigations performed in several models [79, 211].

Taken together, the present data indicates that NO and mtCx43 can be linked to the signal transduction cascade of cardioprotection. A promising candidate for the underlying cardioprotective mechanism could be SNO of mtCx43 cysteine reside 271 leading to HC opening inducing protection via mitochondrial K^+ influx and moderately increased ROS formation.

4.3 Study limitations

The present study demonstrates that NO triggers an increase in mitochondrial permeability, particularly for K^+, and ROS formation in a Cx43 dependent manner. Mitochondrial K^+ influx through mitoK_{ATP} channels leads to a moderate increase in ROS formation inhibiting MPTP opening following ischemia/reperfusion [29, 115, 167, 245]. This study suggests that two factors necessary for cardioprotection are regulated by SNO of mtCx43. This study provides evidence that IPC triggers SNO of mtCx43 and increases mitochondrial permeability. In addition, pharmacological preconditioning by nitrite increases SNO of mtCx43 to a similar extent as rIPC does, giving rise to the notion that NO in physiological concentrations could mediate preconditioning via SNO of mtCx43. Taken together, a potential link between NO and mtCx43 in the signal transduction cascade of cardioprotection is most likely. However, the study lacks direct evidence that SNO of mtCx43 mediates cardioprotection by preconditioning because it remains unclear whether or not SNO of mtCx43 is sufficient for cardiomyocyte preconditioning.

Future studies need to be performed to provide evidence that SNO of mtCx43 is essential for mediating myocardial PC. This could be done by performing Cx43 cysteine epitope replacement studies in a stable transfected cell lines or transgenic mouse models. Thus, the sites of mtCx43 that are S-nitrosated and are responsible for mediating increased mitochondrial ion fluxes and ROS formation could be identified. Furthermore, the exact mechanism of mtCx43 HC involvement in mediating cardioprotection remains unclear. Further studies are needed to investigate

if ion fluxes through mitochondrial Cx43 HC directly mediate preconditioning or if increased mtCx43 HC open probability regulates other mitochondrial channels like mitoK_{ATP} channels.

5. Summary

S-nitrosation of connexin 43 formed channels alters dye uptake in astrocytes and gap junctional communication in endothelial cells. Apart from forming channels in the cell surface membrane of several cell types, connexin 43 is also located at the inner membrane of myocardial subsarcolemmal mitochondria, but not in interfibrillar mitochondria. The absence or pharmacological blockade of mitochondrial connexin 43 decreases mitochondrial dye and potassium uptake. A lack of mitochondrial connexin 43 is associated with the loss of cardioprotection by ischemic preconditioning, which is mediated by formation of reactive oxygen species.

Whether or not mitochondrial Lucifer Yellow, ion uptake, or reactive oxygen generation are affected by S-nitrosation of mitochondrial connexin 43 and whether or not cardioprotective interventions influence S-nitrosation of mitochondrial connexin 43 remains unknown.

Subsarcolemmal mitochondria from rat hearts showed an increased Lucifer Yellow uptake in response to nitric oxide donors (S-nitroso-N-acetyl-DL-penicillamine (SNAP): 38.4 ± 7.1%, $p<0.05$; S-nitrosoglutathione (GSNO): 28.1 ± 7.4%, $p<0.05$) and an increased refilling rate of potassium (SNAP: 227.9 ± 30.1%, $p<0.05$; GSNO: 122.6 ± 28.1%, $p<0.05$). These effects were abolished following blockade of connexin 43 hemichannel by carbenoxolone as well as in interfibrillar mitochondria, which lack connexin 43. Unlike potassium, the sodium permeability was not affected by application of nitric oxide. Furthermore, mitochondrial reactive oxygen species formation was enhanced in response to nitric oxide application compared to control treatment group (SNAP: 22.9 ± 1.8%, $p<0.05$; GSNO: 40.6 ± 7.1%, $p<0.05$), but decreased following nitric oxide treatment in interfibrillar mitochondria compared to control treated interfibrillar mitochondria (SNAP: 14.4 ± 4%, $p<0.05$; GSNO: 13.8 ± 4%, $p<0.05$). Administration of nitric oxide donors to isolated subsarcolemmal mitochondria or nitrite application into the cavity of left ventricles in mice in vivo enhanced S-nitrosation of mitochondrial connexin 43 by 109.2 ± 15.8% and by 59.3 ± 18.2%, respectively ($p<0.05$). Ischemic preconditioning by 4 cycles of ischemia and reperfusion, enhanced S-nitrosation of mitochondrial connexin 43 by 41.6 ± 1.7% ($p<0.05$) in comparison to subsarcolemmal mitochondria from control perfused rat hearts.

These data suggest that S-nitrosation of mitochondrial connexin 43 increases mitochondrial permeability, especially for potassium and leads to increased formation of reactive oxygen species. The increased amount of S-nitrosated mitochondrial connexin 43 by ischemic preconditioning or nitrite administration may link nitric oxide and connexin 43 in the signal transduction cascade of cardioprotection by preconditioning.

6. Zusammenfassung

Neben der Bildung von transmembranen Kanälen an der Zelloberfläche, ist Connexin 43 auch in der inneren Membran von subsarkolemmalen Mitochondrien lokalisiert. In interfibrillären Mitochondrien ist Connexin 43 jedoch nicht nachweisbar. Die Abwesenheit oder pharmakologische Inhibierung von mitochondrialem Connexin 43 verringert die mitochondriale Farbstoff- und Kaliumaufnahme und führt zum Verlust von Kardioprotektion durch ischämische Präkonditionierung, welche durch die moderate Produktion von reaktiven Sauerstoffspezies ausgelöst wird. Die S-Nitrosierung von Connexin 43 gebildeten Membrankanälen führt zu einer veränderten Farbstoffaufnahme in Astrozyten und beeinflusst die auf Gap Junctions basierende Kommunikation zwischen den Zellen des Endothels.

Gegenstand der vorliegenden Untersuchung ist die Analyse der S-Nitrosierung von mitochondrialem Connexin 43 und dessen Einfluss auf die mitochondriale Farbstoffaufnahme, mitochondriale Ioneneinströme, und Formierung reaktiver Sauerstoffspezies. Zusätzlich wurde die S-Nitrosierung vom mitochondrialem Connexin 43 nach kardioprotektiven Interventionen quantifiziert.

In subsarkolemmalen Mitochondrien von Rattenherzen, die mit den Stickstoffmonoxid-Donatoren S-nitrosoglutathione (GSNO) und S-nitroso-N-acetyl-DL-penicillamine (SNAP) behandelt wurden, war die Lucifer Yellow Farbstoffaufnahme (SNAP: 38.4 ± 7.1%, $p<0.05$; GSNO: 28.1 ± 7.4%, $p<0.05$) und die Geschwindigkeit des Kaliumstroms erhöht (SNAP: 227.9 ± 30.1%, $p<0.05$; GSNO: 122.6 ± 28.1%, $p<0.05$). Die Wirkung der Stickstoffmonoxid-Donatoren wurde durch Inhibierung der Connexin 43 Hemikanäle aufgehoben und war in interfibrilären Mitochondrien, die kein Connexin 43 enthalten, nicht nachweisbar. Im Gegensatz zu Kalium, war die Natrium-Permeabilität durch die Verabreichung von Stickstoffmonoxid nicht beeinflussbar. Außerdem wurde die mitochondriale Produktion von reaktiven Sauerstoffspezies durch die Zugabe von Sticksfoffmonoxid-Donatoren (SNAP und GSNO) in subsarkolemmalen Mitochondrien gesteigert (SNAP: 22.9 ± 1.8%, $p<0.05$; GSNO: 40.6 ± 7.1%, $p<0.05$). Im Gegensatz dazu führte die Zugabe von Stickstoffmonoxid in interfibrillären Mitochondrien zu einer Reduktion der Produktion von reaktiven Sauerstoffspezies (SNAP: 14.4 ± 4%, $p<0.05$; GSNO: 13.8 ± 4%, $p<0.05$). Die Verabreichung von Stickstoffmonoxid-Donatoren oder die Injektion von Nitrit in den linken Ventrikel von Mäusen in vivo

führte zu einer Erhöhung der S-Nitrosierung von Connexin 43 in subsarkolemmalen Mitochondrien um 109.2 ± 15.8% bzw. 59.3 ± 18.2%, ($p<0.05$). Ischämische Präkonditionierung, hervorgerufen durch vier Zyklen von Ischämie und Reperfusion, erhöhte die S-Nitrosierung vom mitochondrialem Connexin 43 um 41.6 ± 1.7% ($p<0.05$) im Vergleich zu subsarkolemmalen Mitochondrien von kontroll-perfundierten Rattenherzen.

Die im Rahmen dieser Arbeit erfassten Daten zeigen, dass S-Nitrosierung von mitochondrialem Connexin 43 die mitochondriale Permeabilität für Farbstoff und besonders für Kalium-Ionen erhöht. Die S-Nitrosierung von mitochondrialem Connexin 43 führt zu einer erhöhten Produktion von reaktiven Sauerstoffspezies. Ischämische Präkonditionierung als auch die der Verabreichung von Nitrit führte zu einer erhöhten Menge an S-nitrosiertem mitochondrialen Connexin 43. Schlussfolgernd liegt es nahe, dass die S-Nitrosierung von mitochondrialem Connexin 43 für die Vermittlung des kardioprotektiven Signals von Bedeutung ist.

List of Abbreviations

18αGA	18α-glycyrrhetinic acid
aa	amino acid
ACN	acetonitrile
ADP	adenosine diphosphate
Akt	protein kinase B
AM	acetoxy methyl
AMP	adenosine monophosphate
ANOVA	analysis of variance
ATP	adenosine triphosphate
Bcl-2	B-cell lymphoma 2
BIAM	biotinylated iodoacetamide
BS3	bis(sulfosuccinimidyl)suberate
BSA	bovine serum albumin
Ca^{2+}	calcium
CBX	carbenoxolone
cGMP	cyclic guanosine monophosphate
CID	collision-induced dissociation
CL	cytoplasmic loop
Cl^-	chloride
CsA	cyclosporine A
C-terminal	carboxyl-terminal
Cx	connexin
dH_2O	distilled water
Da	Dalton
DMSO	dimethyl sulfoxide
DTT	dithiothreitol
E	extracellular loop
EDTA	ethylenediaminetetraacetic acid
EGTA	ethylene glycol tetraacetic acid
ERK	extracellular signal-regulated protein kinase
et al.	and others (*et alii*)
EtOH	ethanol

FCCP	p-triflouromethoxyphenylhydrazone
g	gravitational force
GAP26	connexin mimetic peptide
GAPDH	glyceraldehyde 3-phosphate dehydrogenase
GJ	gap junction
G-protein	guanosine nucleotide-binding protein
GSK	glycogen synthase kinase
GSNO	S-nitrosoglutathione
H^+	proton
HC	hemichannel
HDAC	histone deacetylase
HEPES	4-(2-hydroxyethyl)-1-piperazineethanesulfonic acid
HRP	horseradish peroxidase
IgG	immunoglobulin G
IFM	interfibrillar mitochondria
i.p.	intra peritoneal
IP	immunoprecipitation
IPC	ischemic preconditioning
JAK	Janus kinase
JNK	c-Jun N-terminal kinase
kDa	kilo Dalton
kg	kilogram
λ_{ex}	fluorescence excitation wavelength
λ_{em}	fluorescence emission wavelength
LC-MS	liquid chromatography-mass spectrometry
Li	Lithium
LY	Lucifer Yellow CH dilithium salt
MAPK	mitogen-activated protein kinase
mitoK_{ATP}	ATP-dependent potassium
mmHg	millimeters of mercury
MnSOD	manganese superoxide dismutase
MOPS	4-morpholinepropanesulfonic acid
MPTP	mitochondrial permeability transition pore
MS	mass spectrometry

mtCx43	mitochondrial connexin 43
n	sample size
Na^+	sodium
NaCl	sodium chloride
NAD^+	nicotinamide adenine dinucleotide
NADPH	nicotinamide adenine dinucleotide phosphate
NEM	N-ethylmaleimide
NO	nitric oxide
NOS	nitric oxide synthase
ns	not significant
N-terminal	amino-terminal
p	significance level
PBFI	potassium-binding benzofuran isophthalate
PBS	phosphate buffered saline
PC	preconditioning
pH	pondus Hydrogenii or potentia Hydrogenii
PK	protein kinase
PKA	protein kinase A
PKC	protein kinase C
PKG	protein kinase G
rIPC	remote ischemic preconditioning
RISK	reperfusion injury salvage kinases
RITC-dextran	rhodamine B isothiocyanate-dextran 10S
ROS	reactive oxygen species
rpm	rounds per minute
RV	right ventricle
SAFE	survivor activating factor enhancement
SBFI	sodium-binding benzofuran isophthalate
SDS	sodium dodecyl sulfate
SDS-PAGE	sodium dodecyl sulfate polyacrylamide gel electrophoresis
SEM	standard error of the mean
Ser368	serine residue 368
SERCA	sarcoendoplasmic reticulum calcium transport ATPase
SNAP	S-nitroso-N-acetyl-DL-penicillamine

SNO	S-nitrosation
SSM	subsarcolemmal mitochondria
STAT	signal transducer and activator of transcription
TEA	triethanolamine
TM	transmembrane
TMA	trimethylaluminium
TNF-α	tumor necrosis factor
TOM20	translocase of the outer membrane receptor unit 20
Tris	tris(hydroxymethyl)aminomethane)
U	units
UV	ultraviolet
VDAC	voltage dependent anion channel
v-src	viral sarcoma
v/v	volume per volume
wt/vol	weight per volume
y_j	ion energy

S.I. units, elements, and chemicals were abbreviated according to international standards and are not listed here.

List of Figures

List of Tables

Reference List

1. Abascal F, Zardoya R (2013) Evolutionary analyses of gap junction protein families. Biochim Biophys Acta 1828:4-14 doi:10.1016/j.bbamem.2012.02.007
2. Abu-Amara M, Yang SY, Quaglia A, Rowley P, de Mel A, Tapuria N, Seifalian A, Davidson B, Fuller B (2011) Nitric oxide is an essential mediator of the protective effects of remote ischaemic preconditioning in a mouse model of liver ischaemia/reperfusion injury. Clin Sci (Lond) 121:257-266 doi:10.1042/CS20100598
3. Agullo-Pascual E, Delmar M (2012) The noncanonical functions of Cx43 in the heart. J Membr Biol 245:477-482 doi:10.1007/s00232-012-9466-y
4. Agullo-Pascual E, Reid DA, Keegan S, Sidhu M, Fenyo D, Rothenberg E, Delmar M (2013) Super-resolution fluorescence microscopy of the cardiac connexome reveals plakophilin-2 inside the connexin43 plaque. Cardiovasc Res 100:231-240 doi:10.1093/cvr/cvt191
5. Althaus M, Pichl A, Clauss WG, Seeger W, Fronius M, Morty RE (2011) Nitric oxide inhibits highly selective sodium channels and the Na+/K+-ATPase in H441 cells. Am J Respir Cell Mol Biol 44:53-65 doi:10.1165/2009-0335OC
6. Aon MA, Cortassa S, Marban E, O'Rourke B (2003) Synchronized whole cell oscillations in mitochondrial metabolism triggered by a local release of reactive oxygen species in cardiac myocytes. J Biol Chem 278:44735-44744 doi:10.1074/jbc.M302673200
7. Balligand JL, Ungureanu-Longrois D, Simmons WW, Pimental D, Malinski TA, Kapturczak M, Taha Z, Lowenstein CJ, Davidoff AJ, Kelly RA, et al. (1994) Cytokine-inducible nitric oxide synthase (iNOS) expression in cardiac myocytes. Characterization and regulation of iNOS expression and detection of iNOS activity in single cardiac myocytes in vitro. J Biol Chem 269:27580-27588
8. Bao X, Altenberg GA, Reuss L (2004) Mechanism of regulation of the gap junction protein connexin 43 by protein kinase C-mediated phosphorylation. Am J Physiol Cell Physiol 286:C647-654 doi:10.1152/ajpcell.00295.2003
9. Bao X, Chen Y, Reuss L, Altenberg GA (2004) Functional expression in Xenopus oocytes of gap-junctional hemichannels formed by a cysteine-less connexin 43. J Biol Chem 279:9689-9692 doi:10.1074/jbc.M311438200
10. Bao X, Reuss L, Altenberg GA (2004) Regulation of purified and reconstituted connexin 43 hemichannels by protein kinase C-mediated phosphorylation of Serine 368. J Biol Chem 279:20058-20066 doi:10.1074/jbc.M311137200
11. Bargiello TA, Tang Q, Oh S, Kwon T (2012) Voltage-dependent conformational changes in connexin channels. Biochim Biophys Acta 1818:1807-1822 doi:10.1016/j.bbamem.2011.09.019
12. Barouch LA, Harrison RW, Skaf MW, Rosas GO, Cappola TP, Kobeissi ZA, Hobai IA, Lemmon CA, Burnett AL, O'Rourke B, Rodriguez ER, Huang PL, Lima JA, Berkowitz DE, Hare JM (2002) Nitric oxide regulates the heart by spatial confinement of nitric oxide synthase isoforms. Nature 416:337-339 doi:10.1038/416005a
13. Bates TE, Loesch A, Burnstock G, Clark JB (1995) Immunocytochemical evidence for a mitochondrially located nitric oxide synthase in brain and liver. Biochem Biophys Res Commun 213:896-900 doi:10.1006/bbrc.1995.2213
14. Bates TE, Loesch A, Burnstock G, Clark JB (1996) Mitochondrial nitric oxide synthase: a ubiquitous regulator of oxidative phosphorylation? Biochem Biophys Res Commun 218:40-44 doi:10.1006/bbrc.1996.0008

15. Beardslee MA, Laing JG, Beyer EC, Saffitz JE (1998) Rapid turnover of connexin43 in the adult rat heart. Circ Res 83:629-635
16. Beauloye C, Bertrand L, Horman S, Hue L (2011) AMPK activation, a preventive therapeutic target in the transition from cardiac injury to heart failure. Cardiovasc Res 90:224-233 doi:10.1093/cvr/cvr034
17. Beblo DA, Veenstra RD (1997) Monovalent cation permeation through the connexin40 gap junction channel. Cs, Rb, K, Na, Li, TEA, TMA, TBA, and effects of anions Br, Cl, F, acetate, aspartate, glutamate, and NO3. J Gen Physiol 109:509-522
18. Bell RM, Smith CC, Yellon DM (2002) Nitric oxide as a mediator of delayed pharmacological (A(1) receptor triggered) preconditioning; is eNOS masquerading as iNOS? Cardiovasc Res 53:405-413
19. Bell SP, Sack MN, Patel A, Opie LH, Yellon DM (2000) Delta opioid receptor stimulation mimics ischemic preconditioning in human heart muscle. J Am Coll Cardiol 36:2296-2302
20. Bernardi P (1999) Mitochondrial transport of cations: channels, exchangers, and permeability transition. Physiol Rev 79:1127-1155
21. Berthoud VM, Ledbetter ML, Hertzberg EL, Saez JC (1992) Connexin43 in MDCK cells: regulation by a tumor-promoting phorbol ester and Ca2+. Eur J Cell Biol 57:40-50
22. Bijur GN, Jope RS (2003) Rapid accumulation of Akt in mitochondria following phosphatidylinositol 3-kinase activation. J Neurochem 87:1427-1435
23. Birnbaum Y, Hale SL, Kloner RA (1997) Ischemic preconditioning at a distance: reduction of myocardial infarct size by partial reduction of blood supply combined with rapid stimulation of the gastrocnemius muscle in the rabbit. Circulation 96:1641-1646
24. Boengler K, Dodoni G, Rodriguez-Sinovas A, Cabestrero A, Ruiz-Meana M, Gres P, Konietzka I, Lopez-Iglesias C, Garcia-Dorado D, Di Lisa F, Heusch G, Schulz R (2005) Connexin 43 in cardiomyocyte mitochondria and its increase by ischemic preconditioning. Cardiovasc Res 67:234-244 doi:10.1016/j.cardiores.2005.04.014
25. Boengler K, Hilfiker-Kleiner D, Heusch G, Schulz R (2010) Inhibition of permeability transition pore opening by mitochondrial STAT3 and its role in myocardial ischemia/reperfusion. Basic Res Cardiol 105:771-785 doi:10.1007/s00395-010-0124-1
26. Boengler K, Ruiz-Meana M, Gent S, Ungefug E, Soetkamp D, Miro-Casas E, Cabestrero A, Fernandez-Sanz C, Semenzato M, Di Lisa F, Rohrbach S, Garcia-Dorado D, Heusch G, Schulz R (2012) Mitochondrial connexin 43 impacts on respiratory complex I activity and mitochondrial oxygen consumption. J Cell Mol Med 16:1649-1655 doi:10.1111/j.1582-4934.2011.01516.x
27. Boengler K, Schulz R, Heusch G (2006) Connexin 43 signalling and cardioprotection. Heart 92:1724-1727 doi:10.1136/hrt.2005.066878
28. Boengler K, Stahlhofen S, van de Sand A, Gres P, Ruiz-Meana M, Garcia-Dorado D, Heusch G, Schulz R (2009) Presence of connexin 43 in subsarcolemmal, but not in interfibrillar cardiomyocyte mitochondria. Basic Res Cardiol 104:141-147 doi:10.1007/s00395-009-0007-5
29. Boengler K, Ungefug E, Heusch G, Leybaert L, Schulz R (2013) Connexin 43 impacts on mitochondrial potassium uptake. Frontiers in pharmacology 4:73 doi:10.3389/fphar.2013.00073
30. Bolli R, Dawn B, Tang XL, Qiu Y, Ping P, Xuan YT, Jones WK, Takano H, Guo Y, Zhang J (1998) The nitric oxide hypothesis of late preconditioning. Basic Res Cardiol 93:325-338

31. Botker HE, Kharbanda R, Schmidt MR, Bottcher M, Kaltoft AK, Terkelsen CJ, Munk K, Andersen NH, Hansen TM, Trautner S, Lassen JF, Christiansen EH, Krusell LR, Kristensen SD, Thuesen L, Nielsen SS, Rehling M, Sorensen HT, Redington AN, Nielsen TT (2010) Remote ischaemic conditioning before hospital admission, as a complement to angioplasty, and effect on myocardial salvage in patients with acute myocardial infarction: a randomised trial. Lancet 375:727-734 doi:10.1016/S0140-6736(09)62001-8
32. Brink PR, Dewey MM (1980) Evidence for fixed charge in the nexus. Nature 285:101-102
33. Brink PR, Fan SF (1989) Patch clamp recordings from membranes which contain gap junction channels. Biophys J 56:579-593 doi:10.1016/S0006-3495(89)82705-5
34. Brisset AC, Isakson BE, Kwak BR (2009) Connexins in vascular physiology and pathology. Antioxid Redox Signal 11:267-282 doi:10.1089/ars.2008.2115
35. Brissette JL, Kumar NM, Gilula NB, Dotto GP (1991) The tumor promoter 12-O-tetradecanoylphorbol-13-acetate and the ras oncogene modulate expression and phosphorylation of gap junction proteins. Mol Cell Biol 11:5364-5371
36. Brookes P, Darley-Usmar VM (2002) Hypothesis: the mitochondrial NO(*) signaling pathway, and the transduction of nitrosative to oxidative cell signals: an alternative function for cytochrome C oxidase. Free Radic Biol Med 32:370-374
37. Brookes PS (2004) Mitochondrial nitric oxide synthase. Mitochondrion 3:187-204 doi:10.1016/j.mito.2003.10.001
38. Brown GC (2001) Regulation of mitochondrial respiration by nitric oxide inhibition of cytochrome c oxidase. Biochim Biophys Acta 1504:46-57
39. Bruzzone S, Guida L, Zocchi E, Franco L, De Flora A (2001) Connexin 43 hemi channels mediate Ca2+-regulated transmembrane NAD+ fluxes in intact cells. FASEB J 15:10-12 doi:10.1096/fj.00-0566fje
40. Bukauskas FF, Kreuzberg MM, Rackauskas M, Bukauskiene A, Bennett MV, Verselis VK, Willecke K (2006) Properties of mouse connexin 30.2 and human connexin 31.9 hemichannels: implications for atrioventricular conduction in the heart. Proc Natl Acad Sci U S A 103:9726-9731 doi:10.1073/pnas.0603372103
41. Bukauskas FF, Verselis VK (2004) Gap junction channel gating. Biochim Biophys Acta 1662:42-60 doi:10.1016/j.bbamem.2004.01.008
42. Burwell LS, Nadtochiy SM, Tompkins AJ, Young S, Brookes PS (2006) Direct evidence for S-nitrosation of mitochondrial complex I. Biochem J 394:627-634 doi:10.1042/BJ20051435
43. Cadenas E, Boveris A, Ragan CI, Stoppani AO (1977) Production of superoxide radicals and hydrogen peroxide by NADH-ubiquinone reductase and ubiquinol-cytochrome c reductase from beef-heart mitochondria. Arch Biochem Biophys 180:248-257
44. Camelliti P, Green CR, Kohl P (2006) Structural and functional coupling of cardiac myocytes and fibroblasts. Adv Cardiol 42:132-149 doi:10.1159/000092566
45. Chai YC, Hendrich S, Thomas JA (1994) Protein S-thiolation in hepatocytes stimulated by t-butyl hydroperoxide, menadione, and neutrophils. Arch Biochem Biophys 310:264-272 doi:10.1006/abbi.1994.1166
46. Chatterjee S, Stewart AS, Bish LT, Jayasankar V, Kim EM, Pirolli T, Burdick J, Woo YJ, Gardner TJ, Sweeney HL (2002) Viral gene transfer of the antiapoptotic factor Bcl-2 protects against chronic postischemic heart failure. Circulation 106:I212-217
47. Chen Q, Moghaddas S, Hoppel CL, Lesnefsky EJ (2006) Reversible blockade of electron transport during ischemia protects mitochondria and decreases

myocardial injury following reperfusion. J Pharmacol Exp Ther 319:1405-1412 doi:10.1124/jpet.106.110262
48. Chen Y, Deng Y, Bao X, Reuss L, Altenberg GA (2005) Mechanism of the defect in gap-junctional communication by expression of a connexin 26 mutant associated with dominant deafness. FASEB J 19:1516-1518 doi:10.1096/fj.04-3491fje
49. Chen Z, Chua CC, Ho YS, Hamdy RC, Chua BH (2001) Overexpression of Bcl-2 attenuates apoptosis and protects against myocardial I/R injury in transgenic mice. Am J Physiol Heart Circ Physiol 280:H2313-2320
50. Chen ZP, Mitchelhill KI, Michell BJ, Stapleton D, Rodriguez-Crespo I, Witters LA, Power DA, Ortiz de Montellano PR, Kemp BE (1999) AMP-activated protein kinase phosphorylation of endothelial NO synthase. FEBS Lett 443:285-289
51. Cheng A, Chan SL, Milhavet O, Wang S, Mattson MP (2001) p38 MAP kinase mediates nitric oxide-induced apoptosis of neural progenitor cells. J Biol Chem 276:43320-43327 doi:10.1074/jbc.M107698200
52. Cherian PP, Siller-Jackson AJ, Gu S, Wang X, Bonewald LF, Sprague E, Jiang JX (2005) Mechanical strain opens connexin 43 hemichannels in osteocytes: a novel mechanism for the release of prostaglandin. Mol Biol Cell 16:3100-3106 doi:10.1091/mbc.E04-10-0912
53. Chouchani ET, Hurd TR, Nadtochiy SM, Brookes PS, Fearnley IM, Lilley KS, Smith RA, Murphy MP (2010) Identification of S-nitrosated mitochondrial proteins by S-nitrosothiol difference in gel electrophoresis (SNO-DIGE): implications for the regulation of mitochondrial function by reversible S-nitrosation. Biochem J 430:49-59 doi:10.1042/BJ20100633
54. Chouchani ET, Methner C, Nadtochiy SM, Logan A, Pell VR, Ding S, James AM, Cocheme HM, Reinhold J, Lilley KS, Partridge L, Fearnley IM, Robinson AJ, Hartley RC, Smith RA, Krieg T, Brookes PS, Murphy MP (2013) Cardioprotection by S-nitrosation of a cysteine switch on mitochondrial complex I. Nat Med 19:753-759 doi:10.1038/nm.3212
55. Clarke TC, Williams OJ, Martin PE, Evans WH (2009) ATP release by cardiac myocytes in a simulated ischaemia model: inhibition by a connexin mimetic and enhancement by an antiarrhythmic peptide. Eur J Pharmacol 605:9-14 doi:10.1016/j.ejphar.2008.12.005
56. Cohen MV, Walsh RS, Goto M, Downey JM (1995) Hypoxia preconditions rabbit myocardium via adenosine and catecholamine release. J Mol Cell Cardiol 27:1527-1534
57. Cohen MV, Yang XM, Downey JM (1994) Conscious rabbits become tolerant to multiple episodes of ischemic preconditioning. Circ Res 74:998-1004
58. Cohen MV, Yang XM, Liu Y, Solenkova NV, Downey JM (2010) Cardioprotective PKG-independent NO signaling at reperfusion. Am J Physiol Heart Circ Physiol 299:H2028-2036 doi:10.1152/ajpheart.00527.2010
59. Contreras JE, Saez JC, Bukauskas FF, Bennett MV (2003) Gating and regulation of connexin 43 (Cx43) hemichannels. Proc Natl Acad Sci U S A 100:11388-11393 doi:10.1073/pnas.1434298100
60. Contreras JE, Sanchez HA, Eugenin EA, Speidel D, Theis M, Willecke K, Bukauskas FF, Bennett MV, Saez JC (2002) Metabolic inhibition induces opening of unapposed connexin 43 gap junction hemichannels and reduces gap junctional communication in cortical astrocytes in culture. Proc Natl Acad Sci U S A 99:495-500 doi:10.1073/pnas.012589799
61. Contreras JE, Sanchez HA, Veliz LP, Bukauskas FF, Bennett MV, Saez JC (2004) Role of connexin-based gap junction channels and hemichannels in ischemia-

induced cell death in nervous tissue. Brain Res Brain Res Rev 47:290-303 doi:10.1016/j.brainresrev.2004.08.002
62. Cosby K, Partovi KS, Crawford JH, Patel RP, Reiter CD, Martyr S, Yang BK, Waclawiw MA, Zalos G, Xu X, Huang KT, Shields H, Kim-Shapiro DB, Schechter AN, Cannon RO, 3rd, Gladwin MT (2003) Nitrite reduction to nitric oxide by deoxyhemoglobin vasodilates the human circulation. Nat Med 9:1498-1505 doi:10.1038/nm954
63. Costa AD, Garlid KD, West IC, Lincoln TM, Downey JM, Cohen MV, Critz SD (2005) Protein kinase G transmits the cardioprotective signal from cytosol to mitochondria. Circ Res 97:329-336 doi:10.1161/01.RES.0000178451.08719.5b
64. Crow DS, Beyer EC, Paul DL, Kobe SS, Lau AF (1990) Phosphorylation of connexin43 gap junction protein in uninfected and Rous sarcoma virus-transformed mammalian fibroblasts. Mol Cell Biol 10:1754-1763
65. Dang X, Doble BW, Kardami E (2003) The carboxy-tail of connexin-43 localizes to the nucleus and inhibits cell growth. Mol Cell Biochem 242:35-38
66. Davidson JS, Baumgarten IM (1988) Glycyrrhetinic acid derivatives: a novel class of inhibitors of gap-junctional intercellular communication. Structure-activity relationships. J Pharmacol Exp Ther 246:1104-1107
67. Davidson JS, Baumgarten IM (1988) Glycyrrhetinic acid derivatives: a novel class of inhibitors of gap-junctional intercellular communication. Structure-activity relationships. J Pharmacol Exp Ther 246:1104-1107
68. Davidson JS, Baumgarten IM, Harley EH (1986) Reversible inhibition of intercellular junctional communication by glycyrrhetinic acid. Biochem Biophys Res Commun 134:29-36
69. Davies WR, Brown AJ, Watson W, McCormick LM, West NE, Dutka DP, Hoole SP (2013) Remote ischemic preconditioning improves outcome at 6 years after elective percutaneous coronary intervention: the CRISP stent trial long-term follow-up. Circulation Cardiovascular interventions 6:246-251 doi:10.1161/CIRCINTERVENTIONS.112.000184
70. de Groot JR, Veenstra T, Verkerk AO, Wilders R, Smits JP, Wilms-Schopman FJ, Wiegerinck RF, Bourier J, Belterman CN, Coronel R, Verheijck EE (2003) Conduction slowing by the gap junctional uncoupler carbenoxolone. Cardiovasc Res 60:288-297
71. De Maio A, Vega VL, Contreras JE (2002) Gap junctions, homeostasis, and injury. J Cell Physiol 191:269-282 doi:10.1002/jcp.10108
72. De Mello WC (1975) Effect of intracellular injection of calcium and strontium on cell communication in heart. The Journal of physiology 250:231-245
73. Delmar M, Coombs W, Sorgen P, Duffy HS, Taffet SM (2004) Structural bases for the chemical regulation of Connexin43 channels. Cardiovasc Res 62:268-275 doi:10.1016/j.cardiores.2003.12.030
74. Dickson EW, Lorbar M, Porcaro WA, Fenton RA, Reinhardt CP, Gysembergh A, Przyklenk K (1999) Rabbit heart can be "preconditioned" via transfer of coronary effluent. Am J Physiol 277:H2451-2457
75. Dickson EW, Reinhardt CP, Renzi FP, Becker RC, Porcaro WA, Heard SO (1999) Ischemic preconditioning may be transferable via whole blood transfusion: preliminary evidence. J Thromb Thrombolysis 8:123-129
76. Donoso P, Mill JG, O'Neill SC, Eisner DA (1992) Fluorescence measurements of cytoplasmic and mitochondrial sodium concentration in rat ventricular myocytes. The Journal of physiology 448:493-509
77. Duan JM, Karmazyn M (1989) Acute effects of hypoxia and phosphate on two populations of heart mitochondria. Mol Cell Biochem 90:47-56

78. Duffy HS (2012) The molecular mechanisms of gap junction remodeling. Heart Rhythm 9:1331-1334 doi:10.1016/j.hrthm.2011.11.048
79. Duranski MR, Greer JJ, Dejam A, Jaganmohan S, Hogg N, Langston W, Patel RP, Yet SF, Wang X, Kevil CG, Gladwin MT, Lefer DJ (2005) Cytoprotective effects of nitrite during in vivo ischemia-reperfusion of the heart and liver. J Clin Invest 115:1232-1240 doi:10.1172/JCI22493
80. Dutka TL, Mollica JP, Posterino GS, Lamb GD (2011) Modulation of contractile apparatus Ca2+ sensitivity and disruption of excitation-contraction coupling by S-nitrosoglutathione in rat muscle fibres. The Journal of physiology 589:2181-2196 doi:10.1113/jphysiol.2010.200451
81. Ek-Vitorin JF, King TJ, Heyman NS, Lampe PD, Burt JM (2006) Selectivity of connexin 43 channels is regulated through protein kinase C-dependent phosphorylation. Circ Res 98:1498-1505 doi:10.1161/01.RES.0000227572.45891.2c
82. Espey MG, Miranda KM, Thomas DD, Xavier S, Citrin D, Vitek MP, Wink DA (2002) A chemical perspective on the interplay between NO, reactive oxygen species, and reactive nitrogen oxide species. Ann N Y Acad Sci 962:195-206
83. Eugenin EA, Basilio D, Saez JC, Orellana JA, Raine CS, Bukauskas F, Bennett MV, Berman JW (2012) The role of gap junction channels during physiologic and pathologic conditions of the human central nervous system. J Neuroimmune Pharmacol 7:499-518 doi:10.1007/s11481-012-9352-5
84. Evans WH, Carlile G, Rahman S, Torok K (1992) Gap junction communication channel: peptides and anti-peptide antibodies as structural probes. Biochem Soc Trans 20:856-861
85. Fan WJ, van Vuuren D, Genade S, Lochner A (2010) Kinases and phosphatases in ischaemic preconditioning: a re-evaluation. Basic Res Cardiol 105:495-511 doi:10.1007/s00395-010-0086-3
86. Fasciani I, Temperan A, Perez-Atencio LF, Escudero A, Martinez-Montero P, Molano J, Gomez-Hernandez JM, Paino CL, Gonzalez-Nieto D, Barrio LC (2013) Regulation of connexin hemichannel activity by membrane potential and the extracellular calcium in health and disease. Neuropharmacology 75:479-490 doi:10.1016/j.neuropharm.2013.03.040
87. Feliciello A, Gottesman ME, Avvedimento EV (2001) The biological functions of A-kinase anchor proteins. J Mol Biol 308:99-114 doi:10.1006/jmbi.2001.4585
88. Fellet AL, Balaszczuk AM, Arranz C, Lopez-Costa JJ, Boveris A, Bustamante J (2006) Autonomic regulation of pacemaker activity: role of heart nitric oxide synthases. Am J Physiol Heart Circ Physiol 291:H1246-1254 doi:10.1152/ajpheart.00711.2005
89. Flagg-Newton J, Simpson I, Loewenstein WR (1979) Permeability of the cell-to-cell membrane channels in mammalian cell juncton. Science 205:404-407
90. Foote CI, Zhou L, Zhu X, Nicholson BJ (1998) The pattern of disulfide linkages in the extracellular loop regions of connexin 32 suggests a model for the docking interface of gap junctions. J Cell Biol 140:1187-1197
91. Francis D, Stergiopoulos K, Ek-Vitorin JF, Cao FL, Taffet SM, Delmar M (1999) Connexin diversity and gap junction regulation by pHi. Dev Genet 24:123-136 doi:10.1002/(SICI)1520-6408(1999)24:1/2<123::AID-DVG12>3.0.CO;2-H
92. French S, Giulivi C, Balaban RS (2001) Nitric oxide synthase in porcine heart mitochondria: evidence for low physiological activity. Am J Physiol Heart Circ Physiol 280:H2863-2867
93. Fryer RM, Hsu AK, Gross GJ (2001) ERK and p38 MAP kinase activation are components of opioid-induced delayed cardioprotection. Basic Res Cardiol 96:136-142

94. Gao S, Chen J, Brodsky SV, Huang H, Adler S, Lee JH, Dhadwal N, Cohen-Gould L, Gross SS, Goligorsky MS (2004) Docking of endothelial nitric oxide synthase (eNOS) to the mitochondrial outer membrane: a pentabasic amino acid sequence in the autoinhibitory domain of eNOS targets a proteinase K-cleavable peptide on the cytoplasmic face of mitochondria. J Biol Chem 279:15968-15974 doi:10.1074/jbc.M308504200
95. Gho BC, Schoemaker RG, van den Doel MA, Duncker DJ, Verdouw PD (1996) Myocardial protection by brief ischemia in noncardiac tissue. Circulation 94:2193-2200
96. Goldberg GS, Moreno AP, Bechberger JF, Hearn SS, Shivers RR, MacPhee DJ, Zhang YC, Naus CC (1996) Evidence that disruption of connexon particle arrangements in gap junction plaques is associated with inhibition of gap junctional communication by a glycyrrhetinic acid derivative. Exp Cell Res 222:48-53 doi:10.1006/excr.1996.0006
97. Goldberg GS, Moreno AP, Lampe PD (2002) Gap junctions between cells expressing connexin 43 or 32 show inverse permselectivity to adenosine and ATP. J Biol Chem 277:36725-36730 doi:10.1074/jbc.M109797200
98. Gonzalez D, Gomez-Hernandez JM, Barrio LC (2007) Molecular basis of voltage dependence of connexin channels: an integrative appraisal. Prog Biophys Mol Biol 94:66-106 doi:10.1016/j.pbiomolbio.2007.03.007
99. Gonzalez DR, Beigi F, Treuer AV, Hare JM (2007) Deficient ryanodine receptor S-nitrosylation increases sarcoplasmic reticulum calcium leak and arrhythmogenesis in cardiomyocytes. Proc Natl Acad Sci U S A 104:20612-20617 doi:10.1073/pnas.0706796104
100. Goto M, Liu Y, Yang XM, Ardell JL, Cohen MV, Downey JM (1995) Role of bradykinin in protection of ischemic preconditioning in rabbit hearts. Circ Res 77:611-621
101. Grek CL, Zhang J, Manevich Y, Townsend DM, Tew KD (2013) Causes and consequences of cysteine S-glutathionylation. J Biol Chem 288:26497-26504 doi:10.1074/jbc.R113.461368
102. Grund F, Sommerschild HT, Kirkeboen KA, Ilebekk A (1997) Proarrhythmic effects of ischemic preconditioning in anesthetized pigs. Basic Res Cardiol 92:417-425
103. Gutierrez PL (2000) The role of NAD(P)H oxidoreductase (DT-Diaphorase) in the bioactivation of quinone-containing antitumor agents: a review. Free Radic Biol Med 29:263-275
104. Hagar JM, Hale SL, Kloner RA (1991) Effect of preconditioning ischemia on reperfusion arrhythmias after coronary artery occlusion and reperfusion in the rat. Circ Res 68:61-68
105. Handy DE, Loscalzo J (2006) Nitric oxide and posttranslational modification of the vascular proteome: S-nitrosation of reactive thiols. Arterioscler Thromb Vasc Biol 26:1207-1214 doi:10.1161/01.ATV.0000217632.98717.a0
106. Hansford RG, Hogue BA, Mildaziene V (1997) Dependence of H2O2 formation by rat heart mitochondria on substrate availability and donor age. J Bioenerg Biomembr 29:89-95
107. Hare JM (2003) Nitric oxide and excitation-contraction coupling. J Mol Cell Cardiol 35:719-729
108. Harris AL (2002) Voltage-sensing and substate rectification: moving parts of connexin channels. J Gen Physiol 119:165-169
109. Hausenloy DJ, Erik Botker H, Condorelli G, Ferdinandy P, Garcia-Dorado D, Heusch G, Lecour S, van Laake LW, Madonna R, Ruiz-Meana M, Schulz R, Sluijter

JP, Yellon DM, Ovize M (2013) Translating cardioprotection for patient benefit: position paper from the Working Group of Cellular Biology of the Heart of the European Society of Cardiology. Cardiovasc Res 98:7-27 doi:10.1093/cvr/cvt004
110. Hausenloy DJ, Maddock HL, Baxter GF, Yellon DM (2002) Inhibiting mitochondrial permeability transition pore opening: a new paradigm for myocardial preconditioning? Cardiovasc Res 55:534-543
111. Hausenloy DJ, Mwamure PK, Venugopal V, Harris J, Barnard M, Grundy E, Ashley E, Vichare S, Di Salvo C, Kolvekar S, Hayward M, Keogh B, MacAllister RJ, Yellon DM (2007) Effect of remote ischaemic preconditioning on myocardial injury in patients undergoing coronary artery bypass graft surgery: a randomised controlled trial. Lancet 370:575-579 doi:10.1016/S0140-6736(07)61296-3
112. Hausenloy DJ, Tsang A, Mocanu MM, Yellon DM (2005) Ischemic preconditioning protects by activating prosurvival kinases at reperfusion. Am J Physiol Heart Circ Physiol 288:H971-976 doi:10.1152/ajpheart.00374.2004
113. Hawat G, Benderdour M, Rousseau G, Baroudi G (2010) Connexin 43 mimetic peptide Gap26 confers protection to intact heart against myocardial ischemia injury. Pflugers Arch 460:583-592 doi:10.1007/s00424-010-0849-6
114. Heidbreder M, Naumann A, Tempel K, Dominiak P, Dendorfer A (2008) Remote vs. ischaemic preconditioning: the differential role of mitogen-activated protein kinase pathways. Cardiovasc Res 78:108-115 doi:10.1093/cvr/cvm114
115. Heinzel FR, Luo Y, Li X, Boengler K, Buechert A, Garcia-Dorado D, Di Lisa F, Schulz R, Heusch G (2005) Impairment of diazoxide-induced formation of reactive oxygen species and loss of cardioprotection in connexin 43 deficient mice. Circ Res 97:583-586 doi:10.1161/01.RES.0000181171.65293.65
116. Hendgen-Cotta UB, Merx MW, Shiva S, Schmitz J, Becher S, Klare JP, Steinhoff HJ, Goedecke A, Schrader J, Gladwin MT, Kelm M, Rassaf T (2008) Nitrite reductase activity of myoglobin regulates respiration and cellular viability in myocardial ischemia-reperfusion injury. Proc Natl Acad Sci U S A 105:10256-10261 doi:10.1073/pnas.0801336105
117. Herve JC, Derangeon M, Sarrouilhe D, Giepmans BN, Bourmeyster N (2012) Gap junctional channels are parts of multiprotein complexes. Biochim Biophys Acta 1818:1844-1865 doi:10.1016/j.bbamem.2011.12.009
118. Hess DT, Matsumoto A, Kim SO, Marshall HE, Stamler JS (2005) Protein S-nitrosylation: purview and parameters. Nat Rev Mol Cell Biol 6:150-166 doi:10.1038/nrm1569
119. Heusch G, Boengler K, Schulz R (2008) Cardioprotection: nitric oxide, protein kinases, and mitochondria. Circulation 118:1915-1919 doi:10.1161/CIRCULATIONAHA.108.805242
120. Heusch G, Musiolik J, Kottenberg E, Peters J, Jakob H, Thielmann M (2012) STAT5 activation and cardioprotection by remote ischemic preconditioning in humans: short communication. Circ Res 110:111-115 doi:10.1161/CIRCRESAHA.111.259556
121. Hirst-Jensen BJ, Sahoo P, Kieken F, Delmar M, Sorgen PL (2007) Characterization of the pH-dependent interaction between the gap junction protein connexin43 carboxyl terminus and cytoplasmic loop domains. J Biol Chem 282:5801-5813 doi:10.1074/jbc.M605233200
122. Holmuhamedov EL, Oberlin A, Short K, Terzic A, Jahangir A (2012) Cardiac subsarcolemmal and interfibrillar mitochondria display distinct responsiveness to protection by diazoxide. PLoS ONE 7:e44667 doi:10.1371/journal.pone.0044667
123. Hoole SP, Heck PM, Sharples L, Khan SN, Duehmke R, Densem CG, Clarke SC, Shapiro LM, Schofield PM, O'Sullivan M, Dutka DP (2009) Cardiac Remote

Ischemic Preconditioning in Coronary Stenting (CRISP Stent) Study: a prospective, randomized control trial. Circulation 119:820-827 doi:10.1161/CIRCULATIONAHA.108.809723
124. Hoppel CL, Tandler B, Fujioka H, Riva A (2009) Dynamic organization of mitochondria in human heart and in myocardial disease. Int J Biochem Cell Biol 41:1949-1956 doi:10.1016/j.biocel.2009.05.004
125. Hotta Y, Otsuka-Murakami H, Fujita M, Nakagawa J, Yajima M, Liu W, Ishikawa N, Kawai N, Masumizu T, Kohno M (1999) Protective role of nitric oxide synthase against ischemia-reperfusion injury in guinea pig myocardial mitochondria. Eur J Pharmacol 380:37-48
126. Hua VB, Chang AB, Tchieu JH, Kumar NM, Nielsen PA, Saier MH, Jr. (2003) Sequence and phylogenetic analyses of 4 TMS junctional proteins of animals: connexins, innexins, claudins and occludins. J Membr Biol 194:59-76 doi:10.1007/s00232-003-2026-8
127. Huang RY, Laing JG, Kanter EM, Berthoud VM, Bao M, Rohrs HW, Townsend RR, Yamada KA (2011) Identification of CaMKII phosphorylation sites in Connexin43 by high-resolution mass spectrometry. J Proteome Res 10:1098-1109 doi:10.1021/pr1008702
128. Huffman LC, Koch SE, Butler KL (2008) Coronary effluent from a preconditioned heart activates the JAK-STAT pathway and induces cardioprotection in a donor heart. Am J Physiol Heart Circ Physiol 294:H257-262 doi:10.1152/ajpheart.00769.2007
129. Imahashi K, Schneider MD, Steenbergen C, Murphy E (2004) Transgenic expression of Bcl-2 modulates energy metabolism, prevents cytosolic acidification during ischemia, and reduces ischemia/reperfusion injury. Circ Res 95:734-741 doi:10.1161/01.RES.0000143898.67182.4c
130. Imanaga I, Kameyama M, Irisawa H (1987) Cell-to-cell diffusion of fluorescent dyes in paired ventricular cells. Am J Physiol 252:H223-232
131. Ivanics T, Blum H, Wroblewski K, Wang DJ, Osbakken M (1994) Intracellular sodium in cardiomyocytes using 23Na nuclear magnetic resonance. Biochim Biophys Acta 1221:133-144
132. Iwakiri Y, Satoh A, Chatterjee S, Toomre DK, Chalouni CM, Fulton D, Groszmann RJ, Shah VH, Sessa WC (2006) Nitric oxide synthase generates nitric oxide locally to regulate compartmentalized protein S-nitrosylation and protein trafficking. Proc Natl Acad Sci U S A 103:19777-19782 doi:10.1073/pnas.0605907103
133. Jaffrey SR, Snyder SH (2001) The biotin switch method for the detection of S-nitrosylated proteins. Sci STKE 2001:pl1 doi:10.1126/stke.2001.86.pl1
134. Jain SK, Schuessler RB, Saffitz JE (2003) Mechanisms of delayed electrical uncoupling induced by ischemic preconditioning. Circ Res 92:1138-1144 doi:10.1161/01.RES.0000074883.66422.C5
135. Jensen RV, Stottrup NB, Kristiansen SB, Botker HE (2012) Release of a humoral circulating cardioprotective factor by remote ischemic preconditioning is dependent on preserved neural pathways in diabetic patients. Basic Res Cardiol 107:285 doi:10.1007/s00395-012-0285-1
136. John SA, Kondo R, Wang SY, Goldhaber JI, Weiss JN (1999) Connexin-43 hemichannels opened by metabolic inhibition. J Biol Chem 274:236-240
137. Jones SP, Bolli R (2006) The ubiquitous role of nitric oxide in cardioprotection. J Mol Cell Cardiol 40:16-23 doi:10.1016/j.yjmcc.2005.09.011

138. Jung DW, Apel LM, Brierley GP (1992) Transmembrane gradients of free Na+ in isolated heart mitochondria estimated using a fluorescent probe. Am J Physiol 262:C1047-1055
139. Kadle R, Zhang JT, Nicholson BJ (1991) Tissue-specific distribution of differentially phosphorylated forms of Cx43. Mol Cell Biol 11:363-369
140. Kanai AJ, Pearce LL, Clemens PR, Birder LA, VanBibber MM, Choi SY, de Groat WC, Peterson J (2001) Identification of a neuronal nitric oxide synthase in isolated cardiac mitochondria using electrochemical detection. Proc Natl Acad Sci U S A 98:14126-14131 doi:10.1073/pnas.241380298
141. Kanaporis G, Brink PR, Valiunas V (2011) Gap junction permeability: selectivity for anionic and cationic probes. Am J Physiol Cell Physiol 300:C600-609 doi:10.1152/ajpcell.00316.2010
142. Kanaporis G, Mese G, Valiuniene L, White TW, Brink PR, Valiunas V (2008) Gap junction channels exhibit connexin-specific permeability to cyclic nucleotides. J Gen Physiol 131:293-305 doi:10.1085/jgp.200709934
143. Kaszala K, Vegh A, Papp JG, Parratt JR (1996) Time course of the protection against ischaemia and reperfusion-induced ventricular arrhythmias resulting from brief periods of cardiac pacing. J Mol Cell Cardiol 28:2085-2095 doi:10.1006/jmcc.1996.0201
144. Katoh H, Nishigaki N, Hayashi H (2002) Diazoxide opens the mitochondrial permeability transition pore and alters Ca2+ transients in rat ventricular myocytes. Circulation 105:2666-2671
145. Kharbanda RK, Li J, Konstantinov IE, Cheung MM, White PA, Frndova H, Stokoe J, Cox P, Vogel M, Van Arsdell G, MacAllister R, Redington AN (2006) Remote ischaemic preconditioning protects against cardiopulmonary bypass-induced tissue injury: a preclinical study. Heart 92:1506-1511 doi:10.1136/hrt.2004.042366
146. Kim B, Matsuoka S (2008) Cytoplasmic Na+-dependent modulation of mitochondrial Ca2+ via electrogenic mitochondrial Na+-Ca2+ exchange. The Journal of physiology 586:1683-1697 doi:10.1113/jphysiol.2007.148726
147. Kirsch M, Buscher AM, Aker S, Schulz R, de Groot H (2009) New insights into the S-nitrosothiol-ascorbate reaction. The formation of nitroxyl. Org Biomol Chem 7:1954-1962 doi:10.1039/b901046g
148. Kleinbongard P, Dejam A, Lauer T, Rassaf T, Schindler A, Picker O, Scheeren T, Godecke A, Schrader J, Schulz R, Heusch G, Schaub GA, Bryan NS, Feelisch M, Kelm M (2003) Plasma nitrite reflects constitutive nitric oxide synthase activity in mammals. Free Radic Biol Med 35:790-796
149. Kohr MJ, Aponte AM, Sun J, Wang G, Murphy E, Gucek M, Steenbergen C (2011) Characterization of potential S-nitrosylation sites in the myocardium. Am J Physiol Heart Circ Physiol 300:H1327-1335 doi:10.1152/ajpheart.00997.2010
150. Kohr MJ, Sun J, Aponte A, Wang G, Gucek M, Murphy E, Steenbergen C (2011) Simultaneous measurement of protein oxidation and S-nitrosylation during preconditioning and ischemia/reperfusion injury with resin-assisted capture. Circ Res 108:418-426 doi:10.1161/CIRCRESAHA.110.232173
151. Kovanich D, van der Heyden MA, Aye TT, van Veen TA, Heck AJ, Scholten A (2010) Sphingosine kinase interacting protein is an A-kinase anchoring protein specific for type I cAMP-dependent protein kinase. Chembiochem 11:963-971 doi:10.1002/cbic.201000058
152. Kozoriz MG, Church J, Ozog MA, Naus CC, Krebs C (2010) Temporary sequestration of potassium by mitochondria in astrocytes. J Biol Chem 285:31107-31119 doi:10.1074/jbc.M109.082073

153. Krieg T, Qin Q, McIntosh EC, Cohen MV, Downey JM (2002) ACh and adenosine activate PI3-kinase in rabbit hearts through transactivation of receptor tyrosine kinases. Am J Physiol Heart Circ Physiol 283:H2322-2330 doi:10.1152/ajpheart.00474.2002
154. Kronengold J, Srinivas M, Verselis VK (2012) The N-terminal half of the connexin protein contains the core elements of the pore and voltage gates. J Membr Biol 245:453-463 doi:10.1007/s00232-012-9457-z
155. Kwak BR, van Veen TA, Analbers LJ, Jongsma HJ (1995) TPA increases conductance but decreases permeability in neonatal rat cardiomyocyte gap junction channels. Exp Cell Res 220:456-463 doi:10.1006/excr.1995.1337
156. Lacza Z, Pankotai E, Busija DW (2009) Mitochondrial nitric oxide synthase: current concepts and controversies. Front Biosci (Landmark Ed) 14:4436-4443
157. Laird DW, Puranam KL, Revel JP (1991) Turnover and phosphorylation dynamics of connexin43 gap junction protein in cultured cardiac myocytes. Biochem J 273(Pt 1):67-72
158. Lampe PD, Lau AF (2000) Regulation of gap junctions by phosphorylation of connexins. Arch Biochem Biophys 384:205-215 doi:10.1006/abbi.2000.2131
159. Lampe PD, TenBroek EM, Burt JM, Kurata WE, Johnson RG, Lau AF (2000) Phosphorylation of connexin43 on serine368 by protein kinase C regulates gap junctional communication. J Cell Biol 149:1503-1512
160. Lau AF, Hatch-Pigott V, Crow DS (1991) Evidence that heart connexin43 is a phosphoprotein. J Mol Cell Cardiol 23:659-663
161. Li F, Sugishita K, Su Z, Ueda I, Barry WH (2001) Activation of connexin-43 hemichannels can elevate [Ca(2+)]i and [Na(+)]i in rabbit ventricular myocytes during metabolic inhibition. J Mol Cell Cardiol 33:2145-2155 doi:10.1006/jmcc.2001.1477
162. Li G, Whittaker P, Yao M, Kloner RA, Przyklenk K (2002) The gap junction uncoupler heptanol abrogates infarct size reduction with preconditioning in mouse hearts. Cardiovascular pathology : the official journal of the Society for Cardiovascular Pathology 11:158-165
163. Li H, Liu TF, Lazrak A, Peracchia C, Goldberg GS, Lampe PD, Johnson RG (1996) Properties and regulation of gap junctional hemichannels in the plasma membranes of cultured cells. J Cell Biol 134:1019-1030
164. Li L, Lorenzo PS, Bogi K, Blumberg PM, Yuspa SH (1999) Protein kinase Cdelta targets mitochondria, alters mitochondrial membrane potential, and induces apoptosis in normal and neoplastic keratinocytes when overexpressed by an adenoviral vector. Mol Cell Biol 19:8547-8558
165. Li WE, Nagy JI (2000) Activation of fibres in rat sciatic nerve alters phosphorylation state of connexin-43 at astrocytic gap junctions in spinal cord: evidence for junction regulation by neuronal-glial interactions. Neuroscience 97:113-123
166. Li WE, Nagy JI (2000) Connexin43 phosphorylation state and intercellular communication in cultured astrocytes following hypoxia and protein phosphatase inhibition. Eur J Neurosci 12:2644-2650
167. Li X, Heinzel FR, Boengler K, Schulz R, Heusch G (2004) Role of connexin 43 in ischemic preconditioning does not involve intercellular communication through gap junctions. J Mol Cell Cardiol 36:161-163
168. Lieberman SJ, Wasco W, MacLeod J, Satir P, Orr GA (1988) Immunogold localization of the regulatory subunit of a type II cAMP-dependent protein kinase tightly associated with mammalian sperm flagella. J Cell Biol 107:1809-1816

169. Lim SY, Yellon DM, Hausenloy DJ (2010) The neural and humoral pathways in remote limb ischemic preconditioning. Basic Res Cardiol 105:651-655 doi:10.1007/s00395-010-0099-y
170. Lin J, Steenbergen C, Murphy E, Sun J (2009) Estrogen receptor-beta activation results in S-nitrosylation of proteins involved in cardioprotection. Circulation 120:245-254 doi:10.1161/CIRCULATIONAHA.109.868729
171. Liu GS, Thornton J, Van Winkle DM, Stanley AW, Olsson RA, Downey JM (1991) Protection against infarction afforded by preconditioning is mediated by A1 adenosine receptors in rabbit heart. Circulation 84:350-356
172. Loo LW, Berestecky JM, Kanemitsu MY, Lau AF (1995) pp60src-mediated phosphorylation of connexin 43, a gap junction protein. J Biol Chem 270:12751-12761
173. Lundberg JO, Weitzberg E, Gladwin MT (2008) The nitrate-nitrite-nitric oxide pathway in physiology and therapeutics. Nat Rev Drug Discov 7:156-167 doi:10.1038/nrd2466
174. Maeda S, Nakagawa S, Suga M, Yamashita E, Oshima A, Fujiyoshi Y, Tsukihara T (2009) Structure of the connexin 26 gap junction channel at 3.5 A resolution. Nature 458:597-602 doi:10.1038/nature07869
175. Makowski L, Caspar DL, Phillips WC, Goodenough DA (1984) Gap junction structures. V. Structural chemistry inferred from X-ray diffraction measurements on sucrose accessibility and trypsin susceptibility. J Mol Biol 174:449-481
176. Marquez-Rosado L, Solan JL, Dunn CA, Norris RP, Lampe PD (2012) Connexin43 phosphorylation in brain, cardiac, endothelial and epithelial tissues. Biochim Biophys Acta 1818:1985-1992 doi:10.1016/j.bbamem.2011.07.028
177. Martin C, Schulz R, Post H, Boengler K, Kelm M, Kleinbongard P, Gres P, Skyschally A, Konietzka I, Heusch G (2007) Microdialysis-based analysis of interstitial NO in situ: NO synthase-independent NO formation during myocardial ischemia. Cardiovasc Res 74:46-55 doi:10.1016/j.cardiores.2006.12.020
178. Martinez-Ruiz A, Lamas S (2004) S-nitrosylation: a potential new paradigm in signal transduction. Cardiovasc Res 62:43-52 doi:10.1016/j.cardiores.2004.01.013
179. Maulik N, Yoshida T, Engelman RM, Deaton D, Flack JE, 3rd, Rousou JA, Das DK (1998) Ischemic preconditioning attenuates apoptotic cell death associated with ischemia/reperfusion. Mol Cell Biochem 186:139-145
180. Maurer P, Weingart R (1987) Cell pairs isolated from adult guinea pig and rat hearts: effects of [Ca2+]i on nexal membrane resistance. Pflugers Arch 409:394-402
181. McMillin-Wood J, Wolkowicz PE, Chu A, Tate CA, Goldstein MA, Entman ML (1980) Calcium uptake by two preparations of mitochondria from heart. Biochim Biophys Acta 591:251-265
182. Mese G, Richard G, White TW (2007) Gap junctions: basic structure and function. J Invest Dermatol 127:2516-2524 doi:10.1038/sj.jid.5700770
183. Methner C, Schmidt K, Cohen MV, Downey JM, Krieg T (2010) Both A2a and A2b adenosine receptors at reperfusion are necessary to reduce infarct size in mouse hearts. Am J Physiol Heart Circ Physiol 299:H1262-1264 doi:10.1152/ajpheart.00181.2010
184. Miro-Casas E, Ruiz-Meana M, Agullo E, Stahlhofen S, Rodriguez-Sinovas A, Cabestrero A, Jorge I, Torre I, Vazquez J, Boengler K, Schulz R, Heusch G, Garcia-Dorado D (2009) Connexin43 in cardiomyocyte mitochondria contributes to mitochondrial potassium uptake. Cardiovasc Res 83:747-756 doi:10.1093/cvr/cvp157
185. Miura T, Miki T, Yano T (2010) Role of the gap junction in ischemic preconditioning in the heart. Am J Physiol Heart Circ Physiol 298:H1115-1125 doi:10.1152/ajpheart.00879.2009

186. Miura T, Ohnuma Y, Kuno A, Tanno M, Ichikawa Y, Nakamura Y, Yano T, Miki T, Sakamoto J, Shimamoto K (2004) Protective role of gap junctions in preconditioning against myocardial infarction. Am J Physiol Heart Circ Physiol 286:H214-221 doi:10.1152/ajpheart.00441.2003
187. Mocanu MM, Bell RM, Yellon DM (2002) PI3 kinase and not p42/p44 appears to be implicated in the protection conferred by ischemic preconditioning. J Mol Cell Cardiol 34:661-668 doi:10.1006/jmcc.2002.2006
188. Muraski JA, Rota M, Misao Y, Fransioli J, Cottage C, Gude N, Esposito G, Delucchi F, Arcarese M, Alvarez R, Siddiqi S, Emmanuel GN, Wu W, Fischer K, Martindale JJ, Glembotski CC, Leri A, Kajstura J, Magnuson N, Berns A, Beretta RM, Houser SR, Schaefer EM, Anversa P, Sussman MA (2007) Pim-1 regulates cardiomyocyte survival downstream of Akt. Nat Med 13:1467-1475 doi:10.1038/nm1671
189. Murphy E, Steenbergen C (2008) Mechanisms underlying acute protection from cardiac ischemia-reperfusion injury. Physiol Rev 88:581-609 doi:10.1152/physrev.00024.2007
190. Murphy MP (2009) How mitochondria produce reactive oxygen species. Biochem J 417:1-13 doi:10.1042/BJ20081386
191. Murray CI, Kane LA, Uhrigshardt H, Wang SB, Van Eyk JE (2011) Site-mapping of in vitro S-nitrosation in cardiac mitochondria: implications for cardioprotection. Mol Cell Proteomics 10:M110 004721 doi:10.1074/mcp.M110.004721
192. Murry CE, Jennings RB, Reimer KA (1986) Preconditioning with ischemia: a delay of lethal cell injury in ischemic myocardium. Circulation 74:1124-1136
193. Musil LS, Beyer EC, Goodenough DA (1990) Expression of the gap junction protein connexin43 in embryonic chick lens: molecular cloning, ultrastructural localization, and post-translational phosphorylation. J Membr Biol 116:163-175
194. Naga Prasad SV, Barak LS, Rapacciuolo A, Caron MG, Rockman HA (2001) Agonist-dependent recruitment of phosphoinositide 3-kinase to the membrane by beta-adrenergic receptor kinase 1. A role in receptor sequestration. J Biol Chem 276:18953-18959 doi:10.1074/jbc.M102376200
195. Nakamura M, Wang NP, Zhao ZQ, Wilcox JN, Thourani V, Guyton RA, Vinten-Johansen J (2000) Preconditioning decreases Bax expression, PMN accumulation and apoptosis in reperfused rat heart. Cardiovasc Res 45:661-670
196. Neyton J, Trautmann A (1985) Single-channel currents of an intercellular junction. Nature 317:331-335
197. Nguyen TT, Stevens MV, Kohr M, Steenbergen C, Sack MN, Murphy E (2011) Cysteine 203 of cyclophilin D is critical for cyclophilin D activation of the mitochondrial permeability transition pore. J Biol Chem 286:40184-40192 doi:10.1074/jbc.M111.243469
198. Nielsen MS, Nygaard Axelsen L, Sorgen PL, Verma V, Delmar M, Holstein-Rathlou NH (2012) Gap junctions. Comprehensive Physiology 2:1981-2035 doi:10.1002/cphy.c110051
199. Noma A, Tsuboi N (1987) Dependence of junctional conductance on proton, calcium and magnesium ions in cardiac paired cells of guinea-pig. The Journal of physiology 382:193-211
200. O'Rourke B (2004) Evidence for mitochondrial K+ channels and their role in cardioprotection. Circ Res 94:420-432 doi:10.1161/01.RES.0000117583.66950.43
201. Oldenburg O, Qin Q, Sharma AR, Cohen MV, Downey JM, Benoit JN (2002) Acetylcholine leads to free radical production dependent on K(ATP) channels, G(i)

proteins, phosphatidylinositol 3-kinase and tyrosine kinase. Cardiovasc Res 55:544-552
202. Orellana JA, Figueroa XF, Sanchez HA, Contreras-Duarte S, Velarde V, Saez JC (2011) Hemichannels in the neurovascular unit and white matter under normal and inflamed conditions. CNS Neurol Disord Drug Targets 10:404-414
203. Ovize M, Aupetit JF, Rioufol G, Loufoua J, Andre-Fouet X, Minaire Y, Faucon G (1995) Preconditioning reduces infarct size but accelerates time to ventricular fibrillation in ischemic pig heart. Am J Physiol 269:H72-79
204. Ozcan C, Bienengraeber M, Dzeja PP, Terzic A (2002) Potassium channel openers protect cardiac mitochondria by attenuating oxidant stress at reoxygenation. Am J Physiol Heart Circ Physiol 282:H531-539 doi:10.1152/ajpheart.00552.2001
205. Pain T, Yang XM, Critz SD, Yue Y, Nakano A, Liu GS, Heusch G, Cohen MV, Downey JM (2000) Opening of mitochondrial K(ATP) channels triggers the preconditioned state by generating free radicals. Circ Res 87:460-466
206. Palmer JW, Tandler B, Hoppel CL (1985) Biochemical differences between subsarcolemmal and interfibrillar mitochondria from rat cardiac muscle: effects of procedural manipulations. Arch Biochem Biophys 236:691-702
207. Park JW (1988) Reaction of S-nitrosoglutathione with sulfhydryl groups in protein. Biochem Biophys Res Commun 152:916-920
208. Ping P, Zhang J, Pierce WM, Jr., Bolli R (2001) Functional proteomic analysis of protein kinase C epsilon signaling complexes in the normal heart and during cardioprotection. Circ Res 88:59-62
209. Piot CA, Padmanaban D, Ursell PC, Sievers RE, Wolfe CL (1997) Ischemic preconditioning decreases apoptosis in rat hearts in vivo. Circulation 96:1598-1604
210. Piper HM, Sezer O, Schleyer M, Schwartz P, Hutter JF, Spieckermann PG (1985) Development of ischemia-induced damage in defined mitochondrial subpopulations. J Mol Cell Cardiol 17:885-896
211. Pluta RM, Dejam A, Grimes G, Gladwin MT, Oldfield EH (2005) Nitrite infusions to prevent delayed cerebral vasospasm in a primate model of subarachnoid hemorrhage. JAMA 293:1477-1484 doi:10.1001/jama.293.12.1477
212. Prime TA, Blaikie FH, Evans C, Nadtochiy SM, James AM, Dahm CC, Vitturi DA, Patel RP, Hiley CR, Abakumova I, Requejo R, Chouchani ET, Hurd TR, Garvey JF, Taylor CT, Brookes PS, Smith RA, Murphy MP (2009) A mitochondria-targeted S-nitrosothiol modulates respiration, nitrosates thiols, and protects against ischemia-reperfusion injury. Proc Natl Acad Sci U S A 106:10764-10769 doi:10.1073/pnas.0903250106
213. Przyklenk K, Bauer B, Ovize M, Kloner RA, Whittaker P (1993) Regional ischemic 'preconditioning' protects remote virgin myocardium from subsequent sustained coronary occlusion. Circulation 87:893-899
214. Przyklenk K, Darling CE, Dickson EW, Whittaker P (2003) Cardioprotection 'outside the box'--the evolving paradigm of remote preconditioning. Basic Res Cardiol 98:149-157 doi:10.1007/s00395-003-0406-y
215. Purnick PE, Oh S, Abrams CK, Verselis VK, Bargiello TA (2000) Reversal of the gating polarity of gap junctions by negative charge substitutions in the N-terminus of connexin 32. Biophys J 79:2403-2415 doi:10.1016/S0006-3495(00)76485-X
216. Pype JL, Xu H, Schuermans M, Dupont LJ, Wuyts W, Mak JC, Barnes PJ, Demedts MG, Verleden GM (2001) Mechanisms of interleukin 1beta-induced human airway smooth muscle hyporesponsiveness to histamine. Involvement of p38 MAPK NF-kappaB. Am J Respir Crit Care Med 163:1010-1017 doi:10.1164/ajrccm.163.4.9911091

217. Qian J, Zhang Q, Church JE, Stepp DW, Rudic RD, Fulton DJ (2010) Role of local production of endothelium-derived nitric oxide on cGMP signaling and S-nitrosylation. Am J Physiol Heart Circ Physiol 298:H112-118 doi:10.1152/ajpheart.00614.2009
218. Quist AP, Rhee SK, Lin H, Lal R (2000) Physiological role of gap-junctional hemichannels. Extracellular calcium-dependent isosmotic volume regulation. J Cell Biol 148:1063-1074
219. Rassaf T, Bryan NS, Maloney RE, Specian V, Kelm M, Kalyanaraman B, Rodriguez J, Feelisch M (2003) NO adducts in mammalian red blood cells: too much or too little? Nat Med 9:481-482; author reply 482-483 doi:10.1038/nm0503-481
220. Rassaf T, Heiss C, Hendgen-Cotta U, Balzer J, Matern S, Kleinbongard P, Lee A, Lauer T, Kelm M (2006) Plasma nitrite reserve and endothelial function in the human forearm circulation. Free Radic Biol Med 41:295-301 doi:10.1016/j.freeradbiomed.2006.04.006
221. Rassaf T, Totzeck M, Hendgen-Cotta UB, Shiva S, Heusch G, Kelm M (2014) Circulating nitrite contributes to cardioprotection by remote ischemic preconditioning. Circ Res 114:1601-1610 doi:10.1161/CIRCRESAHA.114.303822
222. Ravichandran V, Seres T, Moriguchi T, Thomas JA, Johnston RB, Jr. (1994) S-thiolation of glyceraldehyde-3-phosphate dehydrogenase induced by the phagocytosis-associated respiratory burst in blood monocytes. J Biol Chem 269:25010-25015
223. Remo BF, Giovannone S, Fishman GI (2012) Connexin43 cardiac gap junction remodeling: lessons from genetically engineered murine models. J Membr Biol 245:275-281 doi:10.1007/s00232-012-9448-0
224. Retamal MA, Cortes CJ, Reuss L, Bennett MV, Saez JC (2006) S-nitrosylation and permeation through connexin 43 hemichannels in astrocytes: induction by oxidant stress and reversal by reducing agents. Proc Natl Acad Sci U S A 103:4475-4480 doi:10.1073/pnas.0511118103
225. Retamal MA, Froger N, Palacios-Prado N, Ezan P, Saez PJ, Saez JC, Giaume C (2007) Cx43 hemichannels and gap junction channels in astrocytes are regulated oppositely by proinflammatory cytokines released from activated microglia. J Neurosci 27:13781-13792 doi:10.1523/JNEUROSCI.2042-07.2007
226. Retamal MA, Schalper KA, Shoji KF, Bennett MV, Saez JC (2007) Opening of connexin 43 hemichannels is increased by lowering intracellular redox potential. Proc Natl Acad Sci U S A 104:8322-8327 doi:10.1073/pnas.0702456104
227. Retamal MA, Schalper KA, Shoji KF, Orellana JA, Bennett MV, Saez JC (2007) Possible involvement of different connexin43 domains in plasma membrane permeabilization induced by ischemia-reperfusion. J Membr Biol 218:49-63 doi:10.1007/s00232-007-9043-y
228. Rioufol G, Ovize M, Loufoua J, Pop C, Andre-Fouat X, Minaire Y (1997) Ventricular fibrillation in preconditioned pig hearts: role of K+ATP channels. Am J Physiol 273:H2804-2810
229. Riva A, Tandler B, Loffredo F, Vazquez E, Hoppel C (2005) Structural differences in two biochemically defined populations of cardiac mitochondria. Am J Physiol Heart Circ Physiol 289:H868-872 doi:10.1152/ajpheart.00866.2004
230. Rodriguez-Sinovas A, Boengler K, Cabestrero A, Gres P, Morente M, Ruiz-Meana M, Konietzka I, Miro E, Totzeck A, Heusch G, Schulz R, Garcia-Dorado D (2006) Translocation of connexin 43 to the inner mitochondrial membrane of cardiomyocytes through the heat shock protein 90-dependent TOM pathway and its importance for cardioprotection. Circ Res 99:93-101 doi:10.1161/01.RES.0000230315.56904.de

231. Rodriguez-Sinovas A, Cabestrero A, Lopez D, Torre I, Morente M, Abellan A, Miro E, Ruiz-Meana M, Garcia-Dorado D (2007) The modulatory effects of connexin 43 on cell death/survival beyond cell coupling. Prog Biophys Mol Biol 94:219-232 doi:10.1016/j.pbiomolbio.2007.03.003
232. Rudisuli A, Weingart R (1989) Electrical properties of gap junction channels in guinea-pig ventricular cell pairs revealed by exposure to heptanol. Pflugers Arch 415:12-21
233. Saez JC, Berthoud VM, Branes MC, Martinez AD, Beyer EC (2003) Plasma membrane channels formed by connexins: their regulation and functions. Physiol Rev 83:1359-1400 doi:10.1152/physrev.00007.2003
234. Saez JC, Nairn AC, Czernik AJ, Fishman GI, Spray DC, Hertzberg EL (1997) Phosphorylation of connexin43 and the regulation of neonatal rat cardiac myocyte gap junctions. J Mol Cell Cardiol 29:2131-2145 doi:10.1006/jmcc.1997.0447
235. Saez JC, Retamal MA, Basilio D, Bukauskas FF, Bennett MV (2005) Connexin-based gap junction hemichannels: gating mechanisms. Biochim Biophys Acta 1711:215-224 doi:10.1016/j.bbamem.2005.01.014
236. Sakamoto J, Miura T, Tsuchida A, Fukuma T, Hasegawa T, Shimamoto K (1999) Reperfusion arrhythmias in the murine heart: their characteristics and alteration after ischemic preconditioning. Basic Res Cardiol 94:489-495
237. Saltman AE, Krukenkamp IB, Gaudette GR, Horimoto H, Levitsky S (2000) Pharmacological preconditioning with the adenosine triphosphate-sensitive potassium channel opener pinacidil. Ann Thorac Surg 70:595-601
238. Sanchez HA, Mese G, Srinivas M, White TW, Verselis VK (2010) Differentially altered Ca2+ regulation and Ca2+ permeability in Cx26 hemichannels formed by the A40V and G45E mutations that cause keratitis ichthyosis deafness syndrome. J Gen Physiol 136:47-62 doi:10.1085/jgp.201010433
239. Schalper KA, Sanchez HA, Lee SC, Altenberg GA, Nathanson MH, Saez JC (2010) Connexin 43 hemichannels mediate the Ca2+ influx induced by extracellular alkalinization. Am J Physiol Cell Physiol 299:C1504-1515 doi:10.1152/ajpcell.00015.2010
240. Schulman IH, Hare JM (2012) Regulation of cardiovascular cellular processes by S-nitrosylation. Biochim Biophys Acta 1820:752-762 doi:10.1016/j.bbagen.2011.04.002
241. Schulz R, Gres P, Skyschally A, Duschin A, Belosjorow S, Konietzka I, Heusch G (2003) Ischemic preconditioning preserves connexin 43 phosphorylation during sustained ischemia in pig hearts in vivo. FASEB J 17:1355-1357 doi:10.1096/fj.02-0975fje
242. Schulz R, Heusch G (2004) Connexin 43 and ischemic preconditioning. Cardiovasc Res 62:335-344 doi:10.1016/j.cardiores.2003.12.017
243. Schuppe-Koistinen I, Gerdes R, Moldeus P, Cotgreave IA (1994) Studies on the reversibility of protein S-thiolation in human endothelial cells. Arch Biochem Biophys 315:226-234
244. Schwanke U, Konietzka I, Duschin A, Li X, Schulz R, Heusch G (2002) No ischemic preconditioning in heterozygous connexin43-deficient mice. Am J Physiol Heart Circ Physiol 283:H1740-1742 doi:10.1152/ajpheart.00442.2002
245. Schwanke U, Li X, Schulz R, Heusch G (2003) No ischemic preconditioning in heterozygous connexin 43-deficient mice--a further in vivo study. Basic Res Cardiol 98:181-182
246. Serrano-Martin X, Payares G, Mendoza-Leon A (2006) Glibenclamide, a blocker of K+(ATP) channels, shows antileishmanial activity in experimental murine

cutaneous leishmaniasis. Antimicrob Agents Chemother 50:4214-4216 doi:10.1128/AAC.00617-06
247. Seth D, Stamler JS (2011) The SNO-proteome: causation and classifications. Curr Opin Chem Biol 15:129-136 doi:10.1016/j.cbpa.2010.10.012
248. Shattock MJ, Lawson CS, Hearse DJ, Downey JM (1996) Electrophysiological characteristics of repetitive ischemic preconditioning in the pig heart. J Mol Cell Cardiol 28:1339-1347 doi:10.1006/jmcc.1996.0124
249. Shiki K, Hearse DJ (1987) Preconditioning of ischemic myocardium: reperfusion-induced arrhythmias. Am J Physiol 253:H1470-1476
250. Shimizu M, Tropak M, Diaz RJ, Suto F, Surendra H, Kuzmin E, Li J, Gross G, Wilson GJ, Callahan J, Redington AN (2009) Transient limb ischaemia remotely preconditions through a humoral mechanism acting directly on the myocardium: evidence suggesting cross-species protection. Clin Sci (Lond) 117:191-200 doi:10.1042/CS20080523
251. Shintani-Ishida K, Uemura K, Yoshida K (2007) Hemichannels in cardiomyocytes open transiently during ischemia and contribute to reperfusion injury following brief ischemia. Am J Physiol Heart Circ Physiol 293:H1714-1720 doi:10.1152/ajpheart.00022.2007
252. Shiva S, Gladwin MT (2009) Shining a light on tissue NO stores: near infrared release of NO from nitrite and nitrosylated hemes. J Mol Cell Cardiol 46:1-3 doi:10.1016/j.yjmcc.2008.10.005
253. Shiva S, Huang Z, Grubina R, Sun J, Ringwood LA, MacArthur PH, Xu X, Murphy E, Darley-Usmar VM, Gladwin MT (2007) Deoxymyoglobin is a nitrite reductase that generates nitric oxide and regulates mitochondrial respiration. Circ Res 100:654-661 doi:10.1161/01.RES.0000260171.52224.6b
254. Shiva S, Sack MN, Greer JJ, Duranski M, Ringwood LA, Burwell L, Wang X, MacArthur PH, Shoja A, Raghavachari N, Calvert JW, Brookes PS, Lefer DJ, Gladwin MT (2007) Nitrite augments tolerance to ischemia/reperfusion injury via the modulation of mitochondrial electron transfer. J Exp Med 204:2089-2102 doi:10.1084/jem.20070198
255. Smyth JW, Vogan JM, Buch PJ, Zhang SS, Fong TS, Hong TT, Shaw RM (2012) Actin cytoskeleton rest stops regulate anterograde traffic of connexin 43 vesicles to the plasma membrane. Circ Res 110:978-989 doi:10.1161/CIRCRESAHA.111.257964
256. Solan JL, Lampe PD (2009) Connexin43 phosphorylation: structural changes and biological effects. Biochem J 419:261-272 doi:10.1042/BJ20082319
257. Solan JL, Lampe PD (2008) Connexin 43 in LA-25 cells with active v-src is phosphorylated on Y247, Y265, S262, S279/282, and S368 via multiple signaling pathways. Cell Commun Adhes 15:75-84 doi:10.1080/15419060802014016
258. Solan JL, Marquez-Rosado L, Sorgen PL, Thornton PJ, Gafken PR, Lampe PD (2007) Phosphorylation at S365 is a gatekeeper event that changes the structure of Cx43 and prevents down-regulation by PKC. J Cell Biol 179:1301-1309 doi:10.1083/jcb.200707060
259. Spray DC, Burt JM (1990) Structure-activity relations of the cardiac gap junction channel. Am J Physiol 258:C195-205
260. Stout CE, Costantin JL, Naus CC, Charles AC (2002) Intercellular calcium signaling in astrocytes via ATP release through connexin hemichannels. J Biol Chem 277:10482-10488 doi:10.1074/jbc.M109902200
261. Straub AC, Billaud M, Johnstone SR, Best AK, Yemen S, Dwyer ST, Looft-Wilson R, Lysiak JJ, Gaston B, Palmer L, Isakson BE (2011) Compartmentalized connexin 43 s-nitrosylation/denitrosylation regulates heterocellular communication in

the vessel wall. Arterioscler Thromb Vasc Biol 31:399-407 doi:10.1161/ATVBAHA.110.215939
262. Suchyna TM, Nitsche JM, Chilton M, Harris AL, Veenstra RD, Nicholson BJ (1999) Different ionic selectivities for connexins 26 and 32 produce rectifying gap junction channels. Biophys J 77:2968-2987 doi:10.1016/S0006-3495(99)77129-8
263. Sun J, Morgan M, Shen RF, Steenbergen C, Murphy E (2007) Preconditioning results in S-nitrosylation of proteins involved in regulation of mitochondrial energetics and calcium transport. Circ Res 101:1155-1163 doi:10.1161/CIRCRESAHA.107.155879
264. Sun J, Murphy E (2010) Protein S-nitrosylation and cardioprotection. Circ Res 106:285-296 doi:10.1161/CIRCRESAHA.109.209452
265. Sun J, Picht E, Ginsburg KS, Bers DM, Steenbergen C, Murphy E (2006) Hypercontractile female hearts exhibit increased S-nitrosylation of the L-type Ca2+ channel alpha1 subunit and reduced ischemia/reperfusion injury. Circ Res 98:403-411 doi:10.1161/01.RES.0000202707.79018.0a
266. Sun J, Steenbergen C, Murphy E (2006) S-nitrosylation: NO-related redox signaling to protect against oxidative stress. Antioxid Redox Signal 8:1693-1705 doi:10.1089/ars.2006.8.1693
267. Symersky J, Osowski D, Walters DE, Mueller DM (2012) Oligomycin frames a common drug-binding site in the ATP synthase. Proc Natl Acad Sci U S A 109:13961-13965 doi:10.1073/pnas.1207912109
268. Szabo I, Leanza L, Gulbins E, Zoratti M (2012) Physiology of potassium channels in the inner membrane of mitochondria. Pflugers Arch 463:231-246 doi:10.1007/s00424-011-1058-7
269. Takano H, Manchikalapudi S, Tang XL, Qiu Y, Rizvi A, Jadoon AK, Zhang Q, Bolli R (1998) Nitric oxide synthase is the mediator of late preconditioning against myocardial infarction in conscious rabbits. Circulation 98:441-449
270. Taylor ER, Hurrell F, Shannon RJ, Lin TK, Hirst J, Murphy MP (2003) Reversible glutathionylation of complex I increases mitochondrial superoxide formation. J Biol Chem 278:19603-19610 doi:10.1074/jbc.M209359200
271. Thielmann M, Kottenberg E, Kleinbongard P, Wendt D, Gedik N, Pasa S, Price V, Tsagakis K, Neuhauser M, Peters J, Jakob H, Heusch G (2013) Cardioprotective and prognostic effects of remote ischaemic preconditioning in patients undergoing coronary artery bypass surgery: a single-centre randomised, double-blind, controlled trial. Lancet 382:597-604 doi:10.1016/S0140-6736(13)61450-6
272. Thornton JD, Liu GS, Downey JM (1993) Pretreatment with pertussis toxin blocks the protective effects of preconditioning: evidence for a G-protein mechanism. J Mol Cell Cardiol 25:311-320 doi:10.1006/jmcc.1993.1037
273. Tiravanti E, Samouilov A, Zweier JL (2004) Nitrosyl-heme complexes are formed in the ischemic heart: evidence of nitrite-derived nitric oxide formation, storage, and signaling in post-ischemic tissues. J Biol Chem 279:11065-11073 doi:10.1074/jbc.M311908200
274. Totzeck A, Boengler K, van de Sand A, Konietzka I, Gres P, Garcia-Dorado D, Heusch G, Schulz R (2008) No impact of protein phosphatases on connexin 43 phosphorylation in ischemic preconditioning. Am J Physiol Heart Circ Physiol 295:H2106-2112 doi:10.1152/ajpheart.00456.2008
275. Turrens JF (1997) Superoxide production by the mitochondrial respiratory chain. Biosci Rep 17:3-8
276. Turrens JF, Alexandre A, Lehninger AL (1985) Ubisemiquinone is the electron donor for superoxide formation by complex III of heart mitochondria. Arch Biochem Biophys 237:408-414

277. Turrens JF, Boveris A (1980) Generation of superoxide anion by the NADH dehydrogenase of bovine heart mitochondria. Biochem J 191:421-427
278. van Veen AA, van Rijen HV, Opthof T (2001) Cardiac gap junction channels: modulation of expression and channel properties. Cardiovasc Res 51:217-229
279. Veenstra RD, Wang HZ, Beyer EC, Brink PR (1994) Selective dye and ionic permeability of gap junction channels formed by connexin45. Circ Res 75:483-490
280. Veenstra RD, Wang HZ, Beyer EC, Ramanan SV, Brink PR (1994) Connexin37 forms high conductance gap junction channels with subconductance state activity and selective dye and ionic permeabilities. Biophys J 66:1915-1928 doi:10.1016/S0006-3495(94)80985-3
281. Veenstra RD, Wang HZ, Westphale EM, Beyer EC (1992) Multiple connexins confer distinct regulatory and conductance properties of gap junctions in developing heart. Circ Res 71:1277-1283
282. Venkatakrishnan P, Nakayasu ES, Almeida IC, Miller RT (2009) Absence of nitric-oxide synthase in sequentially purified rat liver mitochondria. J Biol Chem 284:19843-19855 doi:10.1074/jbc.M109.003301
283. Vergara L, Bao X, Cooper M, Bello-Reuss E, Reuss L (2003) Gap-junctional hemichannels are activated by ATP depletion in human renal proximal tubule cells. J Membr Biol 196:173-184 doi:10.1007/s00232-003-0636-9
284. Vikhamar G, Rivedal E, Mollerup S, Sanner T (1998) Role of Cx43 phosphorylation and MAP kinase activation in EGF induced enhancement of cell communication in human kidney epithelial cells. Cell Adhes Commun 5:451-460
285. Wang GY, Wu S, Pei JM, Yu XC, Wong TM (2001) Kappa- but not delta-opioid receptors mediate effects of ischemic preconditioning on both infarct and arrhythmia in rats. Am J Physiol Heart Circ Physiol 280:H384-391
286. Wang H, Viatchenko-Karpinski S, Sun J, Gyorke I, Benkusky NA, Kohr MJ, Valdivia HH, Murphy E, Gyorke S, Ziolo MT (2010) Regulation of myocyte contraction via neuronal nitric oxide synthase: role of ryanodine receptor S-nitrosylation. The Journal of physiology 588:2905-2917 doi:10.1113/jphysiol.2010.192617
287. Wang HZ, Veenstra RD (1997) Monovalent ion selectivity sequences of the rat connexin43 gap junction channel. J Gen Physiol 109:491-507
288. Wang N, De Bock M, Antoons G, Gadicherla AK, Bol M, Decrock E, Evans WH, Sipido KR, Bukauskas FF, Leybaert L (2012) Connexin mimetic peptides inhibit Cx43 hemichannel opening triggered by voltage and intracellular Ca2+ elevation. Basic Res Cardiol 107:304 doi:10.1007/s00395-012-0304-2
289. Wang N, De Vuyst E, Ponsaerts R, Boengler K, Palacios-Prado N, Wauman J, Lai CP, De Bock M, Decrock E, Bol M, Vinken M, Rogiers V, Tavernier J, Evans WH, Naus CC, Bukauskas FF, Sipido KR, Heusch G, Schulz R, Bultynck G, Leybaert L (2013) Selective inhibition of Cx43 hemichannels by Gap19 and its impact on myocardial ischemia/reperfusion injury. Basic Res Cardiol 108:309 doi:10.1007/s00395-012-0309-x
290. Warn-Cramer BJ, Lampe PD, Kurata WE, Kanemitsu MY, Loo LW, Eckhart W, Lau AF (1996) Characterization of the mitogen-activated protein kinase phosphorylation sites on the connexin-43 gap junction protein. J Biol Chem 271:3779-3786
291. Warn-Cramer BJ, Lau AF (2004) Regulation of gap junctions by tyrosine protein kinases. Biochim Biophys Acta 1662:81-95 doi:10.1016/j.bbamem.2003.10.018
292. Warner A, Clements DK, Parikh S, Evans WH, DeHaan RL (1995) Specific motifs in the external loops of connexin proteins can determine gap junction formation between chick heart myocytes. The Journal of physiology 488 (Pt 3):721-728

293. Winmill RE, Hedrick MS (2003) Gap junction blockade with carbenoxolone differentially affects fictive breathing in larval and adult bullfrogs. Respir Physiol Neurobiol 138:239-251
294. Winston BW, Chan ED, Johnson GL, Riches DW (1997) Activation of p38mapk, MKK3, and MKK4 by TNF-alpha in mouse bone marrow-derived macrophages. J Immunol 159:4491-4497
295. Wolfrum S, Schneider K, Heidbreder M, Nienstedt J, Dominiak P, Dendorfer A (2002) Remote preconditioning protects the heart by activating myocardial PKCepsilon-isoform. Cardiovasc Res 55:583-589
296. Wu Y, Zhang F, Wang Y, Krishnamoorthy M, Roy-Chaudhury P, Bleske BE, Meyerhoff ME (2008) Photoinstability of S-nitrosothiols during sampling of whole blood: a likely source of error and variability in S-nitrosothiol measurements. Clin Chem 54:916-918 doi:10.1373/clinchem.2007.102103
297. Xu Z, Ji X, Boysen PG (2004) Exogenous nitric oxide generates ROS and induces cardioprotection: involvement of PKG, mitochondrial KATP channels, and ERK. Am J Physiol Heart Circ Physiol 286:H1433-1440 doi:10.1152/ajpheart.00882.2003
298. Ye ZC, Wyeth MS, Baltan-Tekkok S, Ransom BR (2003) Functional hemichannels in astrocytes: a novel mechanism of glutamate release. J Neurosci 23:3588-3596
299. Yellon DM, Baxter GF, Garcia-Dorado D, Heusch G, Sumeray MS (1998) Ischaemic preconditioning: present position and future directions. Cardiovasc Res 37:21-33
300. Zanella B, Giordano E, Muscari C, Zini M, Guarnieri C (2004) Nitric oxide synthase activity in rat cardiac mitochondria. Basic Res Cardiol 99:159-164 doi:10.1007/s00395-003-0454-3
301. Zhang J, Jin B, Li L, Block ER, Patel JM (2005) Nitric oxide-induced persistent inhibition and nitrosylation of active site cysteine residues of mitochondrial cytochrome-c oxidase in lung endothelial cells. Am J Physiol Cell Physiol 288:C840-849 doi:10.1152/ajpcell.00325.2004
302. Zimmet JM, Hare JM (2006) Nitroso-redox interactions in the cardiovascular system. Circulation 114:1531-1544 doi:10.1161/CIRCULATIONAHA.105.605519
303. Ziolo MT (2008) The fork in the nitric oxide road: cyclic GMP or nitrosylation? Nitric Oxide 18:153-156 doi:10.1016/j.niox.2008.01.008
304. Ziolo MT, Bers DM (2003) The real estate of NOS signaling: location, location, location. Circ Res 92:1279-1281 doi:10.1161/01.RES.0000080783.34092.AF
305. Ziolo MT, Kohr MJ, Wang H (2008) Nitric oxide signaling and the regulation of myocardial function. J Mol Cell Cardiol 45:625-632 doi:10.1016/j.yjmcc.2008.07.015
306. Zundorf G, Kahlert S, Reiser G (2007) Gap-junction blocker carbenoxolone differentially enhances NMDA-induced cell death in hippocampal neurons and astrocytes in co-culture. J Neurochem 102:508-521 doi:10.1111/j.1471-4159.2007.04509.x
307. Zweier JL, Talukder MA (2006) The role of oxidants and free radicals in reperfusion injury. Cardiovasc Res 70:181-190 doi:10.1016/j.cardiores.2006.02.025

Publications

Soetkamp D, Nguyen TT, Menazza S, Hirschhäuser C, Hendgen-Cotta U, Rassaf T, Schlüter KD, Boengler K, Murphy E, and Schulz R (2014) S-nitrosation of mitochondrial connexin 43 regulates mitochondrial function. Basic Res Cardiol (BRIC-D-14-00116R1) (In Press).

Boengler K, Ruiz-Meana M, Gent S, Ungefug E, Soetkamp D, Miro-Casas E, Cabestrero A, Fernandez-Sanz C, Semenzato M, Di Lisa F, Rohrbach S, Garcia-Dorado D, Heusch G, Schulz R (2012) Mitochondrial connexin 43 impacts on respiratory complex I activity and mitochondrial oxygen consumption. J Cell Mol Med 16:1649-1655 doi:10.1111/j.1582-4934.2011.01516.x

Presentations (Poster)

Soetkamp D, Nguyen TT, Menazza S, Hirschhäuser C, Boengler K, Aponte A, Gucek M, Murphy E, and Schulz R: S-Nitrosylation of Mitochondrial Connexin 43: A possible Mechanism Mediating Ischemic Preconditioning in Rat Hearts. American Heart Association's Scientific Sessions 2013, Dallas, TX, USA.

Soetkamp D, Nguyen TT, Menazza S, Appachi S, Murphy E, and Schulz R: S-Nitrosylation of Mitochondrial Connexin 43: A possible Mechanism Mediating Ischemic Preconditioning in Rat Hearts? ISHR XXI World Congress, San Diego, CA, USA.

Selbstständigkeitserklärung

Hiermit versichere ich, die vorgelegte Thesis selbständig und ohne unerlaubte fremde Hilfe und nur mit den Hilfen angefertigt zu haben, die ich in der Thesis angegeben habe. Alle Textstellen, die wörtlich oder sinngemäß aus veröffentlichten Schriften entnommen sind, und alle Angaben, die auf mündlichen Auskünften beruhen, sind als solche kenntlich gemacht. Bei den von mir durchgeführten und in der Thesis erwähnten Untersuchungen habe ich die Grundsätze guter wissenschaftlicher Praxis, wie sie in der ’Satzung der Justus-Liebig-Universität Gießen zur Sicherung guter wissenschaftlicher Praxis’ niedergelegt sind, eingehalten. Ich stimme einer Überprüfung der Thesis mittels Anti-Plagiatssoftware gemäß § 25 Abs. 6 der Allgemeinen Bestimmungen für modularisierte Studiengänge zu.

_____ _____

(Datum) (Unterschrift)

Acknowledgements

I would like to express my special appreciation and thanks to Prof. Dr. Rainer Schulz for his supervision, guidance, and advice in scientific, career related, and non-scientific questions. I thank him for giving me scientific freedom, for giving me the opportunity to participate in several conferences, for introducing me to the scientific society of cardiovascular research, for the quick answers night and day to various questions, and for motivating me during times where I could not envision success. Especially, I want to thank him for introducing me to Elizabeth Murphy and to the NIH society in Bethesda, Maryland, where I met my wife.

I thank my supervisor Prof Dr. Michael Martin for his scientific expertise, and for supporting and reviewing my thesis.

I thank PD Dr. Kerstin Boengler for great scientific discussions, her smart advice during experimental troubleshooting, reviewing manuscripts, presentations, and applications, as well as being there when experiments did not work out and listening to my complaints.

Elizabeth (Tish) Murphy, PhD was my supervisor during my time at the NIH, in Bethesda MD, USA. Special thanks to her for giving me this opportunity and introducing me to a different kind of scientific world, the NIH. I thank her for the scientific support, her critical thoughts reminding me to have a critical view on my own data, and for having a great time and fun with her and her lab members. The time at NIH was very special to me and will be always memorable. Accordingly, I thank Dr. Sara Menazza for Italian nights and her, Tiffany T. Nguyen, and Dr. Sun I thank for being great friends and for the support to obtain the first data for my thesis.

I thank Dr. Ulrike Hendgen-Cotta, Dominik Semmler, and Prof. Dr. Tienush Rassaf from the Institute of Molecular Cardiology at the Heinrich-Heine University of Düsseldorf for a very successful collaboration investigating the mechanism of remote preconditioning.

Prof Dr. Günther Lochnit from the Biochemical Institute of the Justus-Liebig University and Dr. Marian Gucek from the NIH in Bethesda, MD, USA I thank for their support and cooperation performing proteomic analysis.

I thank Prof. Dr. Klaus-Dieter Schlüter and Peter Volk for their support doing Langendorff perfusion experiments,

Special thanks also belong to the members of my group. The technical support of Elvira Ungefug, Anna Reis, and Sabrina Böhme is gratefully acknowledged. When time was tight they were a great support.

I thank Christine Hirschhäuser and Tarek El-Madany for proofreading my thesis. Additionally I thank them for being great friends and for understanding what science means.

My family Nesrin, Gabriel, Mustapha, Samia, Evelyn, Theo, and Lisa words can't say what you all did. Without you this would have not been possible.

Der Lebenslauf wurde aus der elektronischen Version der Arbeit entfernt.

The curriculum vitae was removed from the electronic version of the paper.